Master Thesis

TVVR 22/5015

Longshore Sediment Transport Along the Coast of Ystad Municipality

Cause and Effect

Isa Berin

Johanna Jacobson Löwdin

Division of Water Resources Engineering
Department of Building and Environmental Technology
Lund University

Longshore Sediment Transport Along the Coast of Ystad Municipality

Cause and Effect

By:
Isa Berin
Johanna Jacobson Löwdin

Master Thesis

Division of Water Resources Engineering
Department of Building & Environmental Technology
Lund University
Box 118
221 00 Lund, Sweden

Water Resources Engineering
TVVR 22/5015
ISSN 1101-9824

Lund 2022
www.tvrl.lth.se

Master Thesis
Division of Water Resources Engineering
Department of Building & Environmental Technology
Lund University

English title:	Longshore Sediment Transport Along the Coast of Ystad Municipality
Swedish title:	Kustparallell sedimenttransport längs Ystad kommuns kust
Authors:	Isa Berin Johanna Jacobson Löwdin
Supervisors:	Caroline Hallin, Anna Adell
Examiner:	Magnus Larson
Language	English
Year:	2022
Keywords:	Coastal erosion; sediment dynamics; longshore sediment transport; CERC; shoreline change

Acknowledgements

First and foremost we would like to thank our supervisors, Caroline and Anna, for your encouragement, knowledge and support throughout this whole process. It was very reassuring knowing you were only a phone call or email away during times of confusion. Thank you, Anna, for assisting us during the first days of field study and unwaveringly holding on to the equipment despite strong winds and large waves.

To our families, who provided us with love and care and constant supply of encouragement, we are very grateful. Through good times and bad times, you were on our side forever more, that's what family is for. Thank you, Maria and Anna, for introducing us to Photoshop and teaching us the basics so our very farfetched dreams of calling ourselves illustrators could come true.

Last, but not least, thanks to our four-pawed friend, Otis. You provided us with the emotional support needed to wrap this up and added an ambient sound of snoring, that created a calming environment.

Abstract

The coast of Ystad municipality has historically been subject to erosion, leading to the loss of recreational areas and near-beach structures, consequently resulting in the implementation of mitigating measures. With the ongoing climate change, erosion is expected to continue. This generates a need for a better understanding of sediment dynamics and sediment transport patterns, in order to further plan for coastal management in Ystad municipality. This thesis focused on obtaining further information about the coast of Ystad municipality through field surveys and modelling of longshore sediment transport. The modelled sediment transport showed an overall eastern transport direction, with some coastal stretches indicating an alternating transport direction, which was confirmed through observations. The greatest transport magnitudes were found along beaches that have historically been subjected to erosion and accumulation. Further, small changes in shoreline orientation had a large impact on both direction and magnitude of the modelled sediment transport. Grain size statistics derived from sediment field samples resulted in a correlation between median grain size, sorting, and beach face slope. The results showed a correlation between eroded beaches and coarser, less sorted sediment and a steeper beach face slope, whereas accumulated beaches were correlated with a finer, more well sorted material and a gentler slope. Nourished beaches were found to affect the correlations negatively, since nourishing both impacts the shape of the beach profile and the distribution of grain sizes. Further recurring field sampling is recommended for broader comprehension of grain size patterns along the coast and how nourishing affects these on a longer timescale.

Contents

1 Introduction

1.1 Background

Sandy beaches constitute a great part of the southernmost coast of Sweden and offer appreciated recreational areas and valuable natural environments. They also contribute to the local tourism industry. In addition to being an economic asset, the beach acts as protection against flooding in the event of a storm or increased water-levels, mitigating the impact on existing constructions and infrastructure inland from the beach (Ystad Municipality, 2018). Unfortunately, many stretches of the coast in Scania are presently subject to erosion facing a risk of withdrawal of the shoreline. Further, the increase in water-level due to climate change is predicted to exacerbate the erosion and expedite the consequences (Malmberg Persson et al., 2016).

Sediment transport is a process that occurs continuously on the coast, giving rise to erosion and accumulation due to naturally occurring variations in wave climate and water level (Nyberg et al., 2020). An explanation for the erosion could be a sediment deficit due to sediment transport by an alongshore driven current. Since the coast of Scania lacks significant supplement of sediment from rivers and streams, the dynamics of the coastal changes in Scania are primarily determined by a variation in gradients of the longshore sediment transport (LST) (Fredriksson et al., 2017), which can either erode, accumulate, or preserve the beach. The morphological evolution of the beach can be monitored through observations, and erosion managed accordingly. To pre-empt shoreline recession and optimize mitigating measures, models predicting sediment transport can be an important resource. By simplification of physical processes, some models estimate the longshore transport using only relatively few and easily attainable input parameters, while others are more complex, requiring additional data and measurements (Davidson-Arnott, 2010). Regardless of the model used, the analysis and implementation of the model given results require extensive knowledge concerning the complexity of sediment dynamics and the correlation with transport.

The exposed and eroded coast of Scania has led to Ystad municipality being at the forefront of coastal management in Sweden. The municipality has worked extensively to prevent shoreline recession at multiple locations. In addition, they recently initialised a plan of action with the purpose of providing guidelines for coastal protection and a policy for future strategies (Ystad Municipality, 2018). To facilitate the conduction of the coastal planning policy, a greater and wider knowledge of correlations between present sediment dynamics and general transport patterns is beneficial. Further, by utilizing a transport model that is suitable for the coast of Ystad, coastal management can be more precise and protective measures better directed and implemented at coastal stretches facing erosive stress. This can minimize the risk of flooding or undermining of infrastructure along this coast.

1.2 Objectives

The overall purpose of this project is to increase the knowledge of the sediment dynamics along the coastline of Ystad municipality. This is done by analysing the distribution of grain sizes and modelling sediment transport along the coast on a beach scale (up to a few hundred meters) and on a coastal scale (20-40 kilometres). The aim is also to evaluate the applicability

of sediment transport models in this region. To fulfil the objectives of this project, the thesis aims to answer the following questions:

- What are the general sediment transport patterns along the coast?
    - How do results of modelled potential transport correlate with sediment patterns derived from natural and artificial indicators, such as sand build-up at groynes?
    - How applicable are sediment transport models for the coast of Ystad municipality?
    - What advantages and disadvantages are there for using shoreline change as observed values when estimating transport along this coast?
    - What is the impact on the predicted transport rate when using a transport model that includes site-specific parameters such as grain size?
- Based on field data collection, what correlations are there between beach characteristics such as grain size statistics and beach face slope?
    - How do these parameters vary between eroding and accumulating beaches?

1.3 Methodology

1.3.1 Literature Study

A literature study was performed to gather relevant information regarding coastal processes, including sediment transport and sediment transport modelling. Current site conditions and previous mitigating measures were also studied. Since Ystad has a long history of erosion and coastal measures, this information was attainable both from consultancy reports as well as the municipality itself and provided significant background. The literature review also aimed to identify data needed for the transport rate modelling.

1.3.2 Available Data

Wave climate data for the period 1979 to 2019 was obtained from Adell et al. (2021) and is also available online through the Swedish Geotechnical Institute's (SGI) wave portal. Soil maps and marine geological maps are available through the Swedish Geological Survey and orthophotos through Lantmäteriet and GoogleEarth. Values for the historical shoreline change were obtained from Fredriksson et al. (2017).

1.3.3 Field Study

Additional information and data regarding grain sizes and beach profiles were obtained through a field survey conducted between the 16th and 20th of November in 2020. Sediment samples were collected, and beach profiles were measured along the entire coastline of Ystad municipality, where the shore could be reached. Beach profiles were measured using RTK-GPS and sediment samples were sieved and weighed.

1.3.4 Modelling

Wave climate data from the years 1979-2019 was used to predict the potential sediment transport rate along the coast. The rate was modelled using the CERC model (U.S. Army Corps of Engineers, 1984), which was calibrated for Ystad using EPR-values.

Longshore transport was also modelled for the same years with the Bayram model (Bayram et al., 2007), which uses grain size data as an input parameter.

1.4 Report Outline

Chapter 2 – The Coastal Zone and Processes provides theoretical background information for the objectives presented in this thesis.

Chapter 3 – Description of Study Area. In this chapter, the coastline is divided into smaller sections and descriptions of current use, wave climate and geological conditions are given. A short historical background regarding previous mitigating actions is also provided.

Chapter 4 – Methods and Data, first details how the field sampling was carried out, where methodology and equipment are described. The chapter also details how the sediment transport modelling was performed by both the CERC-transport model and the Bayram model, including input parameters. A description of the calibration of the CERC-model is also presented.

Chapter 5 – Results and Discussion. This chapter first presents the results from the modelling, including transport directions, and a discussion regarding the fit of the CERC model. A comparison with the Bayram model is also included. This is followed by a presentation and brief discussion of the results and correlations conducted on the gathered field data.

Chapter 6 – Conclusions, presents the most important conclusions of the finding in this report. Thoughts and recommendations for future studies are also provided.

2 The Coastal Zone and Processes

2.1 The Coastal Zone

The coastal area is a representation of the boundary between land and sea (Masselink & Gehrels, 2014), where the on-and offshore boundaries can vary up to several kilometres (Davidson-Arnott, 2010). The zone can generally be divided into four head sections stretching from the most landward point to the most seaward: the coast, the beach, the nearshore and the offshore (Dean & Dalrymple, 2001). The beach and nearshore can also be called *the littoral zone*. The head sections can then be divided into sub sections. These can be seen in Figure 2.1 below, which shows a cross section, or beach profile, of a typical beach denoting the different areas of the coast.

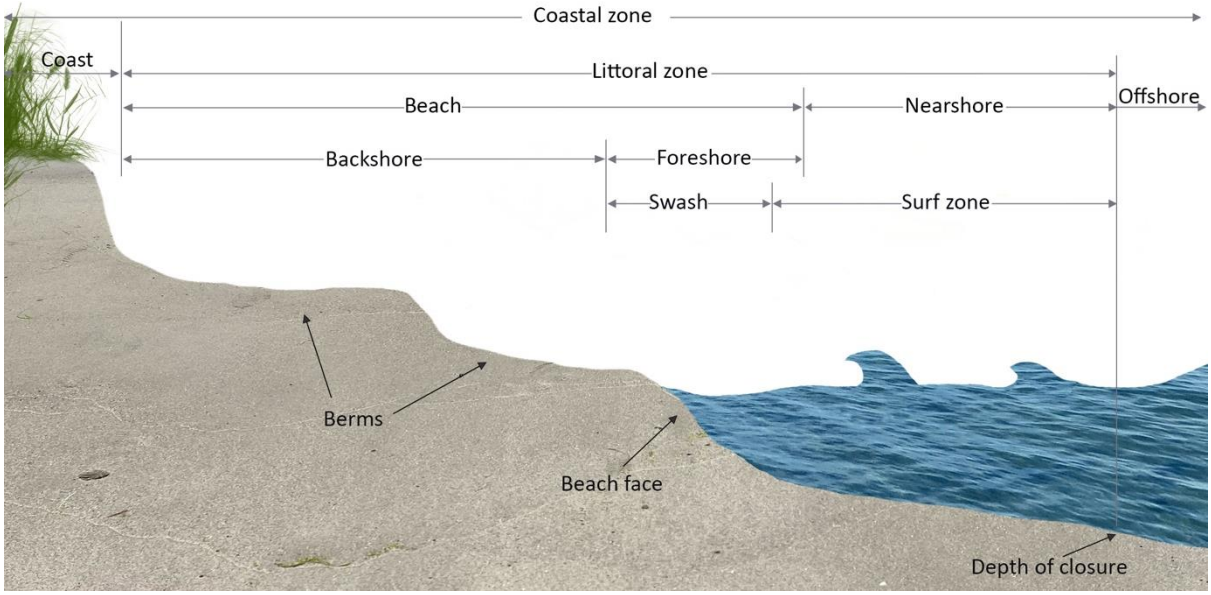

Figure 2.1. The coastal zone. Modified from U.S Army Corps of Engineers (1984).

The most seaward section of the profile is the offshore zone where there is no significant wave-induced sediment transport. Rather, sediment transport mainly occurs in the littoral zone. The boundary between the offshore zone and the littoral zone can be defined as the limit where significant wave-induced sediment transport no longer occurs (Davidson-Arnott, 2010), also called the *depth of closure* (Masselink & Gehrels, 2014). The beach section of the profile is subject to wave action and can be divided into the foreshore, which is exposed to waves during calm conditions, and the backshore, which is only exposed to waves during stormy conditions (Davidson-Arnott, 2010). On this part of the beach, berms can form at the highest limit of wave reach by sediment transported through wave uprush (Dean & Dalrymple, 2001). The surf zone is where waves break and it stretches from the breaker zone (within the nearshore) to the foreshore (Davidson-Arnott, 2010). The surf zone varies with changing wave and environmental conditions (Wright & Short, 1984). The swash zone is situated between the landward point of the surf zone and the seaward limit of the backshore. In the swash zone, the shoreline oscillates due to wave run-up and backwash on the beach face (Hughes & Baldock, 2020). The beach face is defined as the beach sector below the berm, the sub-aerial beach sector, with the beach face slope often representing the steepest slope of the beach profile. As

mentioned, the beach face sector is exposed to wave swash, a process which impact will be further explained in later sections with regards to sediment transport (Reis & Gama, 2010).

2.2 Ocean Waves

The motion of the ocean can be induced by several mechanisms including, amongst others, a gravitational pull causing tidal waves and waves generated by wind climate (U.S. Army Corps of Engineers, 1984). Waves are the major factor responsible for erosion and sediment transport and thus of greatest significance with regards to composition and formation of beaches (Davidson-Arnott, 2010). With the asserted impact from waves on the coast, it becomes important to thoroughly comprehend the mechanisms and dynamics of waves in order to plan for adequate coastal management. The motion of waves varies greatly and in an irregular sea a large range of conditions are to be found with more and less complex wave forms (U.S. Army Corps of Engineers, 1984). Although no theory can fully explain the complexity that is nature, several theories have been developed with the attempt to provide an elementary physical understanding of waves' characteristics. Comprised of only linear equations, the Airy wave theory (linear-wave theory) is generally adequate to describe some of the fundamental properties and since it presents rather simple mathematical forms, it makes it widely used in practical engineering problems (Davidson-Arnott, 2010).

2.2.1 Wave Formation and Characteristics

Wind-generated waves are the dominant input of energy to the littoral zone, primarily as energy dissipates when the wave breaks. The waves are formed as wind transfers energy to the water- surface and due to pressure fluctuations creating a vertical displacement of the surface. With a greater pressure on the windward side while simultaneously a minimum at the leeward, the oscillating movement of the wave is reinforced. Described using linear-wave theory, waves will appear in a periodic and perfectly sinusoidal matter, characterized by a repetitive motion of succeeding wave crests and troughs (Figure 2.2) (Davidson-Arnott, 2010). Fundamentally it is described by three parameters; a height H, vertical distance between the highest part of the wave, a crest, to the lowest part called a trough, a length L, defined as the horizontal distance between two crests or two troughs, and the time between two successive crests called a period, T. The distance from the ocean bed to the mean sea level, is defined by a depth d

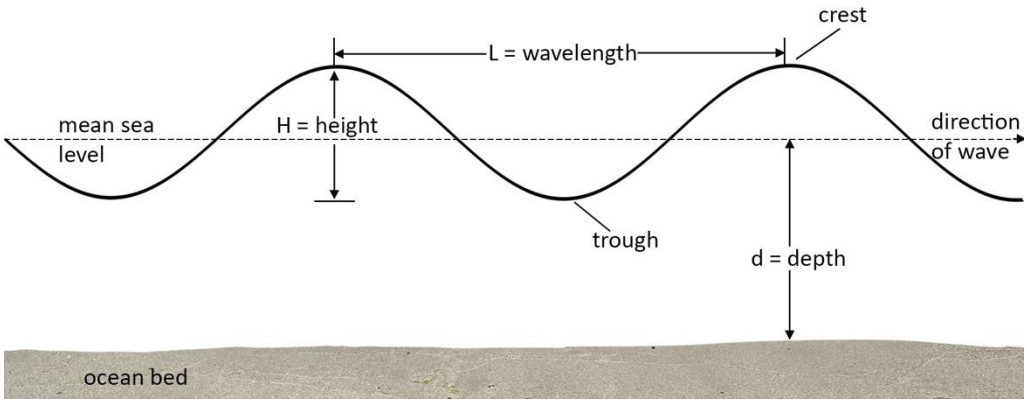

Figure 2.2. Schematic image of wave characteristics. Modified from U.S Army Corps of Engineers (1984).

and the celerity of which the wave propagate is referred to as C (U.S. Army Corps of Engineers, 1984).

The size of the waves is generally determined by the wind speed, the wind duration, and the distance over which the wind blows, referred to as the fetch. These parameters vary regularly, causing a wide range of wave heights and periods. To facilitate the analysis of the wave climate, particular wave heights are instead extracted to be further used in computations and since the wave energy is described to be proportional to the square of the wave height, it is usually the largest waves that are considered for different engineering applications. The significant wave height, H_s, is an important parameter for the statistical distribution of waves and is commonly used to account for large waves and is considered to approximate the mean of the third-highest waves (Davidson-Arnott, 2010).

2.2.2 Wave Propagation and Transformation

The constant changing conditions of the ocean have an impact on the shape and variability of the advancing of waves and direction of propagation and waves approaching shallow and nearshore waters will have a wide range of incident angles in relation to the shoreline (U.S. Army Corps of Engineers, 1984).

The progress of waves as they advance from deep waters to decreasing depth is described as shoaling and is the concept where wave properties vary with regards to change of depth. As the waves reach shallower conditions, they begin to interact with the ocean bed, causing the length and celerity to progressively decrease while simultaneously increasing the wave height and steepness and keeping the period fixed. The wave will proceed until they become unstable and ultimately break (Komar, 1976). Further, the direction of propagation is also affected by interaction with the ocean bed. Waves advancing obliquely to the shore will continuously bend to align themselves with the bottom contours. This concept is called refraction and the process results from a decrease in celerity upon shoaling leading to a varying velocity within the wave where the part in deeper water is moving faster than the part in more shallow water, ultimately causing the wave crest to bend (Davidson-Arnott, 2010). As the wave travels towards the shore, the refraction changes the path of the wave allowing it to advance, break and reach the shore from a different direction than that of the incident deep water wave. Refraction combined with shoaling are two main factors regulating the wave properties and influence how the wave energy is dispersed along the coast (U.S. Army Corps of Engineers, 1984).

2.2.3 Wave Breaking

As waves move into shallower water, the wave height will increase and wavelength decrease, causing an increase in the steepness of the wave. The development of the wave will continue until the wave reaches a critical limit where the crest becomes oversteepened and the wave ultimately breaks (Komar, 1976). The initiation of breaking occurs at what is referred to as breaking depth, d_b, which varies depending on individual wave characteristics (U.S. Army Corps of Engineers, 1984). Although other factors may impact initiation of breaking, one common expression to predict breaking depth is as follows

$$\frac{H_b}{d_b} = 0.78 \tag{2.1}$$

where $H_b$and d_b are the wave height and depth at breaking, respectively, denoting that waves will break at a depth slightly greater than the wave height. Consequently, the incident wave height and length are the parameter initially determining the location of the breaking combined with the bathymetry of the coast (Davidson-Arnott, 2010).

2.3 Sediment Dynamics

2.3.1 Grain Size Distribution

Beaches are often differentiated by shape and character with great variation. One such difference is the beach composition, with regards to sediment size and character (U.S. Army Corps of Engineers, 1984), which greatly influences the transportation, deposition, and erosion of sediments (Davidson-Arnott, 2010). The littoral material is generally classified in accordance with grain size (Davidson-Arnott, 2010; U.S. Army Corps of Engineers, 1984) and Table 2.1 presents particles ranging from clay to boulder, using the scale according to ISO 14688-1:2017 (ISO, 2017). Based on the sediment found upon the beach they can be categorized as sandy beaches with fine sediment, gravel beaches dominated by coarser sediment or mixed beaches, composed of both fine and coarse sediment (Davidson-Arnott, 2010). In order to characterise the beach, the median grain size d_{50} is a commonly used measure, which corresponds to the grain size where the cumulative weight reaches 50%. To extend the comprehension of the beach characteristics, the sorting is also useful to assess. Sorting is a measurement of the spread, or the range of grain sizes found in the sample, meaning that a lower value indicates a lower spread with a more uniform grain size distribution and therefore a more well sorted material (Dean & Dalrymple, 2001).

Table 2.1. Grain size classification according to ISO 14688-1:2017 (ISO, 2017).

Name			Size (mm)
Very coarse soil		Large boulder	>630
		Boulder	200 – 630
		Cobble	63 – 200
Coarse soil	Gravel	Coarse gravel	20 – 63
		Medium gravel	6.3 – 20
		Fine gravel	2.0 – 6.3
	Sand	Coarse sand	0.63 – 2.0
		Medium sand	0.2 – 0.63
		Fine sand	0.063 – 0.2
Fine soil	Silt	Coarse silt	0.02 – 0.063
		Medium silt	0.0063 – 0.02
		Fine silt	0.002 – 0.0063
	Clay	Clay	≤0.002

2.3.2 Sediment Transport

The presence and balance of sediment can be analysed through the budget of sediments, understood as the conservation of mass in the littoral system. The balance is reflected through different sources and sinks in a given sedimentary compartment and involves transport in and out of the system (Komar, 1976). Barriers dividing different sediment compartments or systems from each other can be either natural, such as headlands and shallow waters, or man-made constructions (Nyberg et al., 2021).

For transportation to occur, forces due to wave activity, storm surge and, in some places, tidal currents, generate an impact on the bed sediments. If the force exceeds the threshold for initiation of movement, this will induce an onset of grain motion on the bed. The initiation of motion is usually in reference to shear velocity, which is directly related to the sediment properties. Important properties of individual particles include size, shape and composition, which all greatly influence the capacity to initiate movement and sustain the particles in the water (Dean & Dalrymple, 2001; U.S. Army Corps of Engineers, 1984).

Transport of sediment can occur through different processes. Some particles are suspended and diffused uniformly in the water column while sustained by turbulence. These can be finer sediments in the range of silt and clay. When placed in suspension, they are removed seaward or alongshore to finally settle offshore and therefore do not occur in substantial amounts in the nearshore. Under the influence of energetic waves in the surf zone, sand and gravel can also be transported in suspension. They are readily exchanged between the beach, nearshore and the surf-zone and tend to dominate the active beach profile, which is where significant sediment transport occurs, limited seawards by the depth of closure (Davidson-Arnott, 2010). Another mode of transport is bedload, which is sediment in motion while in close contact with the seabed. The particles tend to be sliding and rolling along the bed and this is primarily the case for coarser particles like sand and gravel. Sediments can also move collectively as a layer along the bottom, commonly referred to as sheet flow (Dean & Dalrymple, 2001).

A common motion and direction of the particles is through cross-shore transport, where sediment moves normal to the shore, and longshore sediment transport with a flow directed alongshore. Although these are usually distinguished as two separate processes, they occur simultaneously affecting the presence of sediment (Davidson-Arnott, 2010). Both will be further explained in the following sections.

2.3.3 Longshore Sediment Transport

Longshore sediment transport is a mode of transport that occurs along the coastline. With the transport being parallel to the shoreline it can be directed in two ways and as an observer standing on land and looking towards the ocean, the longshore transport is directed either to the right or to the left (U.S. Army Corps of Engineers, 1984). The transport is primarily driven by wave action that can generate beach drifting on the swash slope or create a longshore current in the surf-zone. The longshore sediment transport has a substantial impact on sediment dynamics, like erosion and sedimentation, along the coast and is considered of great importance on many coastlines (Davidson-Arnott, 2010).

Longshore Currents

As waves propagate towards shore some will approach obliquely to the shoreline orientation. Upon breaking, a portion of the momentum flux, the longshore component of motion, is directed alongshore the coast inducing a current in the surf-zone (Davidson-Arnott, 2010). The angle at which the waves approach and break, is defined between the wave crest and the orientation of the shoreline. A peak longshore current will occur when the incident angle is 45, whereas angles smaller or larger than 45 will decrease the capacity of the flow (Dean & Dalrymple, 2001). Similarly, an approaching wave with the wave crest aligned parallel with the shoreline does not induce any transport along the coast (Komar, 1983). Although the incident angle of the wave primarily governs the current velocity, the volume rate is better determined by the wave height at breaking conditions (U.S. Army Corps of Engineers, 1984).

Beach Drift

Another mode of transport is beach drift. When waves approach at an oblique angle, wave run-up will occur traverse the foreshore of the beach in the direction of wave approach. The run-up, or swash, is primarily driven by the momentum of the wave and occurs perpendicular to the wave crest while the backwash, governed by gravity, flows straight down the foreshore slope making the transport of sediment appear as a saw-toothed motion alongshore. The significance of this mode of transport varies with beach conditions. Coarser beaches dominated by gravel and cobble, tend to have a steeper foreshore with a narrow surf-zone. Here most of the breaking of waves occur on the foreshore and beach drift is a substantial fraction of the transport. On beaches with medium to coarse sand particles, the significance of the beach drift varies with the shape of the foreshore and wave climate (Davidson-Arnott, 2010).

Transport Rates

The forcing from waves at breaking creates turbulent fluctuations, which can act to dislodge sediment particles (Dean & Dalrymple, 2001). If the threshold of motion is exceeded, entrainment of sediment, and subsequent longshore transport, is induced (Davidson-Arnott, 2010). The rate of the littoral drift is usually defined as volume sediment transported per unit time (U.S. Army Corps of Engineers, 1984), denoted Q_{lst} in this study. When considering the impact on the shoreline evolution due to erosion and accretion, the rate of the transport is preferably given for a longer period of time, commonly as the annual transport. The annual gross transport, Q_G, is the instantaneous volumes transported during a year in both directions past a given point. It is the summation of transported sediment to the right, Q_R, and to the left, Q_L.

$$Q_G = Q_R + Q_L \tag{2.2}$$

Similarly, the annual net transport, Q_N, can be generated from the difference between the opposing transport volumes (Davidson-Arnott, 2010).

$$Q_N = Q_R - Q_L \tag{2.3}$$

The net transport informs of the balance between transported volumes as well as the dominating direction of transport. This is crucial for understanding the dynamics of a specific area and when evaluating the shoreline evolution. A larger output of sediment from the system than input of sediment, will induce a retreat of shoreline. Similarly, a larger input than output will advance the shoreline (Figure 2.3). Of course, interannual variations of littoral transport can be large, thus it can be important to not rely solely on a single value of annual transport (Dean & Dalrymple, 2001; U.S. Army Corps of Engineers, 1984).

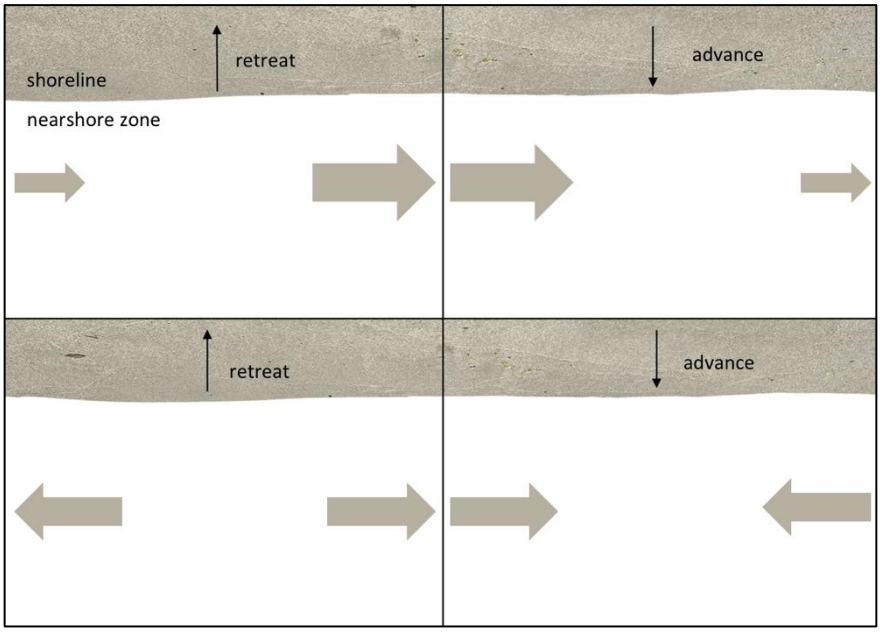

Figure 2.3. Schematic image showing two modes of retreat and advance of shoreline, depending on the direction and magnitude of the longshore transport.

2.3.4 Cross-shore Sediment Transport

As mentioned previously, the instantaneous motion of a particle often has a longshore direction as well as a cross-shore, both contributing extensively to the formation of the coastline. Transportation of sediment on-offshore is primarily driven by water motions due to the waves and the resulting undertow, a current driven by an off-shore directed pressure gradient. Compared to the longshore transport that typically engenders a long-term impact, the cross-shore transport can cause a slow change as well as a rapid transformation where a storm can change the formation of the beach significantly in the order of a few hours (Dean & Dalrymple, 2001). The on-offshore transfer of sediment is largely responsible for variations of the beach profile outline as well as the existence of sandbars (Komar, 1976).

Sea Level Rise

Sea levels are expected to rise as a consequence of the ocean's response to climate change. Thermal expansion of the oceans and melting ice caps are projected to accelerate the response (IPCC, 2019). A rise in sea level, either gradual or rapid through storm surges, increases the water depth throughout the surf zone. As the sea level rises, the beach profile will respond by redistributing sediment to reach equilibrium (Dean & Dalrymple, 2001).

One of the common ways of estimating the shoreline response to sea level rise is through the use of the *Bruun rule*. The Bruun rule predicts a landward displacement of the beach profile, in response to a rise in sea level. Further, it assumes that the shape and mass of the beach profile is maintained through the rise (and fall) of sea level, while sediment is redistributed across the profile (Masselink & Gehrels, 2014).

2.4 Beach Morphology

Beaches are dynamic systems comprised of unconsolidated sediments that have been transported and deposited by wave motion, currents, and wind-induced motion (aeolian deposits) (Davidson-Arnott, 2010). The characteristics of a beach are, thus, governed by factors such as soil composition, wave climate and sediment transport. A beach serves as a buffer for near-shore infrastructure by dissipating wave energy, the ability of which is determined by the shape and availability of sediment, i.e. the loss and gain of sediment (Komar, 1976). The loss or gain of sediment can be either short-term, affected by the seasons or long term-changes determined by permanent erosion and accretion.

2.4.1 Seasonal Changes

Seasonal variability of beach profiles is driven by the beach's response to wave forcing, where it strives to dissipate wave energy as efficiently as possible by changing its shape. Ultimately, the beach tries to reach an equilibrium with the wave energy, causing the profile to shift with the ever-changing wave energy governed by wind climate. The most dramatic changes in wind conditions occur between storms and calm weather (U.S. Army Corps of Engineers, 1984) or between winter and summer. The beach can be described by either a storm profile or calm weather profile (Figure 2.4). During storms, high energy waves erode the berm and transport and deposit sediment across the lower part of the profile, forming one or several bars (Komar, 1976). If undisturbed by other changes, such as man-made structures, the beach normally recovers to its original state during calmer weather (Nyberg et al., 2020), where sediment will be redeposited onto the beach plain to reform the berm (Komar, 1976). A storm profile will typically have a narrower beach plain with a gentler beach face slope, whereas a calm weather profile has a wider beach plain and steeper beach face slope (U.S. Army Corps of Engineers, 1984).

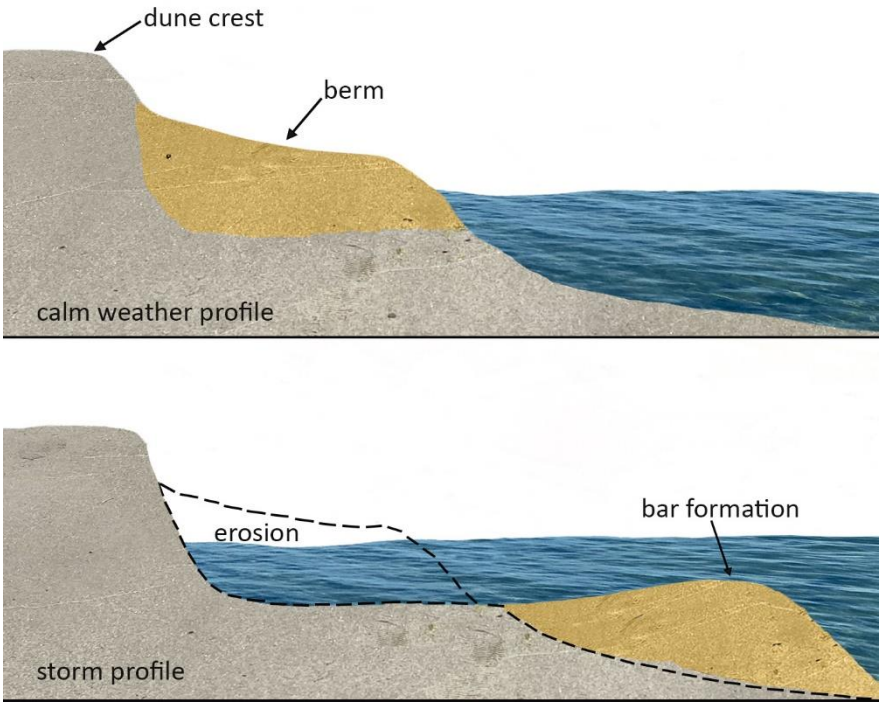

Figure 2.4. Calm weather and storm profiles. Modified from U.S Army Corps of Engineers (1984).

2.4.2 Long-term Variability

Beaches are also affected by long-term net loss and gain of sediment, which can be either man-induced or natural. Man-induced causes include altering the coastal area by building sediment trapping constructions, which hinders it from reaching other beaches, while widening another area. Dredging harbours, fortifying eroding cliffs or building dams in rivers also interferes with natural sources of sediment. Natural causes of long-term shoreline variability include rising sea levels, increasing frequency of storm events and longshore sediment transport. All these events lead to the increased transport of sediment in the coastal area, consequently leading to a long-term retreat of the shoreline (U.S. Army Corps of Engineers, 1984).

2.4.3 Shoreline Change

Estimating the longshore sediment transport, in terms of annual rate and direction, can have several practical applications. One of the main purposes is to predict shoreline change in order to plan and design mitigating structures or other measures (Bayram et al., 2007).

One way of estimating the rate of shoreline change is through the use of digitized shorelines from historical aerial photos (Dean & Dalrymple, 2001). Although this provides information regarding how the shoreline has varied between points in time, it does not reflect how the sediment has been relocated. Instead, measurements of actual sediment rate can be carried out in the field, usually designed to either determine an instantaneous rate or provide measurements for a longer stretch of period. A common method to obtain the direction and magnitude of transport rates is to utilize a sediment tracer. Such experiment is usually constructed using sediment of similar characteristics that have been tagged and then monitored throughout their movement in the surf zone (Dean & Dalrymple, 2001). Further, the direction

of transport, and to some length the rate, can be estimated by evaluating accretion or erosion of sand at coastal barriers. Man-made structures like pits and breakwaters can act as sediment traps and depending on where the entrapment of sediment occurs which could provide an inclination of the prevailing direction of transportation (Komar, 1976). In addition to artificial indicators, natural features might also provide an indication of direction as a diversion of a river mouth to either direction testifies to an existing net direction of transportation (Davidson-Arnott, 2010).

Transport Models

Wave parameters obtained either through wave-recording instruments or hindcasting, can provide correlation between the sediment transport rate and the longshore component of wave energy flux through developed transport models (Komar, 1976). By simplification of physical processes these formulas derive an estimation of the longshore transport using only relatively few and easily attainable input parameters (Davidson-Arnott, 2010). There are several equations that have been developed to obtain the longshore sediment transport. The most widely used equation was developed by the Coastal Engineering Research Center (CERC) and is usually referred to as the CERC equation (Bayram et al., 2007). It is also recommended by the Shore Protection Manual (SPM) (U.S. Army Corps of Engineers, 1984).

With the objective of improving the transport estimations, new models are constantly developed with an aim to simulate further influences on sediment transport. This requires additional parameters such as wave steepness, beach slope and sediment size or including several modes of transport. A more intricate model will require an increase in data, with no definite consensus on what model is most suitable, since they tend to perform differently and provide variated outcome depending on study site (Davidson-Arnott, 2010).

3 Description of Study Area

The area of study is limited to the coast of Ystad municipality. Ystad is situated in the south of Sweden and its coast encompasses around 40 kilometres (Figure 3.1). The coast is of high value to the municipality as there are many homes and holiday houses in the near beach areas. In addition, the sandy beaches attract tourists all year around and are a major source of income for local businesses (Skoog, 2008). The area has previously had problems with erosion (explained further in later sections) and the preservation of the coast is in the interest of the entire municipality. The following subsections will expand on the study area further, describing the current situation and previous protective measures that have been implemented in different areas. A description of the soil composition and the marine geology in the active profile will also be given. As previously mentioned, the seaward limit of the active profile coincides with the depth of closure, which in this region is approximately six metres (Fredriksson et al., 2017).

The coast of Ystad municipality is facing towards the southern Baltic Sea basin, which can be thought of as a semi-closed basin, as its only point of sea water exchange is at the narrow straits of Denmark. The coastal system can be categorised as a low-energy system since the change in water level due to tide can be considered negligible (SMHI, 2022) and the fetch is limited due to nearby landmasses that border the southern Baltic Sea.

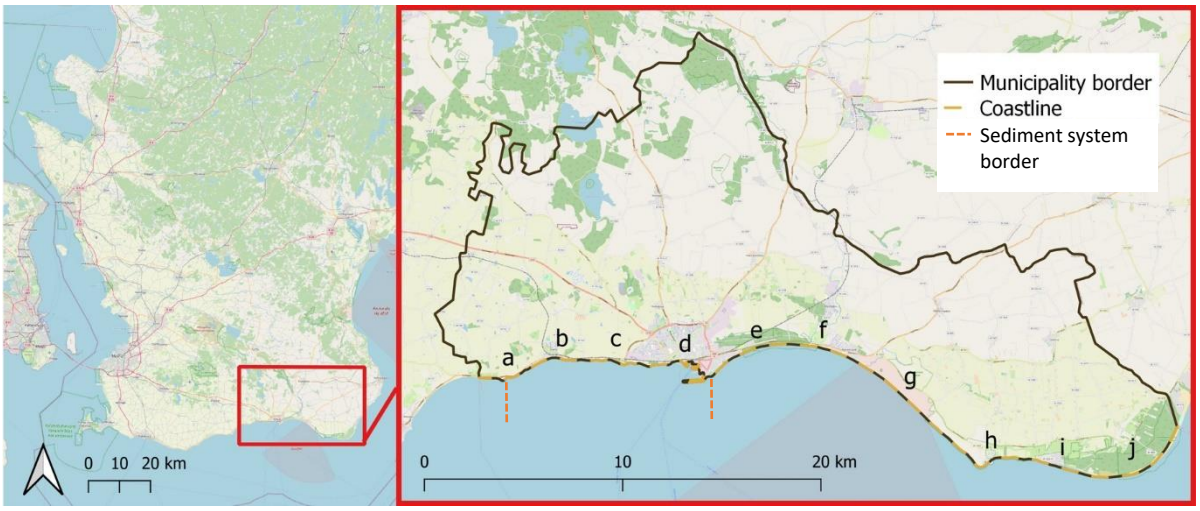

Figure 3.1. Location of the study area. Left image shows the south of Sweden, while the right image displays a close-up of Ystad municipality and the approximate location of the areas described below: a – West of Svarte, b – Svarte, c – Lilleskog, d – Ystad e – Ystad Sandskog, f – Nybrostrand, g – Hammars backar, h – Kåseberga, I – Löderups Strandbad and Hagestad, j – Sandhammaren. Data source: Swedish Geological Survey and OpenStreetMap.

The coast of Ystad municipality is divided into two sediment systems, divided to the right of Ystad harbour (Figure 3.1) (Nyberg et al., 2021). The marine sediment along the coast varies from soft clay to boulders. The western parts are dominated by cobbles and boulders, while the sand content increases when moving to the east with the greatest sand content outside of Sandhammaren (Figure 3.2). A more detailed description of the soil types and marine geology of the different locations along the coast can be found in appendix A1.

The wave climate also varies along the coast, with the majority of waves approaching from a south-west direction for all locations excluding Sandhammaren, which also has a high frequency of waves approaching from the east (Figure 3.3).

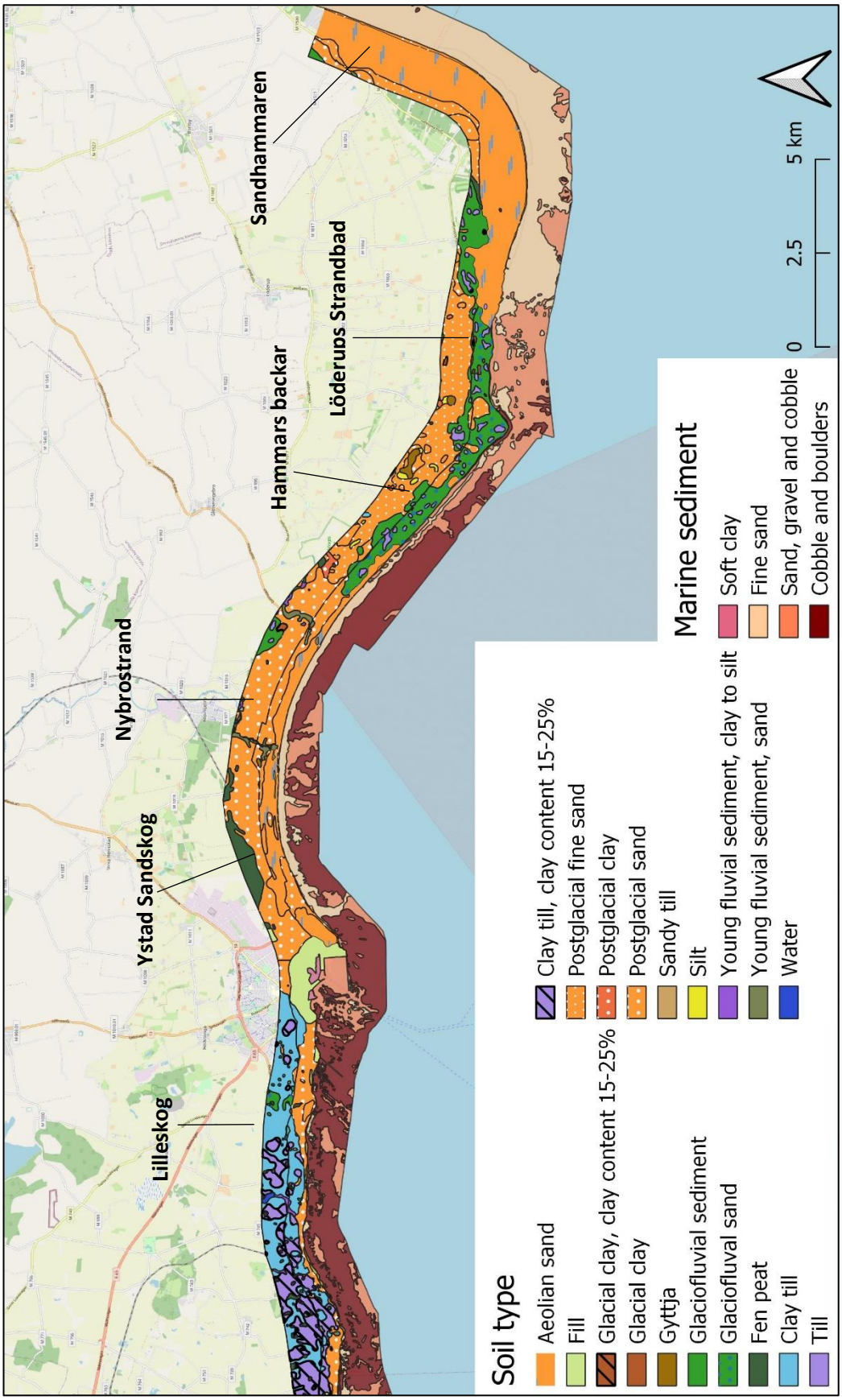

Figure 3.2. Soil composition and marine geology of the coast of Ystad municipality. Data acquired from the Swedish Geological Survey. The marine geology layer uses combined data from the topmost layer and the underlaying layer. Background map obtained from OpenStreetMap.

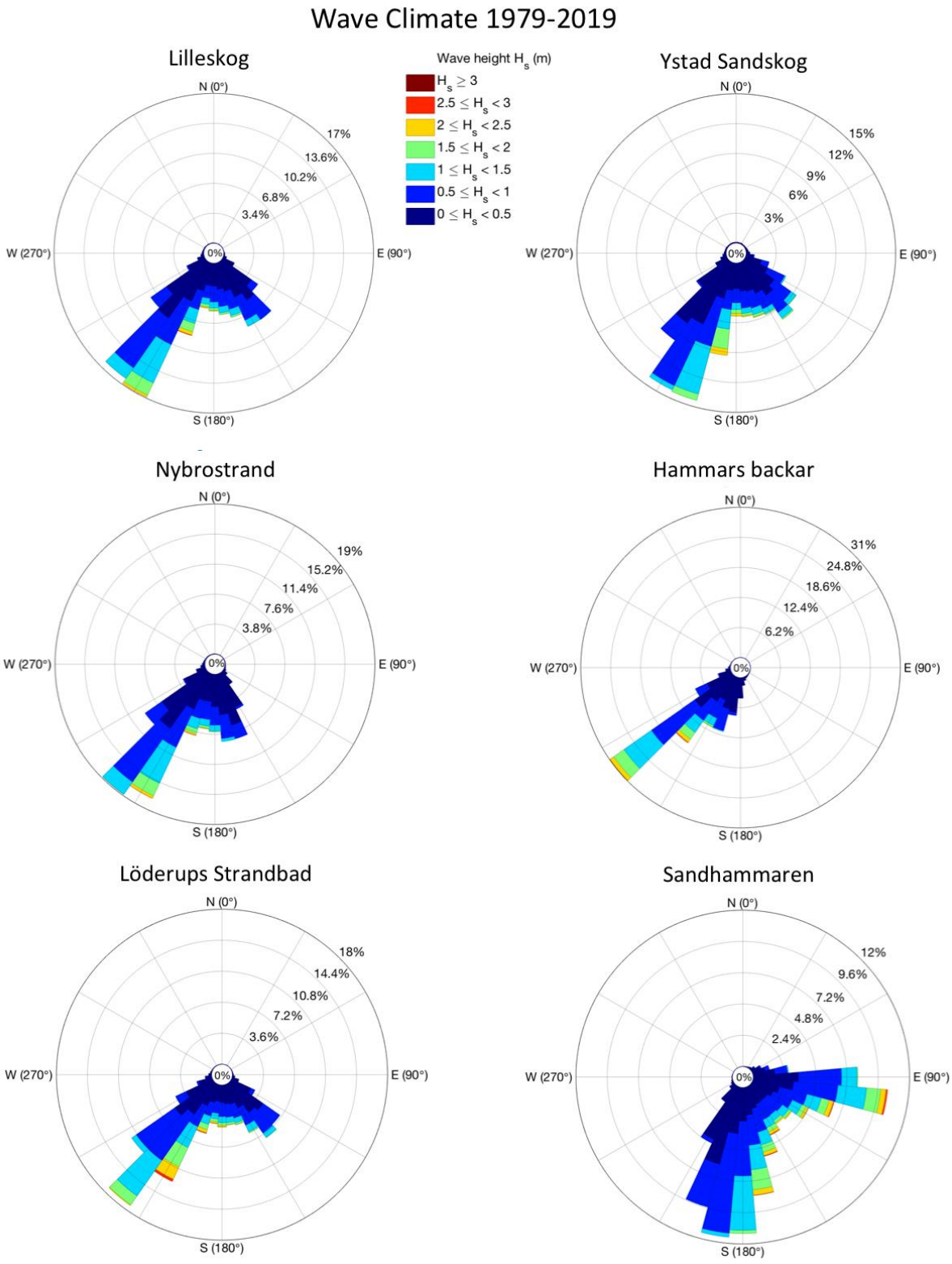

Figure 3.3. Wave roses from six points along the coast showing significant wave height, direction and frequency of incoming waves for the years 1979-2019 at six metres depth (Adell et al., 2021). Note that the wave roses have different frequency ranges.

Given that the coast is 40 kilometres long, the use and characteristics of the coast vary between locations. Table 3.1 below provides a summary of the characteristics of the locations denoted in Figure 3.1. Following the table is a further presentation of the locations describing the use and historical development, in terms of mitigating measures, of the coast.

Table 3.1. A summary of the characteristics of the coastal stretches in the municipality. Information regarding beach characteristics and protective measures obtained from Ystad Municipality (2018), marine sediment obtained from the Swedish Geological Survey, wave direction obtained from Adell et al. (2021) and shoreline orientation obtained from Lantmäteriet.

Location	Beach characteristics	Marine sediment	Dominant wave direction	Shoreline orientation	Protective measures
a) West of Svarte	Narrow and coarse-grained beach, farmland directly inland, **stable beach**	Cobble and boulders throughout active profile, small patches of sand	SSW 		No
b) Svarte	Narrow and flat, sand and coarse-grained beach at small community of Svarte otherwise farmland directly inland, **stable beach**	Cobble and boulders throughout active profile, small patches of sand	SSW 		Stone revetments by house owners
c) Lilleskog	Narrow and flat coarse beach, featuring some stretches of sandy beach, and some stretches of almost non-existing beach **active erosion**	Some fine sand close to shore followed by cobble and boulder and patches of sand and gravel	S and SSW 		Revetments and two groynes
d) Ystad	Sandy beach with recreational purpose, a harbour and water treatment plant, area around treatment plant has **slight erosion**	Cobble and boulder, sand and gravel in the harbour with small patches of clay	SW and SSW 		Slope stabilising construction, stone revetments

Location	Beach characteristics	Marine sediment	Dominant wave direction	Shoreline orientation	Protective measures
e) Ystad Sandskog	Sandy beach, popular for recreation, residential houses, **erosion**	Fine sand close to shore, gravel and boulders further offshore	SW and SSW 		5 groynes, 5 detached breakwaters, nourishment and fences
f) Nybrostrand	Sandy beach, residential houses, **stable beach**	Fine sand close to shore, sand and gravel furthest west, cobble and boulder in the east	SW and SSW 		No
g) Hammars backar *h) Kåseberga*	Narrow and coarse-grained beach, Kåseberga ridge located close to shoreline, **stable beach**	Fine and coarser sand close to shore, cobble and boulders further offshore	SW 		Concrete slabs in Kåseberga harbour
i) Löderups Strandbad and Hagestad	Sandy beach intersected with stone revetments, popular for recreation, **considerable erosion**	Coarser sediment in profile in the west, fine sand throughout profile furthest east	SW and SSW 		Groynes and breakwaters, revetments of rocks and boulders, nourishment
j) Sandhammaren	Wide sandy beach with large dune build-up, popular for recreation, **considerable accumulation**	Fine sand throughout active profile	Wide range from S to E 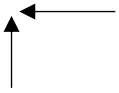		No

3.1 West of Ystad Harbour

This part stretches from the municipality border west of Svarte to Ystad harbour (a-d in Figure 3.1) and encompasses around 12 kilometres, which constitutes approximately 1/4 of the coast of Ystad municipality. There are several residential houses along the coast, primarily in Svarte and the western part of Ystad. The national road number 9 is considered a vital infrastructure and runs alongside the coast for almost the entire stretch. At several locations the road runs extremely close to the beach, no more than a few meters (Figure 3.4) and is considered at risk due to present erosion on the beach (Ystad Municipality, 2018).

Figure 3.4. Images of the beach on the western shore of Ystad. Left: Mixed sediment beach, close to a main road. Right: Revetment. Photo: Johanna Löwdin, 2020-11-17.

Ongoing erosion is present at several locations and causes a threat to the road as well as residential houses and recreational areas, such as sandy beaches. Some revetments have been installed as a measure to protect the shoreline (Figure 3.4) (Skoog, 2008).

3.2 Ystad Sandskog

Ystad Sandskog stretches from the outskirts of Ystad city, directly east of Ystad harbour, to Nybrostrand. The area holds several businesses and many holiday houses, as well as a large seaside hotel. Further, the national road 9, stretches alongside the coastline and at some locations it runs not more than 150 meters from the shoreline. The eastern part of Sandskogen is regarded to have a very high recreational value and nature worth preserving harbouring several highly regarded ecosystem services (Ystad Municipality, 2018).

3.2.1 Historical Shoreline Change and Protective Measures

Ystad Sandskog is subjected to erosion (Figure 3.5). Observations of erosion have been recorded throughout the last century, and digital shoreline analyses have established a 15-30m (+-15 m) withdraw of the shoreline dating back to 1940 (Ystad Municipality, 2018). Measures to prevent further erosion have since been implemented. In the 1950's groynes were placed perpendicular to shore in order to seize sediment transported along shore and stabilise the beach (Hågeryd et al., 2005). The groynes have since been fully refurbished and constructed to also serve as swimming docks during summer (Irminger Street et al., 2016). Today, five groynes are located at Ystad Sandskog, aligned from the hotel (Figure 3.5), and stretching about a kilometre along the beach. Further east, five detached breakwaters have been placed, serving the same purpose; to capture alongshore transported sand (Clinton Marine Survey, 2020).

Figure 3.5. Left: Erosion of sandy beach in Ystad Sandskog. Right: One of the groynes located along Ystad Sandskog. Photo: Johanna Löwdin, 2020-11-18.

During recent years the beach has been nourished, transporting large amount of sediment from an offshore sediment deposit, located outside of Sandhammaren, to replenish the eroded stretch. The beach has been nourished four times, 2011, 2014, 2017 and 2020 using between 55 000 and 80 000 m^3 of sand each time (Ystad Municipality, 2018, 2021), which has mainly been deposited between the groynes (Figure 3.6) (M. Skoog, personal communication, 2022). This has been successful in both preventing the shoreline from eroding further back, whilst also averting damage downstream as eroded sediment from the nourished stretch helps prevent erosion on stretches downstream.

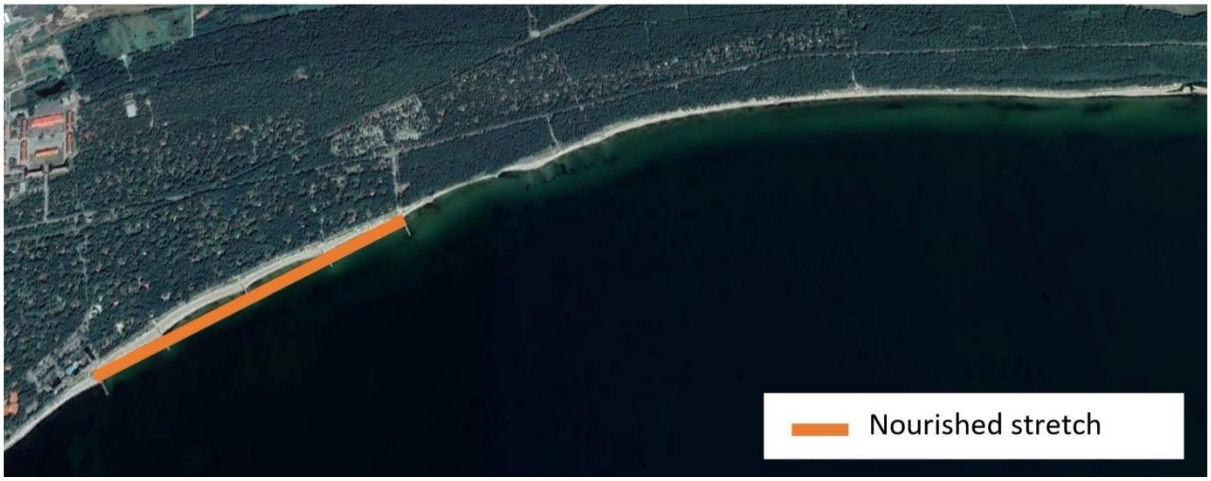

Figure 3.6. The nourished part of Ystad Sandskog. Satellite image from GoogleEarth, 2019.

3.3 Nybrostrand

The beach is confined between two rivers, the river mouth of Nybroån in the west and river mouth of Kabusaån east of the community Nybro. The community has a current population of approximately 600 people, consisting mainly of residential houses with some buildings located 40-50 meters from the water. The municipality believes there are great prospects for further exploitation. It also holds a campsite in the western part and a small area of vegetation close to the beach that is appreciated for recreational purposes. The national road 9 runs through the community (Ystad Municipality, 2018).

3.3.1 Historical Shoreline Change and Protective Measures

Analyses of historical photographs of shoreline and empirical observations have shown that this area is both subjected to erosion and accumulation at a similar rate, meaning that the beach can naturally recuperate from erosion. This leads to overall stable conditions for the beach (Ystad Municipality, 2018). Parts of the beach, however, widened 20 meters since 1956/1957 and 2001 (Hågeryd et al., 2005). Figure 3.7 shows the results of accumulation and dune build-up, where a fishing hut is partly covered by sand.

Figure 3.7. Left: Sandy beach in the eastern part. Right: Structure almost covered by dune build-up. Photo: Johanna Löwdin, 2020-11-18.

3.4 Kabusa Military Field, Hammars Backar and Kåseberga

The Kabusa military field has in general a flat topography and is traditionally used for cattle grazing. The landscape grows considerably hillier to the east where the flat field transitions into the Kåseberga ridge at the nature reserve of Hammars backar. The ridge continues to the east past the village of Kåseberga, which is located at the base of the ridge on the seaward side. The ridge is situated right at the water edge past Hammars backar and Kåseberga bay, due to erosion, creating a height difference between the beach and crest of 30-40 meters. The beach itself is narrow and coarse-grained (Ystad Municipality, 2018).

3.4.1 Historical Shoreline Change and Protective Measures

The coastal stretch between Kabusa and Kåseberga has in general been classified as stable. The stretch has previously been eroded, depleting the beach of fine sediment, and leading to a coarser coastline, creating a natural defence against further erosion (Skoog, 2008). There are some areas that have experienced some accumulation and some that have been eroded, although protective measures have only been seen as necessary in Kåseberga harbour, where concrete slabs have been added to the slope of the road leading down to the harbour.

3.5 Löderups Strandbad

Löderups Strandbad is located directly east of Kåseberga bay at the base of Kåseberga ridge and is comprised mainly of holiday homes, which are located all the way up to the waterfront (Ystad Municipality, 2018). Löderups Strandbad is one of the most eroded areas in Sweden, where several hundred meters of land has been lost (Figure 3.8) (Nyberg et al., 2020).

East of Löderups Strandbad there is a nature reserve called Hagestad, which is of great recreational value and also holds a popular beach and camping site (Ystad Municipality, 2018).

The area has been affected by the erosion occurring in Löderups Strandbad, leading to a shoreline withdrawal of around 85 meters between the years 1999 and 2010 (Irminger Street et al., 2016).

Figure 3.8. Left: Erosion at the campsite east of Löderup. Right: Revetment at Löderup beach. Photo: Johanna Löwdin, 2020-11-19.

3.5.1 Historical Shoreline Change and Protective Measures

Erosion in this area was first notice in the 1940s and has been a problem since then, leading to loss of beach sediment and undermining of structures, consequently resulting in the loss of several homes. To mitigate these effects, in 1959, a 40-meter-long row of piles were driven into the sediment along the shore and were filled with rocks and branches. The erosion continued and during the 70's, breakwaters and groynes were constructed to stop the loss of sediment (Almström & Hanson, 2014). Homeowners in the area also continued to fortify their beachward borders with rocks and boulders (Figure 3.8), inadvertently moving the erosion eastward along Löderups Strandbad. At most, around 200 metres of beach have been eroded since 1940 (Irminger Street et al., 2016). During the 90's six groynes were constructed in the area to mitigate the erosion and trap sand in the area. This proved to be insufficient, and the beach was therefore nourished during the same events as for Sandskogen, adding between 15 000 – 27 000 m^3 sand per event (Ystad Municipality, 2018) at two points along the beach (Figure 3.9).

Figure 3.9. The parts of Löderups Strandbad that were nourished during 2020 (Skoog, 2020). Satellite image from GoogleEarth, 2019.

3.6 Sandhammaren

Sandhammaren makes up the most eastern part of Ystad coastline, and the most south-eastern part of Scania, where the shoreline curves northwards. The area is limited by the nature reserve in the west and the municipality border in the north-east. The area is known for its wide sandy beaches (Figure 3.10) and is a popular recreational site. Sandhammaren stretches is around five kilometres with beaches up to 200 metres wide, made up with dunes created by aeolian deposits (Ystad Municipality, 2018).

Figure 3.10. Sandhammaren beach with its wide fine grained beach plane to the left and the edge of the dunes on the right. Photo: Johanna Löwdin, 2020-11-20.

3.6.1 Historical Shoreline Change and Protective Measures

The shoreline in Sandhammaren has both experience erosion and accumulation. Between 1971 and 2001, the beach widened with over 100 meters. Orthophotos of the shoreline in 1956 show that the beach was wider then, than in 1971, meaning that erosion was dominating during those years and the beach has since begun to build back up (Hågeryd et al., 2005).

4 Methods and Data: Potential Longshore Transport Rate Modelling

4.1 CERC model

The CERC model is an empirical bulk formula based on the assumption that the longshore sediment transport rate is proportional to the longshore wave power per unit beach length (Bayram et al., 2007; Mil-Homens et al., 2013). The equation assumes that transport is only dependent on wave-induced currents and does not account for other mechanisms such as wind-induced currents or the influence of grain size or beach slope (Bayram et al., 2007; E. R. Smith et al., 2009). The CERC model is given by

$$Q_{lst} = \frac{\rho K \sqrt{\frac{g}{\gamma_b}}}{16(\rho_s - \rho)(1 - P)} H_{sb}^{2.5} \sin(2\alpha_b) \tag{4.1}$$

where Q_{lst} is the potential sediment transport rate, K is an empirical coefficient, ρ is the sea water density, ρ_s is the sediment density, g is the acceleration due to gravity, γ_b is the breaker index, P is the sediment porosity, H_{sb} is the significant wave height at breaking and α_b is the wave angle at breaking (U.S. Army Corps of Engineers, 1984). A positive transport rate is defined as transport to the right when looking seawards from shore and a negative transport rate is defined as transport to the left. In this study, positive and negative rates indicate western and eastern transport, respectively and Q_{lst} is presented in cubic metres per year (m^3/year). In Table 4.1 below, the values for the input parameters, excluding breaking wave conditions, are presented.

Table 4.1. Values of input parameters to the CERC model.

Input parameter	Value
ϱ	1025 kg/m^3
ϱ_s	2600 kg/m^3
g	9.81 m/s^2
P	40 %
γ_b	0.78

As mentioned previously, the CERC model does not account for mechanisms such as wind-induced currents or beach specific conditions such as slope or grain size. It does, however, include a transport coefficient K, that can be chosen to reflect influences on transport rate. The SPM (U.S. Army Corps of Engineers, 1984) recommends a value of 0.39 when using significant wave height (H_s). The transport coefficient should, however, preferably be calibrated against observations.

By assuming straight and parallel bottom contours, and using offshore wave conditions as input parameters, the significant wave height and angle at breaking can be obtained by using the conservation of wave energy flux (Equation 4.2) and Snell's law (Equation 4.3).

$$H_{s0}^2 C_{g0} \cos\alpha_0 = H_{sb}^2 C_{gb} \cos\alpha_b \tag{4.2}$$

$$\frac{sin\alpha_0}{C_0} = \frac{\sin \alpha_b}{C_b} \tag{4.3}$$

where H_s is the significant wave height, C_g is the group velocity, C is the phase velocity and α the wave angle. The subscripts 0 and b denotes the offshore point and breaking point, respectively.

The CERC model is applied through a FORTRAN-program written by the Division of Water Resources Engineering at Lund University of Technology. Further input is required in the form of significant wave height, peak period, wave direction and shoreline orientation.

Offshore wave parameters were obtained using the third generation SWAN (Simulating WAves Nearshore) spectral model (Booij et al., 1999), which generates and propagates waves towards the shore. The model uses wave data obtained from Adell, et al. (2021) from the period 1979-2019 and constitutes wave climate parameters H_s and wave direction from 137 points along the coast at six meters depth with 3h resolution. Using Equations 4.2 and 4.3 the waves were then propagated to the breaking point to obtain breaking wave conditions to use as input for the CERC model.

4.1.1 Calibration

The calibration of the model coefficient K was done by comparing predicted shoreline change of the coast of Ystad, obtained using the CERC model, with observed values for the historical shoreline change. The observed shoreline change rates used for the calibration in this project were obtained from Fredriksson et al. (2017), who used digitized vegetation lines from orthophotos from the years 1960 and 2012 to compute End Point Rate (EPR) which is a measurement of the shoreline change movement in metres per year (Equation 4.4) (Himmelstoss et al., 2018).

$$EPR = \frac{distance\ in\ m\ between\ oldest\ and\ youngest\ shoreline}{time\ between\ oldest\ and\ youngest\ shoreline} \tag{4.4}$$

The predicted longshore transport rates used in the comparison with the observed data was computed using the CERC model. The coastline was smoothed using QGIS and stretches of coastline were chosen based on the following criteria: they had to be relatively uniform, they had to be continuous without hard structures, their shoreline orientation had to be relatively uniform, and all stages (eroding, accumulating, stable) should be represented in the selection. With EPR$\leq$|0.5|m/yr regarded as stable and a stretch with EPR$<$0.5 m/yr considered eroding and EPR$>$0.5 m/yr defined as accumulating (see Figure 4.1), this resulted in six stretches matching the criteria, which were used to calibrate K.

Figure 4.1. The coast is divided into categories (eroding, stable, accumulating) based on EPR values obtained from Fredriksson et al. (2017). Background map ©Swedish Geological Survey.

Two stretches are in the eastern part of Ystad Sandskog, two stretches in Hagestad and two stretches in Sandhammaren (Figure 4.1). Transport gradients for each stretch were created by taking the difference in annual net sand transport between the starting and end point of the stretch (Figure 4.2). The gradient ($\Delta V_{LST}/\Delta t$) for each stretch was then converted into shoreline change ($\frac{\Delta x}{\Delta t}$) by dividing with the length of the stretch (Δy) and height of the active profile ($D_c + D_b$) according to Equation 4.5.

$$\frac{\Delta x}{\Delta t} = \frac{\Delta V_{LST}/\Delta t}{\Delta y * (D_c + D_b)} \tag{4.5}$$

where D_c is the depth of closure and D_b the maximum height of the beach plain above mean sea level, which is estimated to 2 meters (Fredriksson et al., 2017).

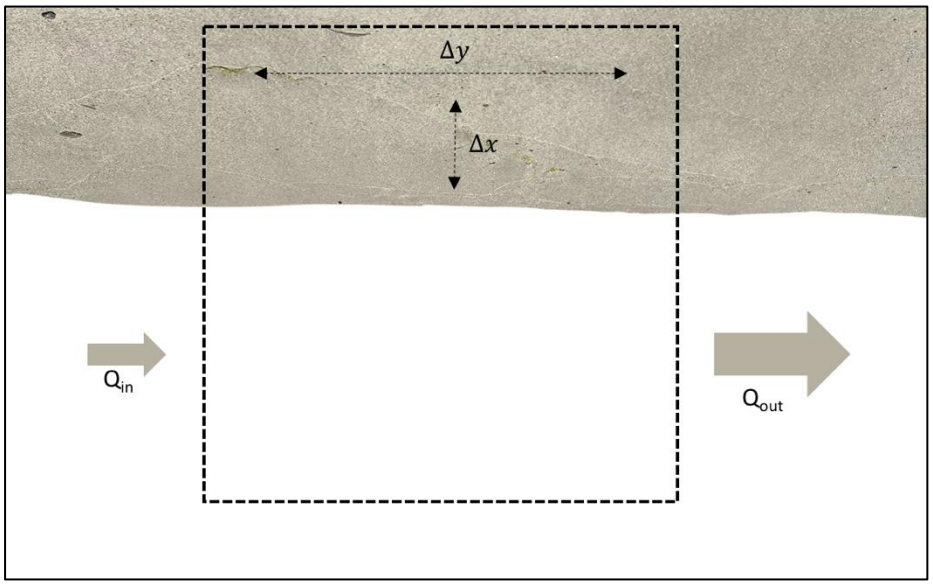

Figure 4.2. Longshore sediment transport along a specified stretch of coast (Δy). The net sediment transport (Q_{in} - Q_{out}) causes a gradient and consequently a response in shoreline change (Δx).

To compare the predicted values with EPR, the average observed shoreline change for each stretch was used as a representative value. The fit of each calibration was then evaluated using root mean square error (RMSE), which is a measure of the deviation of the prediction errors.

4.1.2 Model Setup

Only the eastern shore of Ystad was used when running the model, as the western shore, to a great extent, consisted of coarse material or boulders with few sandy stretches. The CERC model was applied to datapoints situated approximately every 200 meters along the shore, which resulted in estimated net transport rates for the years 1979-2019. The shoreline was then divided into stretches with an orientation representative for the section with start and end point near the datapoints. Using the same method as during calibration, the net transport was used to create new transport gradients to calculate the estimated shoreline change in meters per year. The performance of the model was then evaluated using RMSE. Additionally, a sensitivity analysis was conducted to determine the immediate impact of the orientation on the potential longshore transport using CERC.

4.2 Bayram Model

To further analyse the CERC model performance, it was compared to another commonly used method in predicting longshore sediment transport rate; the Bayram formula (Bayram et al., 2007). It shares the basic premises with CERC, accounting for the longshore component of the wave-energy as directly correlated to the longshore transport. CERC, however, only accounts for wind-generated currents whereas the Bayram model considers that the breaking of waves is required to stir up and mobilise sediment to subsequently be transported by different modes of currents. Further, it assumes that the sediment remains in suspension, maintaining an average concentration distribution in the surf zone (Bayram et al., 2007). The Bayram model can be written according to Equation 4.6.

$$Q_{lst} = \frac{\varepsilon}{(\rho_s - \rho)(1 - P)w_s g} F\bar{V} \tag{4.6}$$

where ρ is the sea water density, ρ_s is the sediment density, g is the acceleration due to gravity and P is the sediment porosity. F is a fraction of the flux energy, and when considered oblique incident waves the fraction is expressed by

$$F = E_b C_{gb} cos\alpha_b \tag{4.7}$$

$$E_b = \frac{1}{8}\rho g H_b^2 \tag{4.8}$$

$$C_{gb} = \sqrt{g\frac{H_b}{\gamma_b}} \tag{4.9}$$

with E_b representing the energy per unit crest width, C_{gb} is the group velocity and $cos\alpha_b$ is the incident angle. γ_b is the breaker index. The subscript b denotes breaking point.

Further, in Equation 4.6 ε is a non-dimensional transport coefficient that expresses the efficiency of the waves in keeping sediment grains in suspension, making use of the peak wave period T_p and the settling velocity w_s.

$$\varepsilon = \left(9 + 4\frac{H_b}{w_s T_p}\right) \tag{4.10}$$

The settling velocity is also present in Equation 4.7, where the amount of work needed to keep the sediment in suspension is accounted for by the product of the concentration and the submerged weight with fall speed velocity w_s, thereby introducing the effect of the sediment grain size (Bayram et al., 2007). The equations used to derive w_s (Equations 4.11, 4.12 and 4.13) were developed by Ahrens (2000) for natural sand particles.

$$w_s = \frac{\nu}{d_{50}}\left(C_1 D_{gr}^3 + C_2 D_{gr}^{1.5}\right) \tag{4.11}$$

$$C_1 = 0.055tanh\left[12D_{gr}^{-1.77}\exp\left(-0.004D_{gr}^3\right)\right] \tag{4.12}$$

$$C_1 = 1.06tanh\left[0.016D_{gr}^{1.5}\exp\left(-\frac{120}{D_{gr}^3}\right)\right] \tag{4.13}$$

With d_{50} denoting the mean grain size and v is the kinematic viscosity of water. D_{gr} is the effective diameter of the grain size and expressed in Equation 4.14 below.

$$D_{gr} = d_{50}\left(\frac{g\left(\frac{\rho_s}{\rho} - 1\right)}{v^2}\right)^{\frac{1}{3}} \tag{4.14}$$

The current has been estimated to a representative mean current, $\bar{V}$ (Equation 4.15), calculated with the use of specific wave and beach profile characteristics. The friction coefficient c_f is set to be constant.

$$\bar{V} = \frac{5}{32}\frac{\pi\gamma_b\sqrt{g}}{c_f}A^{\frac{3}{2}}sin\alpha_b \tag{4.15}$$

The shape parameter, A (Equation 4.16), is derived using a formula appropriate for sandy beaches (Kriebel et al., 1991).

$$A = \frac{9}{4}\left(\frac{w_s^2}{g}\right)^{\frac{2}{3}} \tag{4.16}$$

Input parameters can be found in Figure 3.3, excluding breaking wave conditions. Parameters used in both CERC and Bayram calculations are the same.

Table 4.2. Values of input parameters to the Bayram model.

Input parameter	**Value**
ϱ	1025 kg/m^3
ϱ_s	2600 kg/m^3
g	9.81 m/s^2
P	40 %
γ_b	0.78
v	1.3*10^{-6} m^2/s
c_f	0.01

4.2.1 Model Setup

The same data and range as used for CERC, with regards to wave height, peak period and angle of incident wave. Additionally, the parameter d_{50} denoting grain size of sediment, was added to the data set. This information was collected during the field survey (see section 5.1.2). The Bayram formula was applied to all sample locations and computation was made using MATLAB with the annual net transport rate derived at each location. These were then used to form ten transport gradients to evaluate the performance of the model and compare with CERC, using end point rate and RMSE.

5 Methods and Data: Field Measurements

5.1 Methodology

Field data collection was performed along Ystad shoreline between the 16th and 20th of November in 2020. This was mainly done to gather site-specific information about the beaches to make correlations between beach characteristics and calculated transport patterns.

Wind conditions at the time offered moderate wind that increased in strength throughout the week, ultimately reaching wind gusts exceeding 20 m/s. Since no wind gage is available in Ystad, measurements from Skillinge were considered adequate to represent the wind conditions along the coast. Water level measurements were retrieved directly from outside of Ystad harbour. The water level shifted in time, deviating significantly on the 20th of November, while otherwise mostly staying below or in line with the mean water level for Ystad at 15.7 cm (Figure 5.1) (SMHI, 2021).

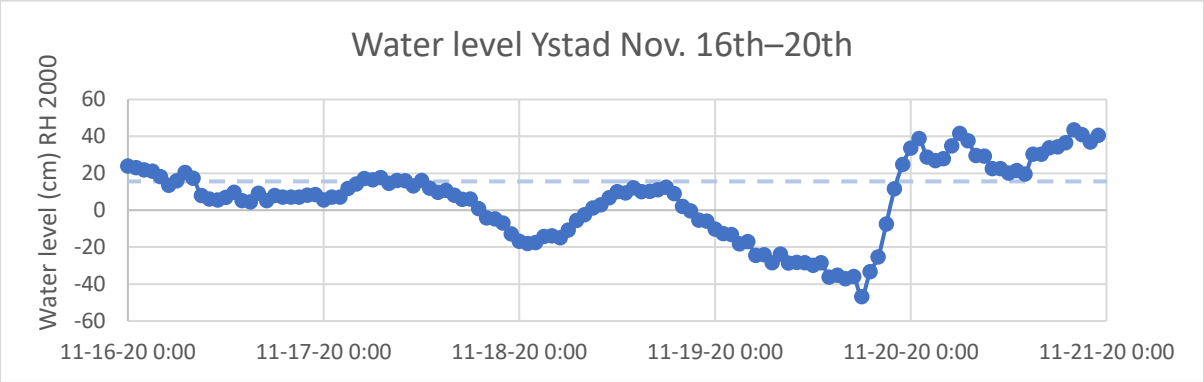

Figure 5.1. Water level and mean water level in Ystad during the time of field measurement. Water level expressed in the RH 2000 reference system (SMHI, 2021).

5.1.1 Beach Profiles

Beach profiles were measured using RTK-GPS (Figure 5.2), beginning above the vegetation line, and extending approximately 10-30 metres into the water, depending on water depth and wave conditions. In total, 60 beach profiles were measured; 25 on the western shore and 35 on the eastern shore (see Figure 5.4 – 5.6).

Figure 5.2. Measuring the beach profile seawards using the RTK-GPS. Photo: Johanna Löwdin, 2020-11-18.

The measured beach profile was used to derive the beach face slope of each profile. A full record of the measured beach face slopes can be found in appendix A2.

5.1.2 Sediment Sampling

Bascom (1951) suggested a standardised method of gathering sediment data for comparison between grain size and beach face slope, which is widely used. The sediment sample should be taken from a point midway between the berm crest and swash zone, where the grain size has small temporal variations and can be used in comparisons as it can be used as a representative grain size for the beach. This point is noted as the "Bascom reference point". Seaward of this point, grain sizes are typically finer, although coarser at the plunge point, and landward it can be either finer or coarser, with the finest sediment found in the dunes.

Sand samples were collected from the Bascom reference point from every beach profile. Although the evident existence of a berm crest varied along the coastline, there was usually some indication of a berm. Figure 5.3 shows a thread of seaweed just before the beach flattens, which helped estimate the location of the Bascom point.

Figure 5.3. Beach stretch at Nybrostrand. The Beach profile shows a linear slope followed by deposition of seaweed which marks a change of the slope where the beach forms a horizontal platform landward. Photo: Johanna Löwdin, 2020-11-18.

The top 3-5 centimetres of the sediment were scraped off and the sample was then taken from the top decimetre using a plastic cup. Approximately two decilitres of sediment were collected from each sampling point. The sediment samples were dried overnight in an oven set to 105 degrees Celsius. 200 grams of each sample was then sieved using stacked woven wire mesh sieves ranging from 0.063 – 2 mm. The sieve stack was shaken to separate grain sizes and the trapped sediment on each sieve was then weighed and recorded. Median grain size (d_{50}) and sorting (σ) was then calculated where d_{50} is the 50th percentile, meaning that 50% of the sediment sample is coarser than the median grain size. Sorting was found using the fraction of the 84th and 16th percentile as seen in Equation 5.1 below.

$$\sigma = \frac{d_{84}}{d_{16}} \tag{5.1}$$

For a full record of sediment characteristics, see appendix A2.

Figure 5.4. Locations of beach profile measurements and sediment sampling on the western shore of Ystad. Background map ©OpenStreetMap.

Figure 5.5. Locations of beach profile measurements and sediment sampling on the eastern shore of Ystad from Sandskogen to Nybrostrand. Background map ©OpenStreetMap.

Figure 5.6. Locations of beach profile measurements and sediment sampling on the eastern shore of Ystad from Löderups Strandbad to Sandhammaren. Background map ©OpenStreetMap.

6 Results and Discussion: Longshore Sediment Transport

6.1 CERC model

6.1.1 Sensitivity Analysis

To assess how a difference in shoreline change impacts the transport rate and, by extension, the calculated gradients and shoreline change, a sensitivity analysis was performed. The orientation was altered with +1, +2, +5 and +10 degrees, for ten transects along Nybrostrand (Figure 6.1). The other model input parameters remained unchanged. In Figure 6.1 the net sediment transport rates for the above-mentioned scenarios are shown.

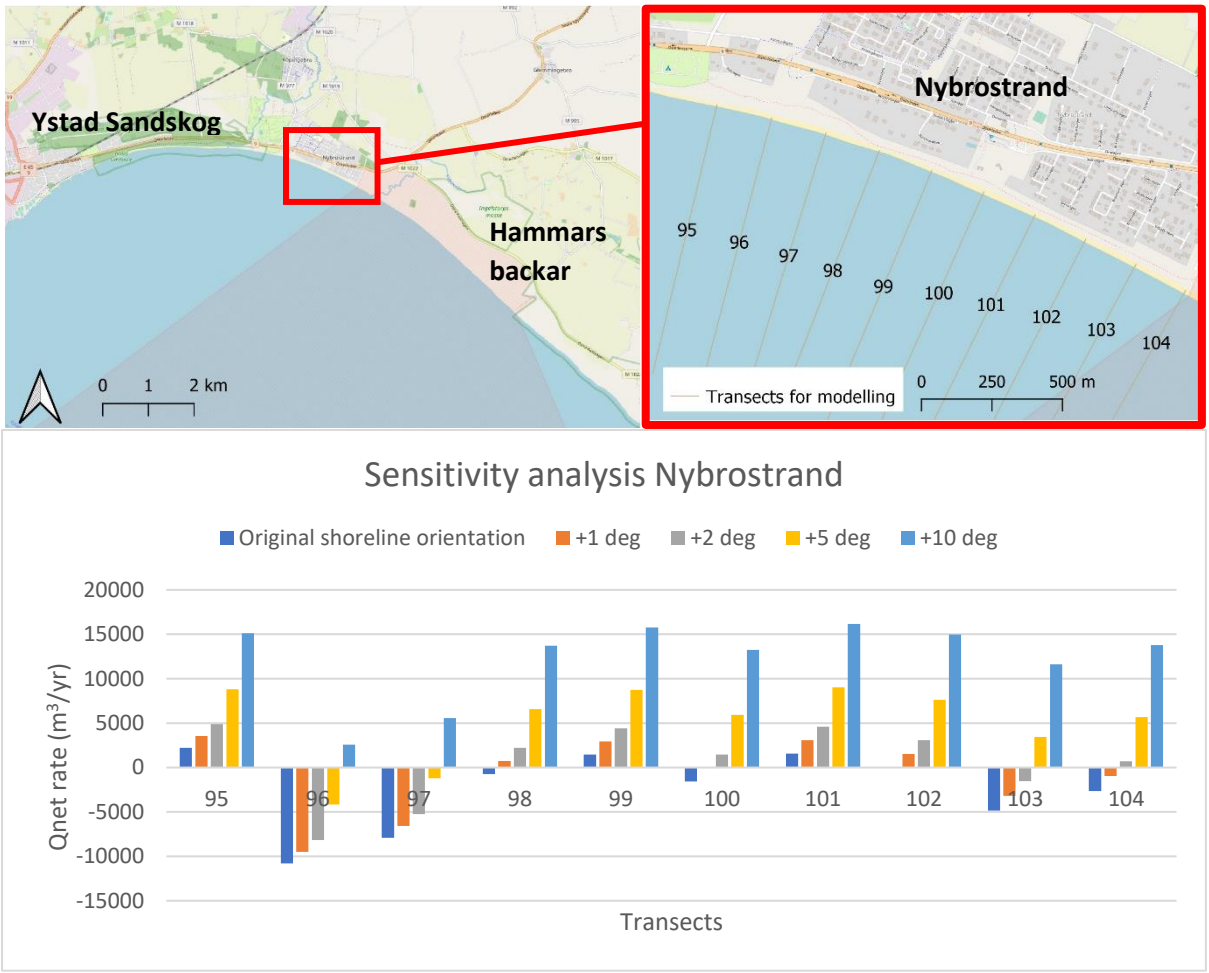

Figure 6.1. Top: Location of the transects used in the sensitivity analysis. Background map ©OpenStreetMap. Bottom: Outcome of analysis of model sensitivity to orientation. The graph shows the predicted transport rate for ten points along Nybrostrand when changing the orientation with +1, +2, +5 and + 10 degrees.

The analysis shows that the CERC model is sensitive to changes in the shoreline orientation. Altering the orientation by +1 degree results in a mean difference of transport rate of 109%, when measured in absolute values. This is influenced by a few outliers where the change, in percentage, is several thousands. A median value instead, results in a difference of approximately 10%. At six locations, the direction of transport changes. This is already observed at +1 degree, though occurring to a greater extent with increased alteration. How readily the model alters direction of transport depends on the angle and frequency of the approaching waves. In Nybrostrand the dominating angle of approach is close to parallel with

the shore, meaning that a small change in shoreline orientation can change the incoming wave direction from the left to the right, in reference to the beach. A location with a dominating angle of approach that is not close to being parallel with the shoreline, should be less sensitive to changes in shoreline orientation.

6.1.2 Transport Gradients and Calibration

During calibration, the recommended value of 0.39 was chosen as a starting point for the transport coefficient K. Ultimately, 0.018 was chosen as the best fit for the model.

When comparing the predicted shoreline change in meters per year with the observed change (Figure 6.2), the predicted change is greater in all cases except for three stretches in Sandhammaren and one stretch in Löderups Strandbad. At two stretches, 17 and 18, the predicted change is misdirected compared to EPR. At stretch 17, the predicted gradient indicates accumulation of approximately five meters per year, whereas the stretch erodes approximately three meter per year according to EPR. At stretch 18, the modelled transport rate predicts accumulation of just under one meter per year, while the observed value shows erosion of around two and a half meters per year. At seven locations the direction of the predicted and observed shoreline change match. The remaining stretches are considered stable by one of the methods (CERC and EPR) and either accumulating or eroding by the other. The discrepancy between predicted and observed values might partly be explained by the selection of gradients and the sensitivity CERC displays for the orientation, as discussed previously.

Calculating the RMSE of the predicted shoreline change compared to observed EPR values resulted in an RMSE of 6.7. Excluding the curved shoreline right before Kåseberga at Kåsehuvud improves the RMSE to a value of 3.0. The sensitivity analysis showed that CERC is sensitive to changes in coastal orientation, which could impact the transport rate and direction. At Kåsehuvud the shoreline orientation changes abruptly from a north-south to a west-east direction, although maintaining the wave climate. This could explain why the fit between the predicted and observed shoreline change here is affecting the overall RMSE negatively. Although the fit improved when excluding Kåsehuvud, the scatterplot in Figure 6.3 confirms a weak correlation between observed and predicted shoreline change with an R^2-value of 0.0174.

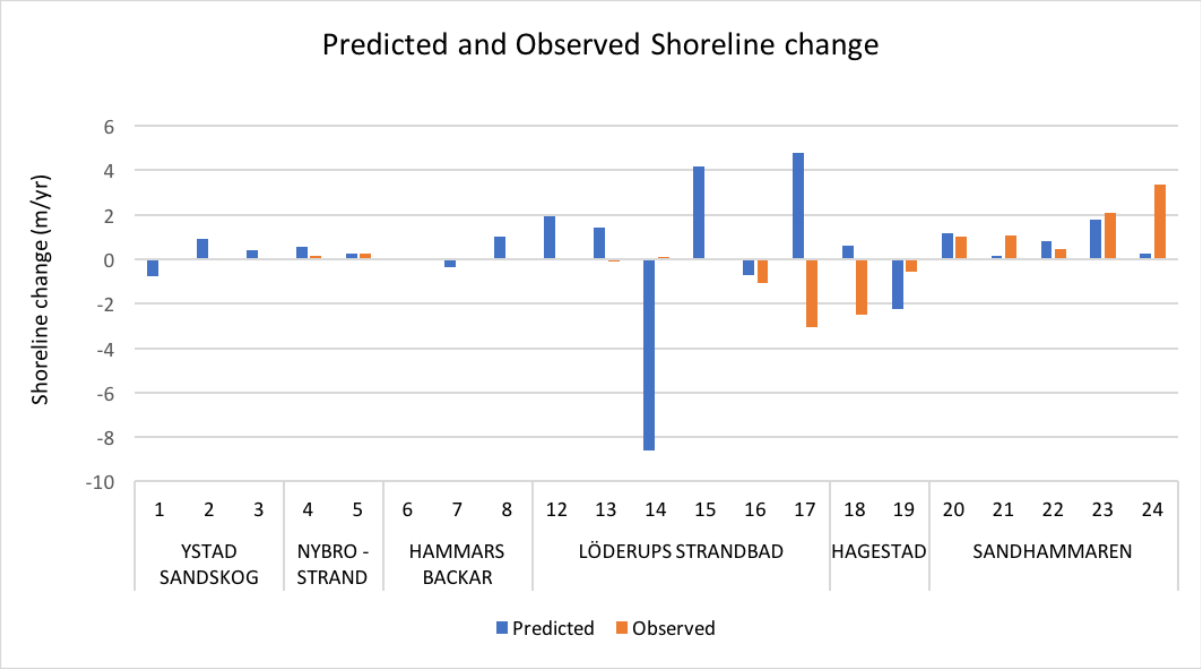

Figure 6.2. Predicted and observed shoreline change (m/yr) for 21 stretches along the eastern shore of Ystad, excluding the curved shoreline of Kåsehuvud.

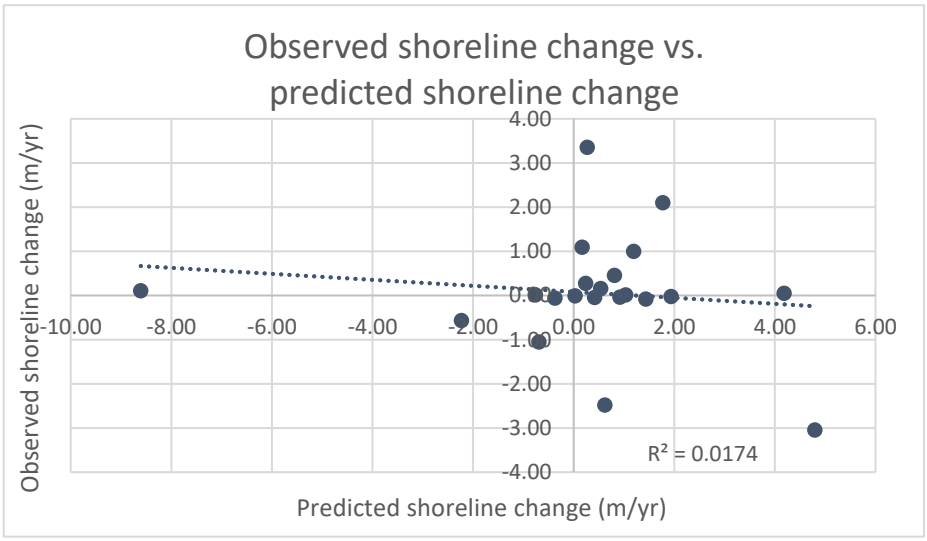

Figure 6.3. Observed shoreline change (m/yr) plotted against predicted shoreline change (m/yr) for the same stretches as shown in .

The calibrated transport coefficient could explain why a majority of the gradients display a larger predicted shoreline change than observed. Only six stretches were used for calibration, which were equally distributed along stable, accumulating and eroding beaches. Since a majority of the coast is defined as stable, according to the EPR, perhaps the stable stretches should have been taken into greater consideration, with additional stable stretches added during calibration. Further, the calibration was performed with regards to the entire coast, which consequently resulted in one transport coefficient being applied for the whole coast. By instead calibrating with regards to specific beach conditions, the transport coefficient would most likely change along the coast. Should the potential sediment transport be computed using different obtained values for K, this would more accurately depict the variation in transport

and beach conditions and possibly reduce the discrepancy between predicted and observed shoreline change. Calibrating for different sets of K was, however, difficult to accomplish given that the stretches considered appropriate for calibration were too few in this study.

Further, the calibration process is based on the observed values of the EPR, thereby assuming that there should be a direct correlation between the transport of sediment and the shoreline change, with the shoreline change being a result of the withdraw and succession of the vegetation line. Observations and measurements along the coast reveal that the loss of sediment is not equally distributed along the profile, instead a majority of the sediment is lost below the water line resulting in a less visible impact on the shoreline (Hanson, 2012). This suggests that, although large amounts of sediments are transported and lost, it might not have an immediate impact on the shoreline. This consequently results in a smaller EPR and possibly a too low estimation of the transport coefficient when calibrating for K. This would suggest that the model will underpredict the potential longshore transport in this area. In addition, nourishing events drive the shoreline seawards, such as in Ystad Sandskog west, which is considered stable as EPR is less than 0.5 m/yr, despite documented erosion from the past decades. Effects of nourishing events on EPR could, however, be considered negligible since EPR is based on changes of the vegetation line, which has a slow response (Fredriksson et al., 2017). Despite the slow response, the collective influence of anthropogenic impact, such as nourishment, groynes and revetments, on sediment transport, likely affects the rate of shoreline displacement. This could have a negative impact on the correlation between the sediment transport and the shoreline change.

When comparing with EPR, values for the predicted shoreline change were calculated using a simplified volume calculation. The depth of closure (D_c) and maximal height above mean sea level (D_b) were assumed to be the same for the entire coast. Using the hindcasted wave climate (Adell et al., 2021), a more specific D_c could have been calculated and applied. However, Fredriksson et al. (2017) consider the variance in D_b to be negligible, and perhaps the same can be said for D_c. Additionally, both the volume conversion and the CERC-model assume an unlimited supply of sediment. The composition and variation of available sediment across the active profile and between beaches is not considered. This could lead to the CERC-model overpredicting sediment transport in places with lower availability of readily moved sediment, which is difficult to account for, when using one transport coefficient for a long coastline.

The resulting calibrated transport coefficient, K, is lower than the USACE suggested value of 0.39, as well as previously used values for the coast of Ystad municipality. Larson and Hanson (1992) proposed a transport coefficient of 0.3 for Ystad when using the root-mean squared wave height, H_{rms}. Since the wave heights are correlated according to $H_s = \sqrt{2}H_{rms}$, the transport coefficient of 0.3 for H_{rms} is equivalent to approximately 0.12, with regards to H_s. Although 0.12 is larger than the obtained value in this study, both coefficients are lower than the USACE recommended, which suggests that calibration is of significance to the coast of Ystad.

Although 0.018 can be considered a relatively small value for the transport coefficient, other studies have obtained similar magnitude of K when calibrated for low-energy coastal climates. Wang et al. (1998) argued that if the recommended value for the transport coefficient is used,

rates are unrealistically high for the studied low-energy coasts. Based on measurements from the streamer trap and short-term impoundments, the study suggested K to be revised to 0.08 for the specific settings. Their study was performed using H_{rms} and when adjusted to H_s, K becomes approximately 0.03. The following year, Wang and Kraus (1999) conducted a study using the same measurement technique at the same site, establishing K to range between 0.044-0.541, depending on measurements pre- and post groyne installation. Adjusting the values to H_s, K would instead have a range between 0.018-0.23. Further, Smith et al. (2003) instead, used a large-scale laboratory facility to simulate and measure transport in a low-energy climate. They too estimated a lower K and after establishing a dependency on breaker type, K was suggested to be either 0.119 or 0.049, depending on spilling or plunging conditions. Although not conducted in the same way, all three studies significantly lowered the transport coefficient through calibration and derived similar values as obtained in this study. This further supports the importance of calibration for low-energy coastal climates and concludes that K could be in the vicinity of, or even as low as, 0.018.

6.1.3 Direction and Magnitude of Longshore Sediment Transport

The sensitivity analysis confirms that shoreline orientation is a sensitive parameter for CERC-calculations. The immediate impact on fluctuations in the parameter was described in section 6.1.1, which shows that a slight alternation of the shoreline orientation changes both the magnitude and, depending on the angle of approach, the direction of transport. There is uncertainty to whether the model provides an accurate direction. Visual, artificial, and natural geomorphological indicators were used to establish a probable direction to validate the results of the model.

The sediment transport direction, obtained from the model, has an overall eastern net direction along the coast of Ystad. Along Kåseberga ridge the direction is predicted to alternate with a westbound direction at several locations. The magnitude of transport is seen to be largest in Ystad Sandskog, Kåseberga and Löderups Strandbad, whereas a smaller magnitude is observed in Nybrostrand and further east along the ridge. A more detailed description of transport direction and magnitude is further presented in this chapter for each coastal stretch, respectively.

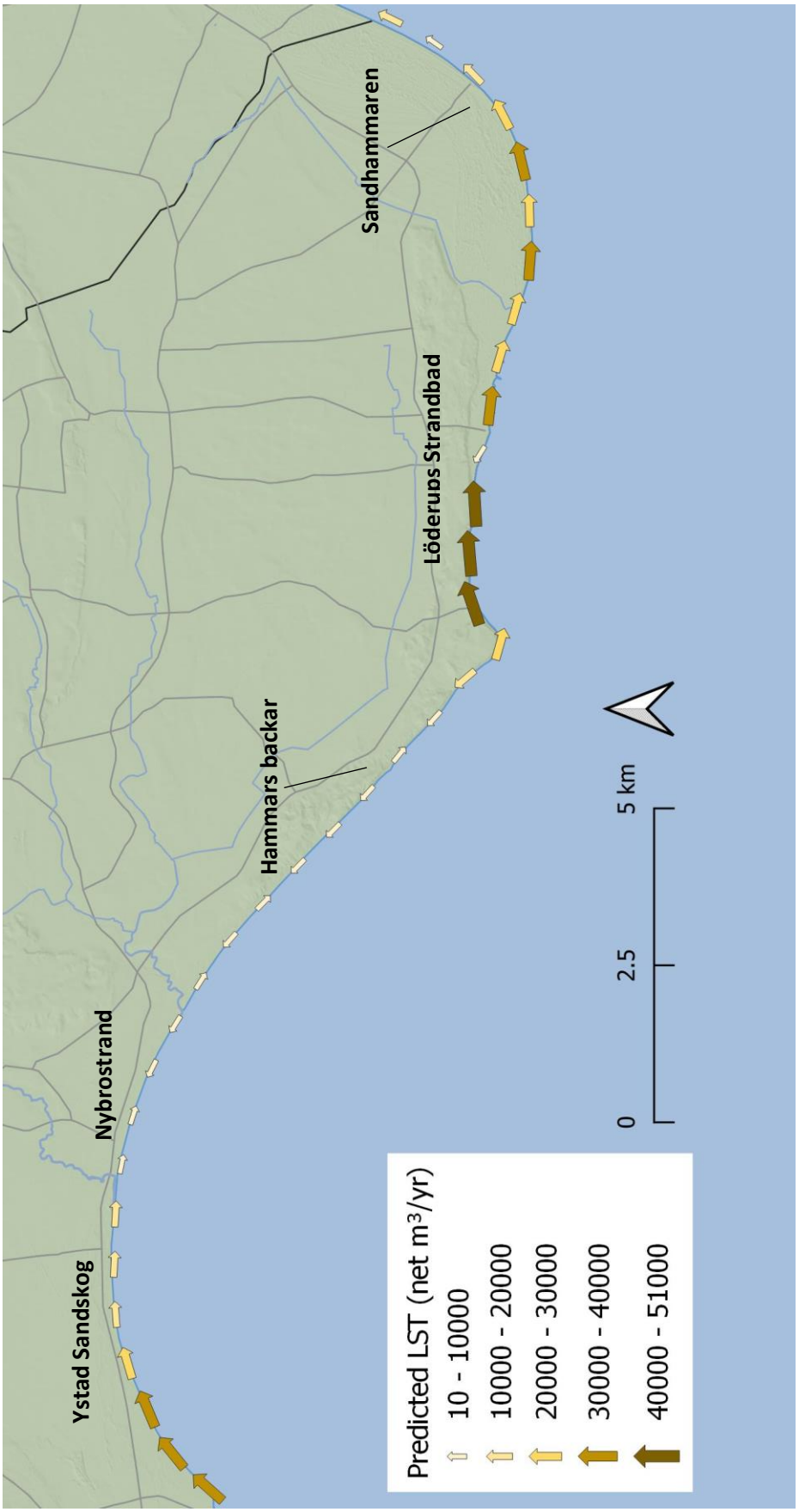

Figure 6.4. Predicted net longshore sediment transport (direction and magnitude) along the coast of Ystad. Background map ©Swedish Geological Survey.

Ystad Sandskog

The transport modelling presents an eastern net direction (Figure 6.5). The wave climate is represented by waves primarily approaching from a south-west direction, as seen in Figure 3.3, which would lead to a longshore transport largely directed to the east. In Ystad Sandskog west the shoreline orientation creates a larger angle of approach and greater magnitude of transport as opposed to Ystad Sandskog east, where the waves are more parallel to the shore and consequently the magnitude smaller. With the harbour acting as a border between the two sediment systems, there is no significant longshore sediment transport input from the west (Nyberg et al., 2021). This, combined with a larger magnitude of transport, indicates an erosive state of this stretch, which coincides well with the observed erosion and where nourishment has been added (section 3.2).

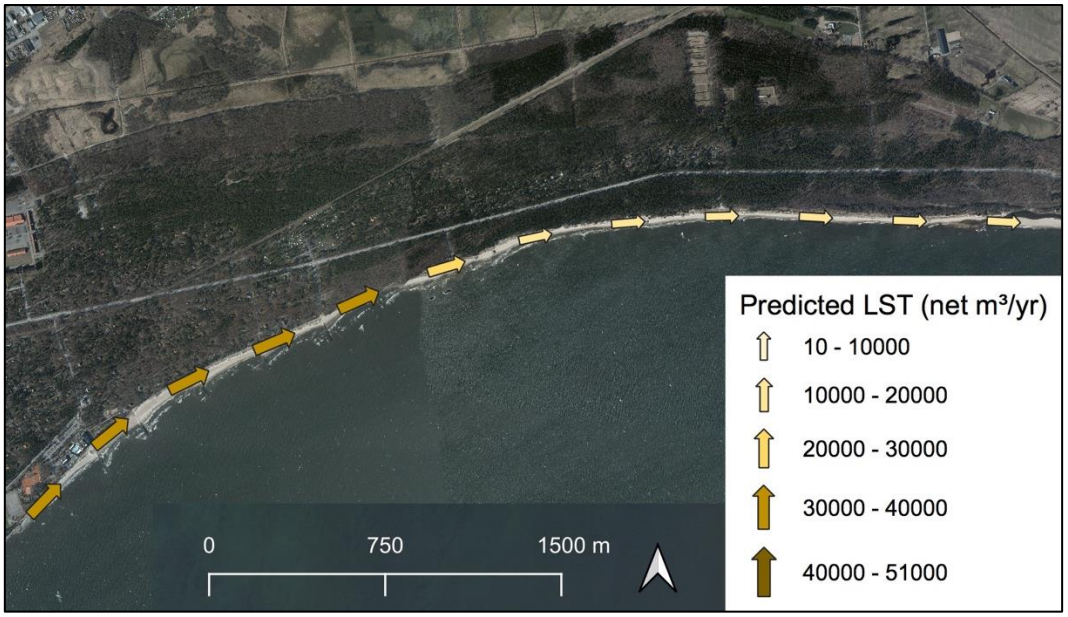

Figure 6.5. Predicted net longshore sediment transport (direction and magnitude) along Ystad Sandskog. Orthophoto ©Swedish Geological Survey.

At Ystad Sandskog west, there are five groynes installed to mitigate erosion. The aim of groynes is to block the sediment transport, leaving an impoundment of sediment on the updrift side of the structure. This can be understood from Figure 6.6 below, which shows a visual build-up to the left of groyne 0 and 4 and indicating a direction of transportation from west to east, supporting the CERC derived transport direction.

Figure 6.6. Groynes built in Ystad Sandskog west to trap sediment. Orthophoto from 2019. ©GoogleEarth

East of the groynes are five detached breakwaters with sediment build-up, or salient, visible between the breakwaters and beach (Figure 6.7). The initial three breakwaters are seen in the left image of Figure 6.7, where some sediment has been trapped. When comparing this with the later instalment of two additional breakwaters, there is a noticeable morphological change as more accretion is present between the five breakwaters, mainly by the two situated most to the west. This indicates that updrift is west of the breakwaters with a probable eastbound net direction of sediment transport.

Figure 6.7. Detached breakwaters in Sandskogen east with sediment build-up on the beach side and to the west. Left: The first three breakwaters. Photo from 2010. Right: Two more breakwaters have been built. Orthophoto from 2019. ©Google earth.

Furthest east is the outlet of Nybroån. The river can serve as a natural indicator of net sediment transport direction as a dominant direction could lead to a diversion of the mouth. According to Hågeryd et al. (2005) the westward diversion of the mouth indicates a westbound direction of transport, however, analyses of satellite photos instead show a continuous alternation in diversion and displacement of the river mouth. A photo taken in 2015 suggests a diversion to the east, whereas in 2018 the river mouth has relocated further west (Figure 6.8) possibly due to deposition from a westbound transportation of sediment. This alternation suggests that the direction of transport at this location instead fluctuates between years.

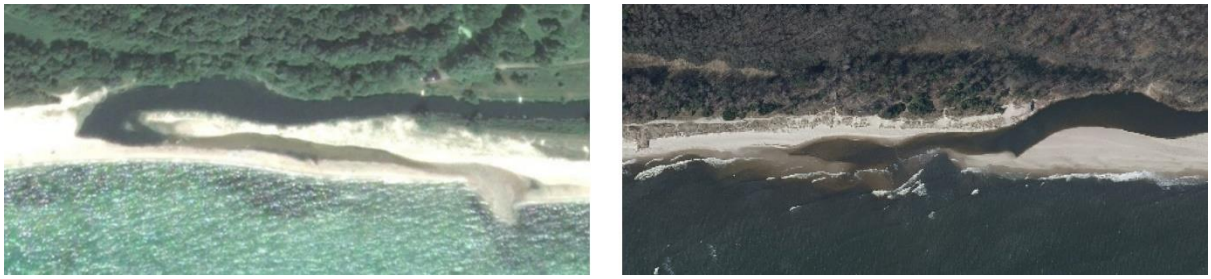

Figure 6.8. River mouth of Nybroån. The outlet alternates shape and direction. Left: Outlet directed to the east. Orthophoto from 2015. ©Google Earth. Right: Outlet directed towards the west. Orthophoto from 2018. ©Swedish Geological Survey.

Nybrostrand

The modelled longshore sediment transport has an alternating direction along this stretch of coast. The magnitude of transport is several times smaller compared to transport in Ystad Sandskog (Figure 6.5 and Figure 6.9).

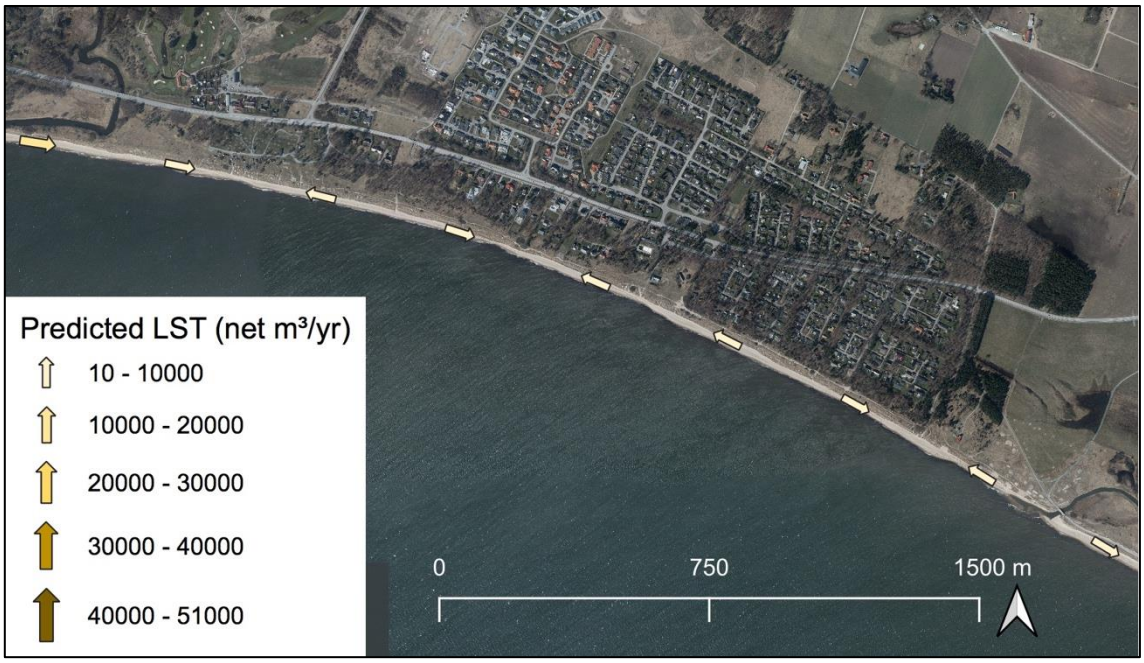

Figure 6.9. Predicted net longshore sediment transport (direction and magnitude) along Nybrostrand. Orthophoto ©Swedish Geological Survey.

The incoming waves approach from a south-western direction and as the waves refract, they will most likely break either parallel to the coastline or with a small angle (Figure 3.3). This explains the magnitude of transport as a small angle of approach consequently results in a small transport alongshore, whereas a wave crest approaching parallel will not induce any longshore transport at all. The altering transport creates several sites where directions converge and sediment potentially accretes, as well as sites with diverging transport possibly resulting in erosion. This coincides with the observed local erosion and accretion patches along this stretch of the coast (see section 3.3).

Kabusaån can serve as a natural indicator with the same argument as for Sandskogen. Looking at the diversion of the river mouth, it has an alternating direction (Figure 6.10) indicating that that transport of sediment changes direction between years. This is supported by the

sensitivity analysis performed in Nybrostrand where a small change in shoreline orientation had significant impact on transport (Figure 6.1), denoting that varying wave climate will alter the transport direction at this location.

Figure 6.10. River mouth of Kabusaån. The outlet alternates shape and direction. Left: Outlet directed to the east. Orthophoto from 2015. ©Google Earth. Right: Outlet directed towards the west. Orthophoto from 2018. ©Swedish Geological Survey.

Kabusa Military Field, Hammars Backar and Kåseberga

The direction of transport is continuously varying over this large stretch of coastline. There is a slight tendency for westbound transport in the west whereas a dominant eastbound transport is observed east of Kåsehuvud (Figure 6.11) The coastline has a uniform orientation in the west with incoming waves approaching from southwest and south-southwest (Figure 3.3), consequently breaking parallel or with a small angle to the shoreline, resulting in a small magnitude of sediment transport. Forcing from waves has historically eroded the coast, driving it to align itself with the incoming waves. The coastline east of Kåsehuvud has also been subjected to erosion, depleting the shore of fine sediment and leading to the fortifying of the shoreline at Kåseberga village (see section 3.4). The coastline east of Kåsehuvud has also been subjected to erosion, depleting the shore of fine sediment, and leading to the fortifying of the shoreline at Kåseberga village (see section 3.4). Since the CERC model assumes unlimited supply of sediment it predicts a large magnitude of transport along this stretch despite an absence of mobile sediment.

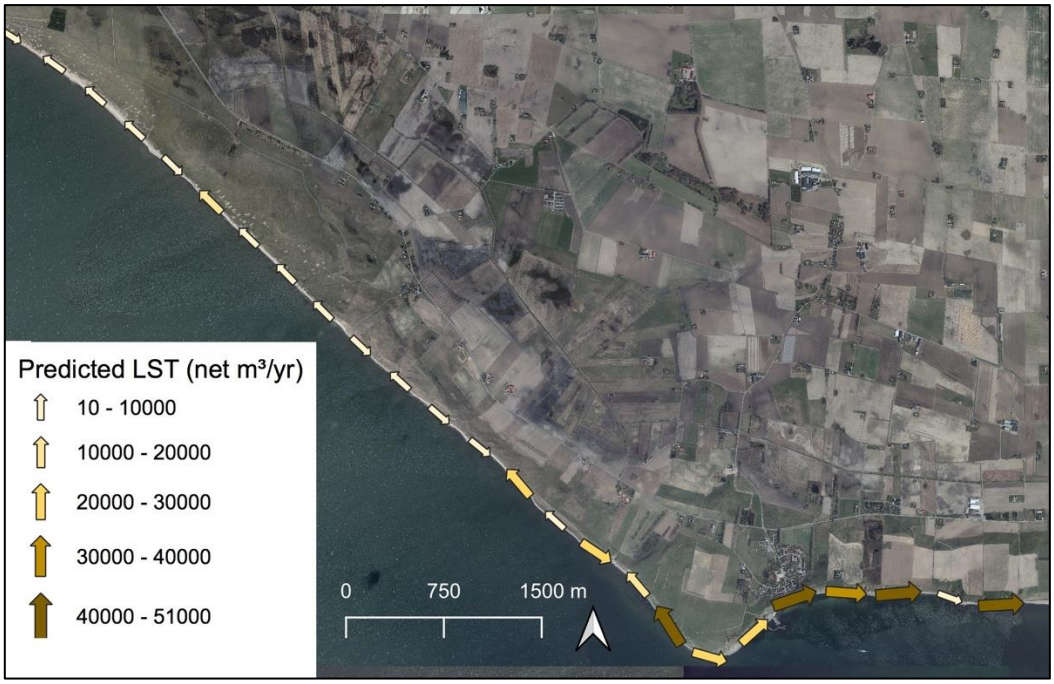

Figure 6.11. Predicted net longshore sediment transport (direction and magnitude) along the stretch Kabusa military field - Kåseberga. Orthophoto ©Swedish Geological Survey.

Löderups Strandbad

The predicted transport is dominantly eastern bound throughout the whole stretch (Figure 6.12). This coincides well with the wave climate approaching from a south-west direction (Figure 3.3). The transport magnitude varies along the stretch with some patches having an estimated transport of up to 51000 m^3/year. This stretch of coastline has experienced severe erosion and has, therefore, been well-documented throughout the years, facilitating the establishment of direction as being eastbound. Early measures taken to prevent erosion in Löderups Strandbad was fortifying the exposed coastline with revetments of large blocks and boulders, consequently constructing a static coastline. This resulted in an increase of erosion further east, suggesting that dominant direction of transportation is from west to east (Almström & Hanson, 2014). Due to the depletion of fine sediment at Kåseberga, it is likely that this stretch is even more exposed to erosion.

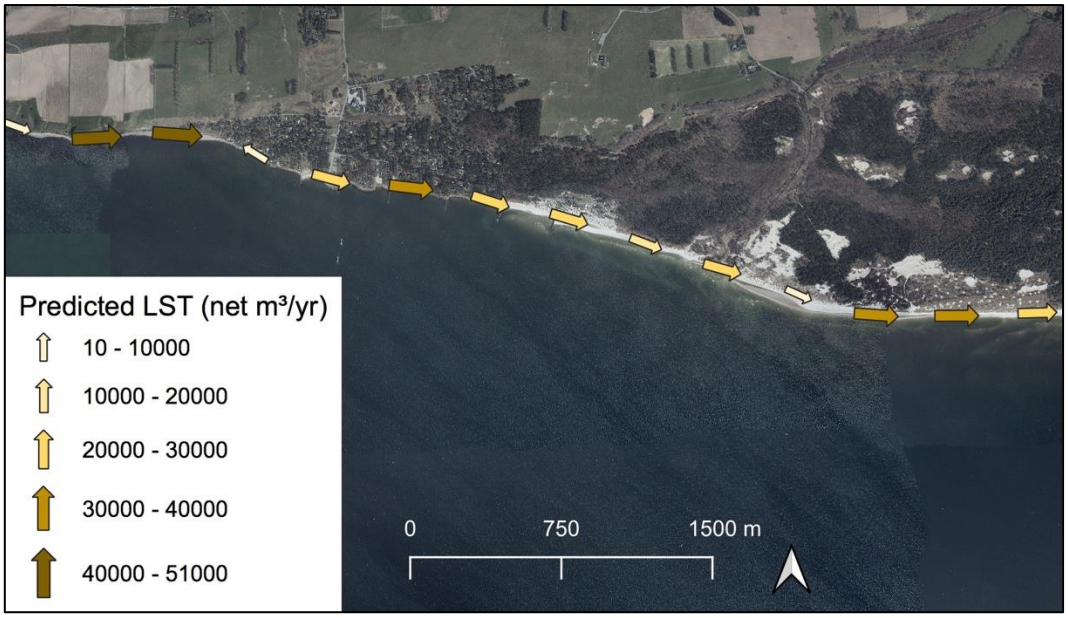

Figure 6.12. Predicted net longshore sediment transport (direction and magnitude) along Löderups Strandbad. Orthophoto ©Swedish Geological Survey.

Sandhammaren

In Sandhammaren the coast curves from a southern orientation into forming the east coast of Scania. The model given direction is dominantly northern and the magnitude of the transport is smaller in comparison to Löderups Strandbad. This area lacks artificial and natural indicators to help establish the direction. The wave data, however, displays a wave climate with incident waves mainly approaching from south-east (Figure 3.3). This suggests an induced current directed to the north, which is in compliance with the model derived direction (Figure 6.13). The input of sediment to is greater than the output. This means that this shoreline should accumulate, which is in accordance with observations (see section 3.6).

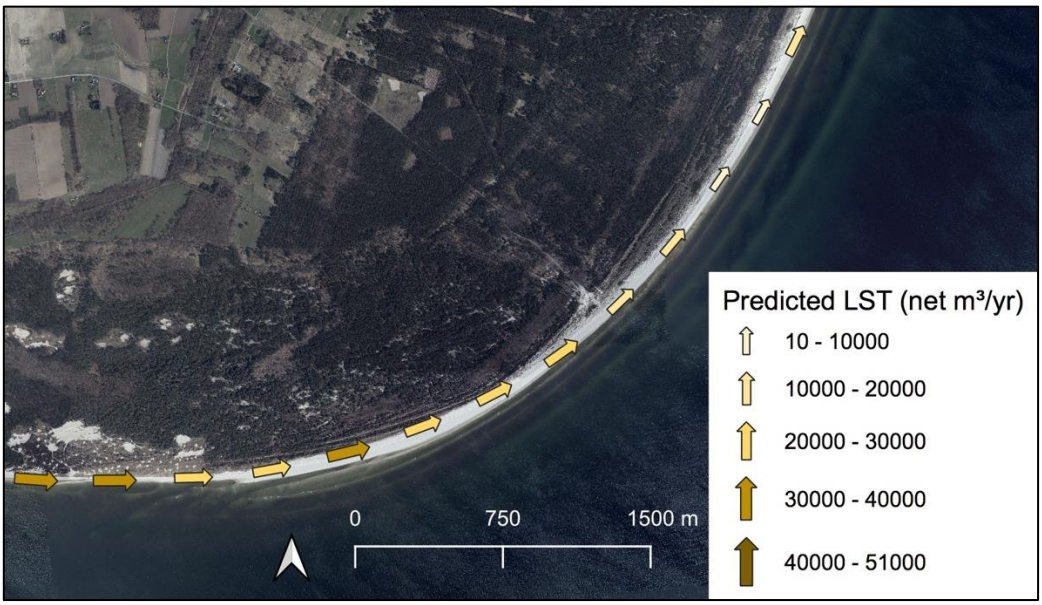

Figure 6.13. Predicted net longshore sediment transport (direction and magnitude) along Sandhammaren. Orthophoto ©Swedish Geological Survey.

6.2 Bayram Model

The RMSE was calculated for the predicted shoreline change using the Bayram and CERC models. The same ten stretches were used for both models and compared with observed yearly shoreline change, EPR. This resulted in an RMSE of 2.3 for CERC and 3.4 for the Bayram model, indicating a slightly better fit for CERC. A comparison might not be entirely valid considering CERC was calibrated with regard to observed shoreline change, while the Bayram model was not calibrated.

A comparison between the models in Figure 6.14 displays the net transport rate to be similar for both models, though the Bayram model predicts a larger net transport at almost all locations. The similarity in transport magnitude throughout the coastline could mean that the calibrated transport coefficient for CERC modelling is suitable for this region. The net direction of transportation is the same at every point of measurement. Considering the Bayram model is a reworked version of CERC, their similarity should be expected.

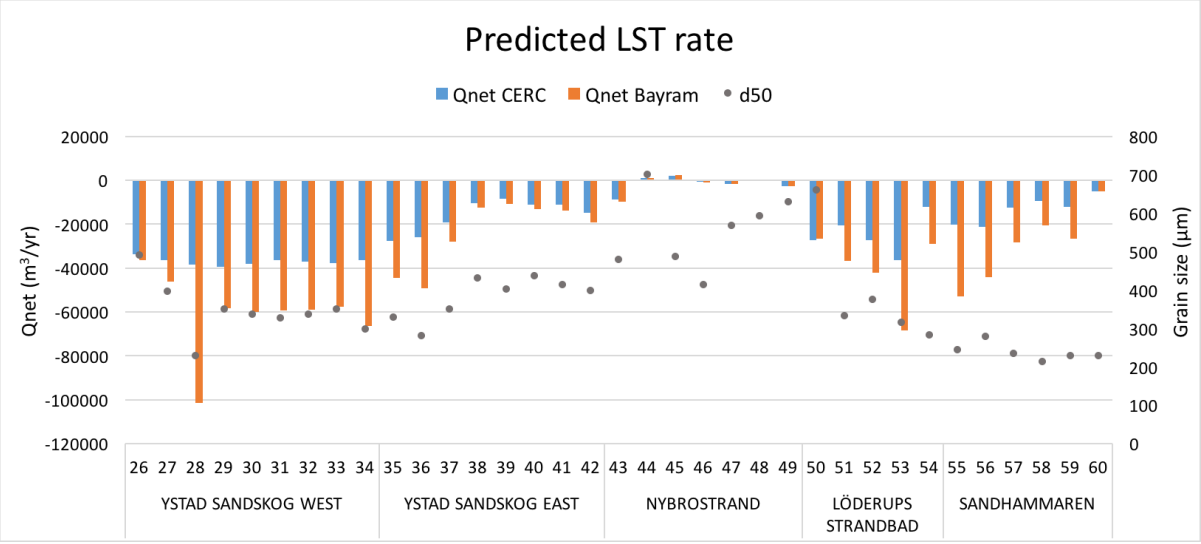

Figure 6.14. A comparison of the potential longshore sediment transport rate calculated with the CERC model and the Bayram model. The grain size (d_{50}) from the sample locations is also included.

A principal different between the models is that the Bayram formula assumes a large portion of the transport to be suspended load and thus accounts for the sediment characteristics present on the beach. As finer particles are more readily set in motion than coarser sediment, this suggests that the Bayram model might predict larger transport at stretches with finer sediment. At points 28-33 and 51-52, the beaches were nourished in 2020, likely lowering the grain sizes at these points. This means that the Bayram model probably predicts a slightly larger transport than what should naturally occur. Additionally, point 28 in Ystad Sandskog exhibits a larger net transport that deviates from adjacent datapoints, suggesting that it might be a result of a smaller median grain size. Likewise, increasing grain sizes in Ystad Sandskog east and Nybrostrand coincide with smaller net transport implying a similar correlation. Since this trend is also present for the CERC-modelled transport, it is likely a consequence of waves breaking with a small angle or parallel to the shoreline, which was discussed in section 6.1.3. At Sandhammaren, the opposite trend can be detected as grain transport decreases with decreasing d_{50}. However, no overall consistent correlation between grain size and magnitude of transport for the entire coast can be found in the analysis presented in Figure 6.14.

Quadrado and Goulart (2020) compared sediment transport rates predicted with the Bayram and CERC models, with in situ measurements in sandy beaches in Brazil and found that the Bayram model underestimated transport rates, while CERC did not show the same tendencies for either under- or overestimation. Considering the similarity between the models in this study, both models should either under-, over-, or correctly predict transport here. This is best verified using measured transport which was not available for this project.

7 Results and Discussion: Field Measurements

7.1 Correlations with Sediment Characteristics

From the sieve size analysis, sediment grain size (d_{50}) and sorting were obtained and used to analyse correlations with longshore distance and observed shoreline change (EPR). Grain size was also correlated with beach face slope.

7.1.1 Longshore Grain Size Variability

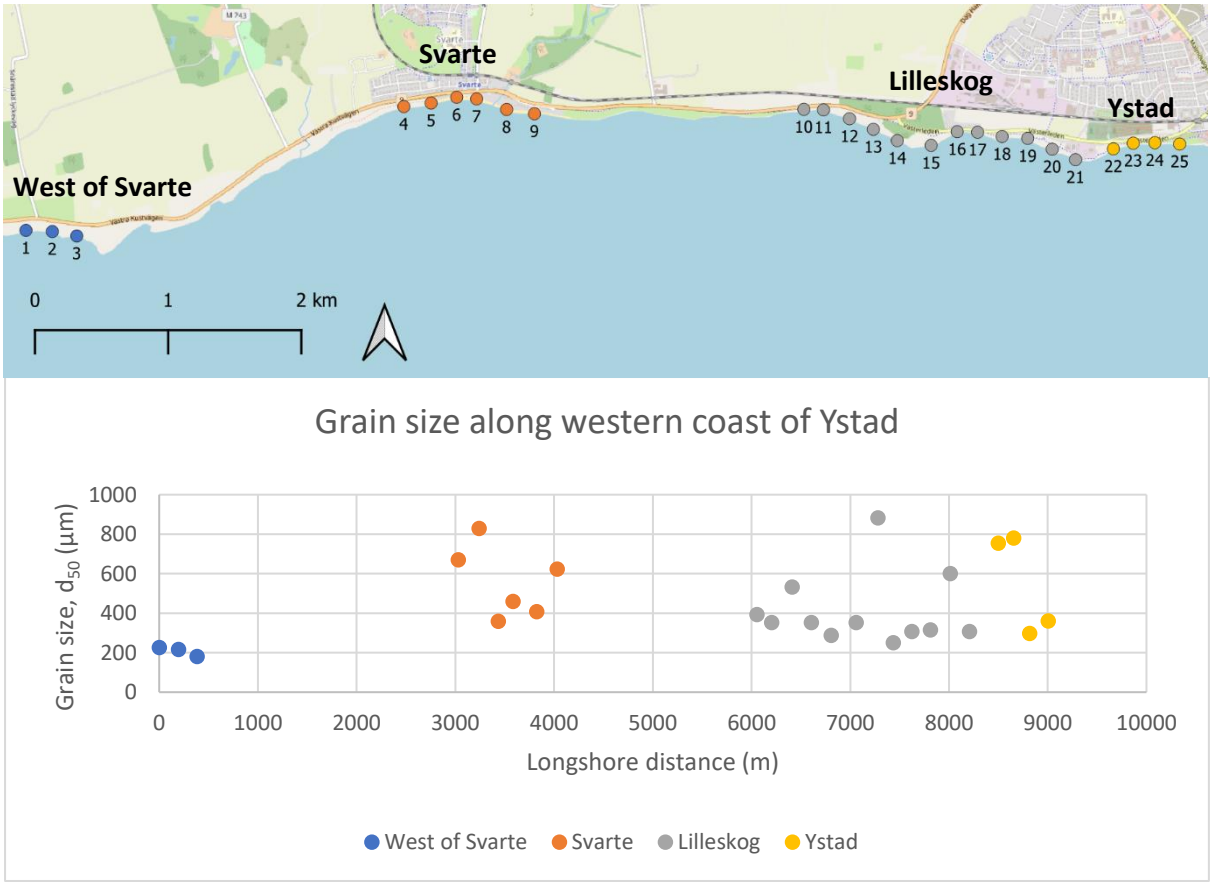

Figure 7.1. Top: Sample locations on the western coast of Ystad. Background map ©OpenStreetMap. Bottom: Grain size (d_{50}) from field samples against longshore distance for the western coast of Ystad.

Figure 7.1 shows that grain sizes along the western shore of Ystad are dispersed and varied, with grain sizes ranging from approximately 200-900 µm. Clear patterns for the locations are not found except for West of Svarte, where the three samples show a slight diminishing in grain size with distance. This location had the finest sediment of the western shore. At Lilleskog and Ystad, the median grain sizes are relatively equal with the majority of the around 350-400 micrometres for the sediment samples with the exception of a few samples that had a coarser grain size of around 800 micrometres.

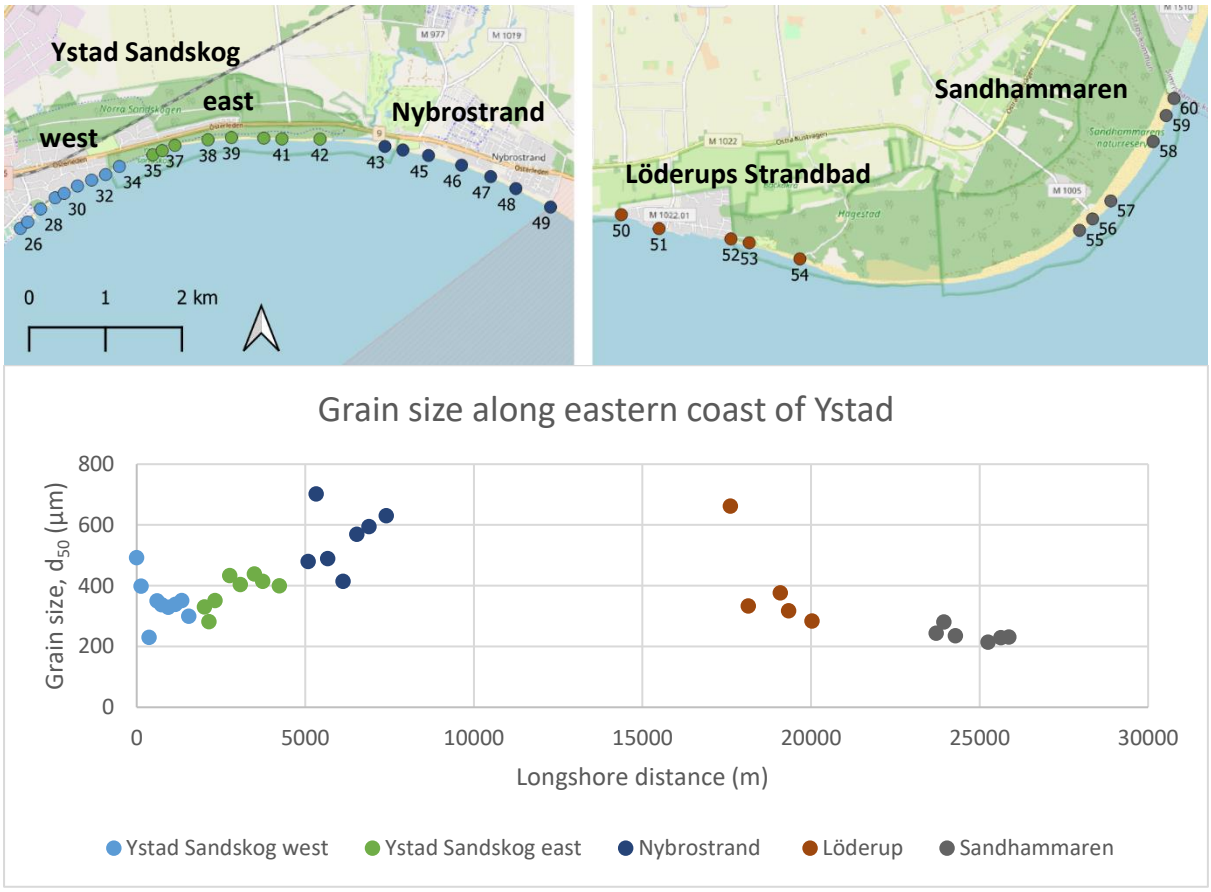

Figure 7.2. Top: Sample locations on the eastern coast of Ystad. Background map ©OpenStreetMap. Bottom: Grain size (d_{50}) from field samples against longshore distance for the eastern coast of Ystad.

Compared to the western shore of Ystad, the eastern coastline has evident patterns in grain size (Figure 7.2). d_{50} increases alongshore from Ystad Sandskog to Nybrostrand and decreases alongshore Löderups Strandbad and Sandhammaren. The gap in the middle indicates lack of data due to the unattainable stretch of beach along the ridge from Kabusa military field to Kåseberga. As finer particles require less energy for suspension, these can be transported longer distances (Kamel, 1962), suggesting that grain size is expected to decrease with transported distance longshore. This is supported by the findings of Hallin et al. (2019) at Ängelholm beach, located 140 kilometres northwest of Ystad, where a decrease in grain size with the direction of travel was observed.

The transport rate calculated by CERC shows an eastern bound transport direction in Ystad Sandskog (Figure 6.5), contradicting the grain size pattern found at Ängelholm by Hallin et al. (2019). Since the bay in Ystad Sandskog is not enclosed, a continuous supplement of sediment can be expected, as well as sediment distribution from rivers, which might influence or disrupt the grain size pattern with distance. The coarsening of sediment with transport direction could also be explained by the nourished stretches of the beach in Ystad Sandskog west. The sediment used for nourishing has, at every occasion, been collected from the eastern parts of Sandhammar sediment deposit (M. Skoog, personal communication, 2022). Measurements conducted at the sediment deposit concludes d_{50} to be approximately 200 µm

in the eastern parts (Marin Miljöanalys AB, 2012), which is finer than the naturally occurring sediment at point 26 and 27, which are located before the nourishment and have grain sizes of approximately 500 and 400 µm. The fine sediment from nourishing might be influencing the grain sizes in an eastern direction, with influence decreasing with distance, as the sediment consists of more native material and less nourished material, leading to a coarsening of sediment.

Should the nourished material have a significant influence on the grain size further along the coast, this would imply that coarser sediment occurs naturally in Nybrostrand, possibly explaining the grain size pattern. This is, however, not supported by the information presented in the marine geology map or the soil composition in this area, which do not differentiate notably from Ystad Sandskog (see Figure 3.2). The ridge to the west of Nybrostrand indicates that coarser materials should exist and the, on occasion, west-bound transport of sediment from this area could provide Nybrostrand with coarser sediment. The suggested effect of the ridge on sediment grain sizes could be supported by sample 50 in western Löderups Strandbad having similar d_{50} to Nybrostrand. It is possible that this section is highly influenced by the present ridge, whereas following samples in Löderup, located further east, are more likely to be affected by the 2020 nourishment at Löderups Strandbad. By also charting the coast along Hammars backar, Kabusa military field and Kåseberga, this could further explain the grain size patterns.

In Löderups Strandbad and Sandhammaren, the grain size decreases with distance, which coincides with the direction of transport calculated with CERC (see section 6.1.3).

7.1.2 Grain Size Sorting

As previously mentioned, sorting is a measurement of how varied the grain sizes are within a sediment sample. A lower sorting indicates a lower variation and therefore a more homogenous sediment sample. The sorting of the sediment field samples was plotted against longshore distance for the western and eastern shore. Figure 7.3 and Figure 7.4 below show the sorting on the western and eastern coast, respectively.

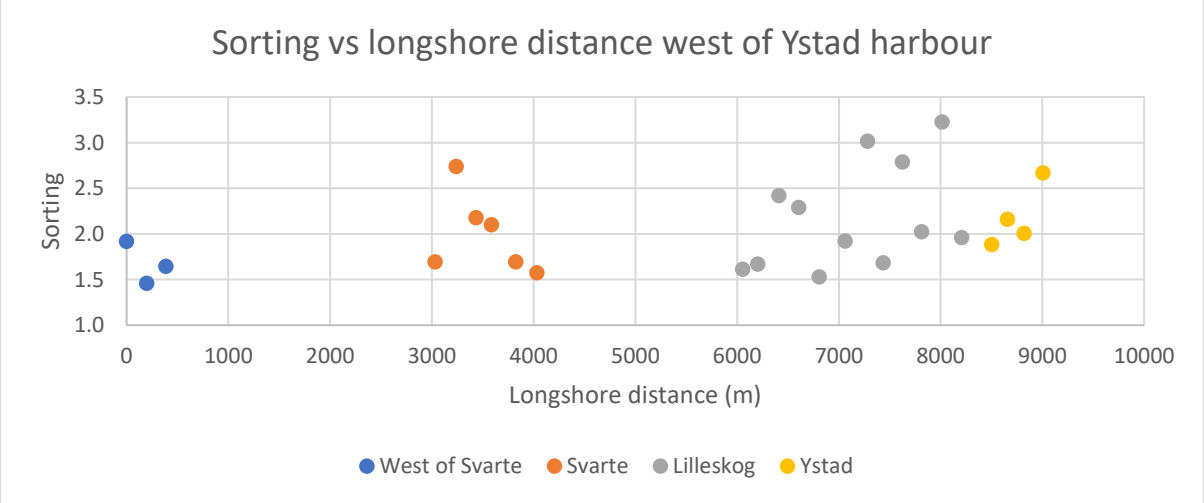

Figure 7.3. Sorting of sediment samples from the western shore of Ystad plotted against longshore distance.

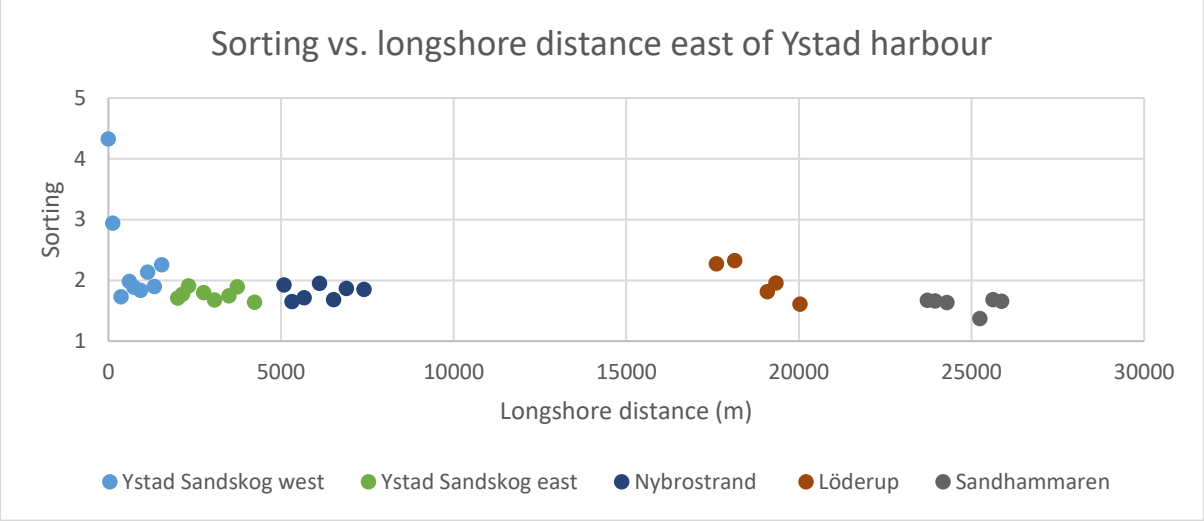

Figure 7.4. Sorting of sediment samples from the eastern shore of Ystad plotted against longshore distance.

There is a noticeable difference between the two parts of the coast, much like the grain size patterns, where the western shore has a more varied sorting than the eastern shore. Except for Svarte, which has a continuous improvement of sorting along the coast, there is no discernible pattern on the western coast. On the eastern coast the samples are more collected and there is a slight pattern of approaching a more well-sorted state along the coast in Sandskogen and an evident pattern of a more well-sorted state further east in Löderups Strandbad.

The pattern can be explained as progressive sorting, understood as the correlation between sorting and travelled distance (Kamel, 1962). It implies that sorting improves with increased distance longshore. This is true for Ystad Sandskog, where sorting slightly improves, and Löderups Strandbad, which both displayed a dominantly eastbound direction of transport (Figure 6.5 and Figure 6.12). As sorting progresses alongshore, the median sediment grain sizes are predicted to decrease with distance, with finer material outdistancing coarser, and the sorting is expected to become better while containing finer sediment (Russell, 1955). This is the case for Löderups Strandbad with an apparent decrease of d_{50} with distance (Figure 7.2) while also approaching a more well-sorted state. Ystad Sandskog displays an opposite pattern of grain size with distance, which was partly explained by the influence of nourished sediment. If the influence deceases with distance to the east, perhaps a different pattern should have been expected for the sorting as well.

The most well sorted sediments are found along the stretch of Sandhammaren, however, no notable pattern with distance is observed. Sandhammaren has the finest d_{50} of the samples, which could explain the sorting on this stretch.

Cumulative Distribution Curves

The sorting can be interpreted further through grain size distribution curves. Distribution curves from all field samples can be found in appendix A4. In Figure 7.5, several samples are plotted together showing the distribution curves from eroding and accumulating stretches. The stretches are confined to |EPR|>0.5 m/yr and only samples from east of Ystad harbour are presented.

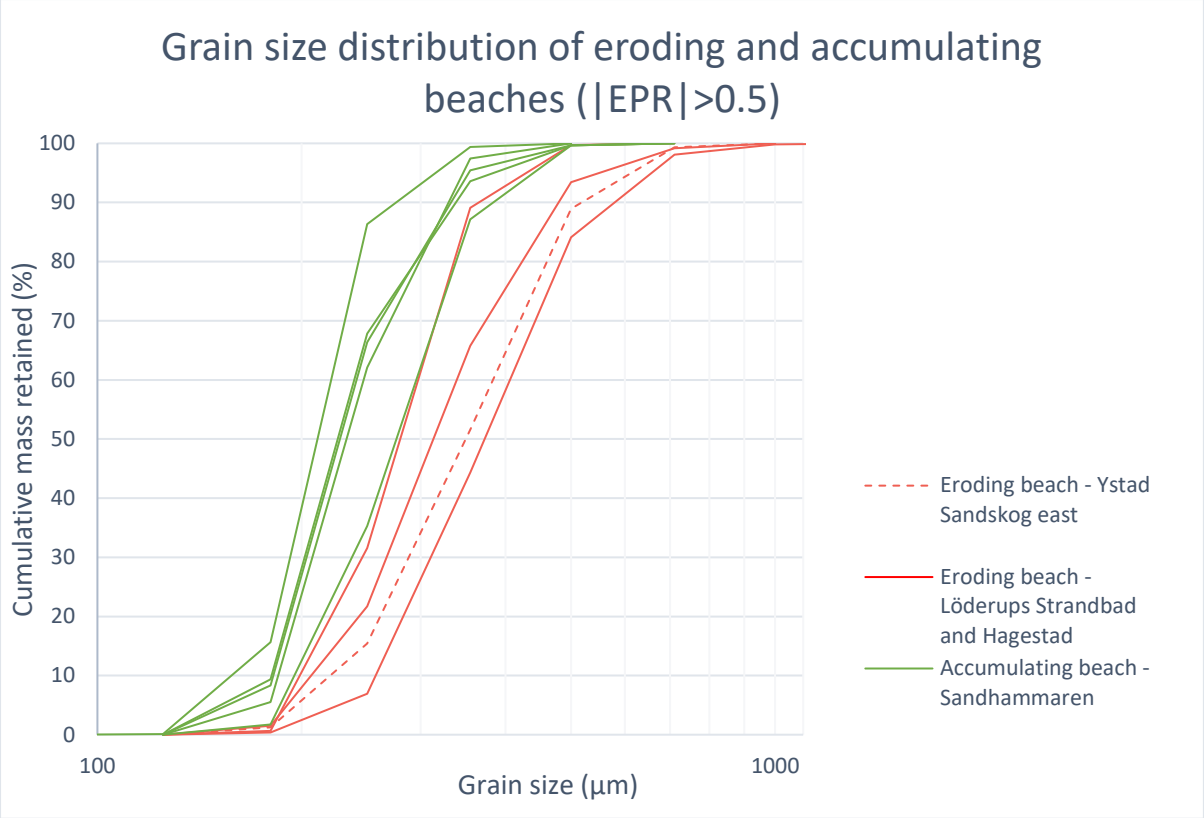

Figure 7.5. Cumulative distribution curves of grain size samples from eroding (EPR < -0.5 m/yr) and accumulating (EPR > 0.5 m/yr) beaches on the eastern shore of Ystad.

The median grain size, d_{50}can be obtained from the distribution curve and corresponds to the particle size represented at 50% mass retained in the cumulative distribution. The accumulating beaches all have finer median grain size in comparison with the eroded beaches. Further, the inclinations of the curves reveal that the accumulating beaches are, in general, better sorted as a steeper slope is obtained as a result of a more uniform sediment sample.

A similar comparison was made presenting the particle distribution of nourished and non-nourished beaches, respectively. Samples from both nourished locations, Ystad Sandskog and Löderups Strandbad, are displayed in Figure 7.6.

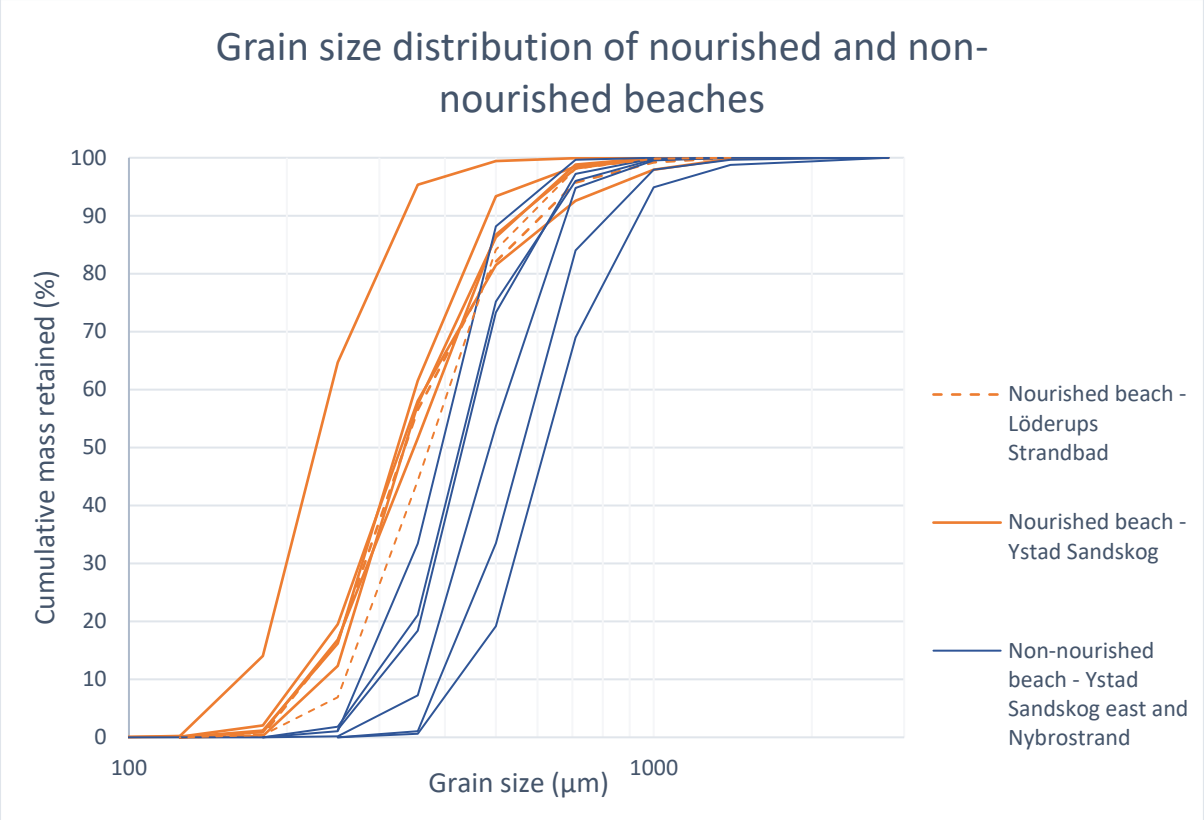

Figure 7.6. Cumulative distribution curves of grain size samples from nourished and non-nourished beaches on the eastern shore of Ystad.

Samples from nourished beaches all display similar distributions, with regards to both d_{50} and sorting, with finer d_{50} than for non-nourished stretches. The distributions for nourished samples all follow a similar curvature, with exception for the curve furthest to the left. There is no evident site specificity amongst the samples from nourished beaches since the sample from Löderups Strandbad displays almost identical properties as samples from Ystad Sandskog. The non-nourished samples are more scattered with a distinguishable difference in median grain size. The nourished material is native to the same sediment deposit and is expected to have similar characteristics. Since sampling was conducted seven months after the last nourishment, it is probable that not enough time had passed to order the sediment to a more natural sediment distribution, which results in similar characteristics for all nourished stretches. The lack of site specificity for the nourished stretches also means that these could be excluded in some analyses since their characteristics are not the result of naturally occurring disturbances. To describe the natural profile behaviour more accurately, the following analysis presents results where these stretches have been excluded.

7.1.3 Median Grain Size vs. Beach Face Slope

The beach profiles measured during field samples were used to derive the beach face slope for all sample locations. The slope was correlated to median grain size for the eastern shore and for the whole coastline. Since sampling and profile measuring was performed shortly after a nourishing event, which effects both grain size and beach face slope, the correlation was also tested for Ystad coastline and the eastern coast, excluding nourished parts. The results can be seen in Figure 7.7 below.

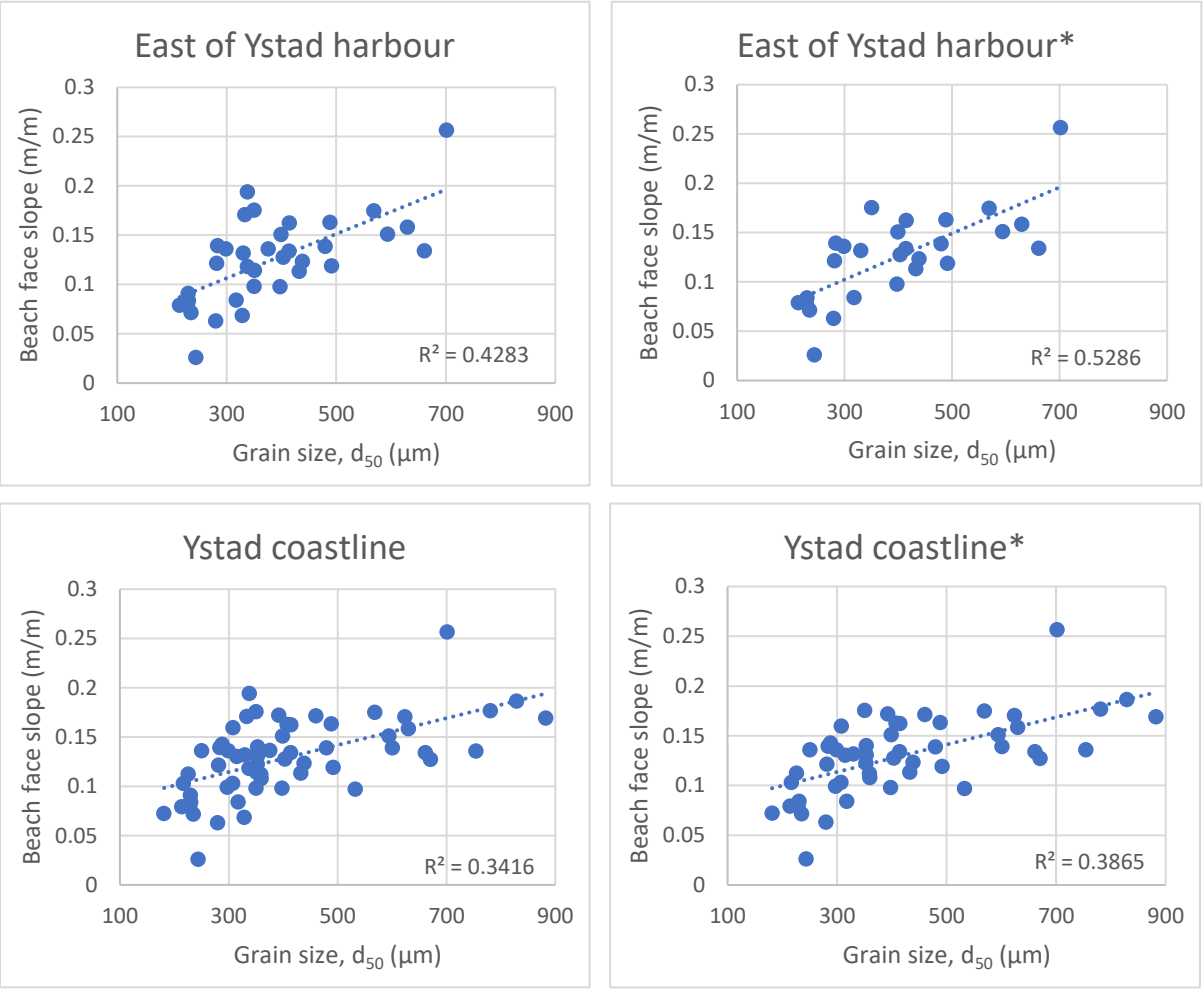

*Figure 7.7. Beach face slope in m/m plotted against grain size (d_{50}) in micrometre. * Nourished stretches have been excluded from the plot.*

A correlation is found for all cases. The stretch east of Ystad harbour presents a greater correlation compared to the entire Ystad coastline for both cases, including and excluding nourished segments, with R^2-values of 0.43 and 0.55, respectively. Excluding nourished beaches strengthens the correlation, indicated by a higher R^2-value. The immediate improved correlation confirms that the recent nourishment event is still likely affecting. the beaches, which was also observed in the distribution curve for nourished beaches (Figure 7.6). The asymmetry of the onshore-offshore transport governs the formation of the slope. When the sediment transported landward and seaward is approximately the same amount the beach face slope will eventually approach a more constant state, defined as dynamic equilibrium (Komar, 1976). With a recent impact on the beach, in the form of nourishing, it is expected that the stretches have yet to reach dynamic equilibrium.

Generally, milder beach face slopes will be associated with finer sediment grain sizes and steeper slopes with coarser grain sizes (McFall, 2019) which is also true for this coast. The correlation is partly explained by the amount of percolation present at the beach which, in turn, is highly governed by sediment characteristics (Komar, 1976). A beach with coarser material will have higher pore space, providing a higher percolation rate that reduces the swash and backwash on the beach. The reduced energy components allow for a steeper beach face to

establish whereas finer sediments, with a lower percolation rate, has a higher backwash velocity that readily removes material and forms milder slopes (Dubois, 1972). This supports the correlation observed in the graphs. In addition to grain size, McLean & Kirk (1969) discussed the importance of sorting with regards to beach face slope and determined sorting to exert a primary influence through permeability. Similar results were not observed in this study with diminutive correlation confirmed between sorting and beach face slope (see appendix A3).

7.1.4 Beach Characteristics vs. EPR

The median grain size, beach face slope and sorting from the field samples were plotted against observed shoreline change (EPR). Only samples where EPR showed either accumulation (EPR>0.5 m/yr) or erosion (EPR<-0.5 m/yr) were included. This left one sample west of Ystad and ten samples east of Ystad. The resulting plots are shown in Figure 7.8 below. Note that the scale of the y-axis differs between the plots.

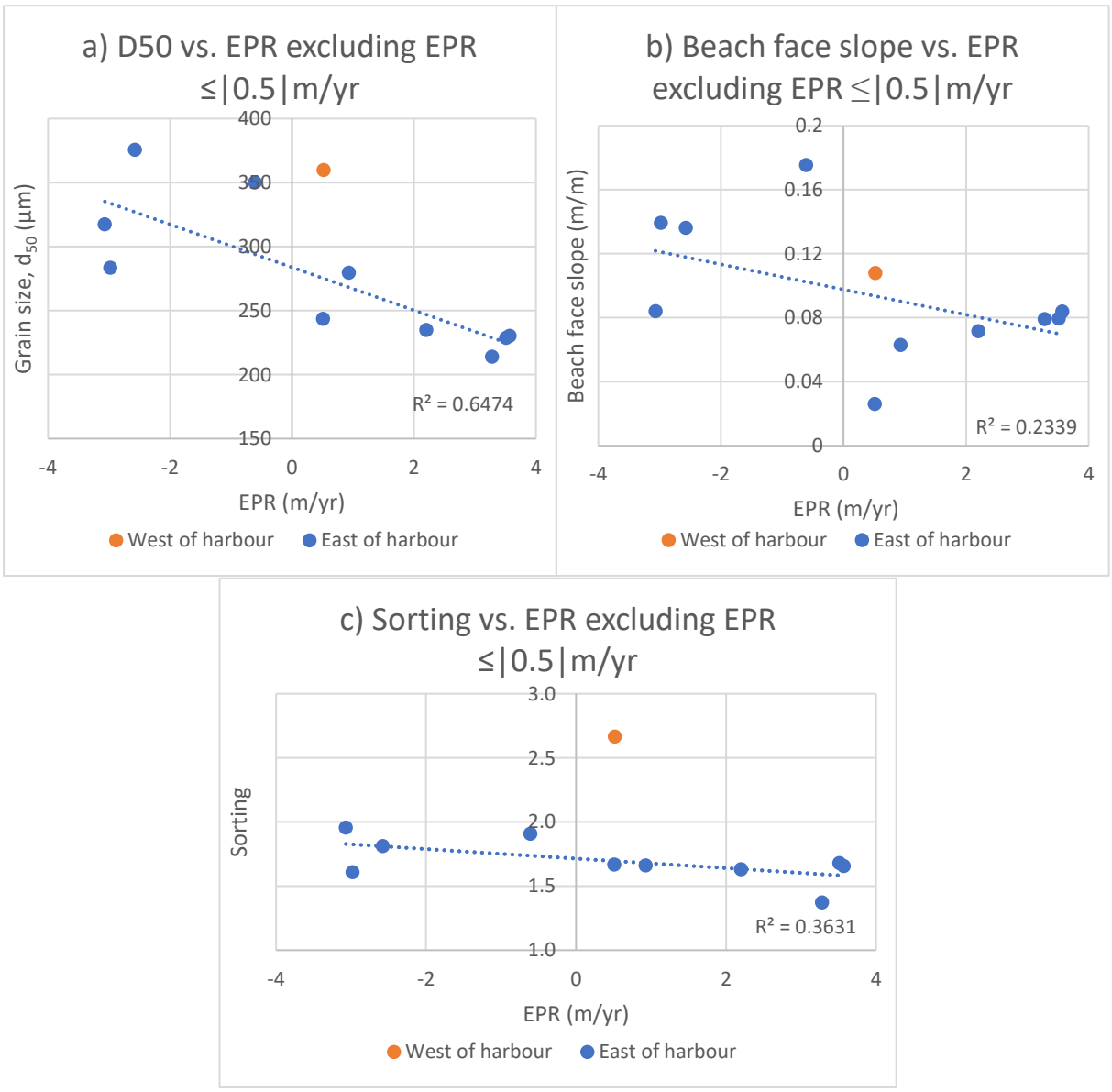

Figure 7.8. Correlation analysis for grain size samples excluding stretches where EPR≤|0.5|m/yr. a) Median grain size for the field samples vs. shoreline change (EPR). b) Beach face slope in m/m derived from the beach profile measurements plotted against observed shoreline change (EPR) in m/year. c) Sorting of beach sediment sample plotted against observed shoreline change (EPR) in m/year.

Correlation is found for all three cases, with the strongest for the relationship between $d_{50}$and EPR, with an R^2-value of 0.65, showing a pattern of finer grain sizes in accumulating areas and coarser in eroding areas (Figure 7.8a). This was also shown by the cumulative distribution curve in Figure 7.5. As stated previously, finer particles are more easily put in suspension, suggesting that a beach subjected to erosive wave forcing should lose fine sediment due to back-wash, coarsening the sediment in the profile and allowing more percolation. This should generally lead to coarser sediment in eroded areas as coarser sediments settle close to the source (Komar, 1976). The sample west of Ystad is coarser than expected for an accumulating beach, although the beach where the sample was collected also has a variety of larger rocks in the surf zone (Figure 3.2) which could dissipate wave energy leading to deposition of material.

For the cases of beach face slope and sorting there is a slight correlation with EPR, with R^2-values of 0.23 and 0.36 (Figure 7.8b-c). Generally, the above plots indicate that in an erosive state, the beach has coarser, less well sorted, sediment and a steeper beach face, whereas a beach in an accumulating state has a finer, more well sorted, sediment with a gentler slope.

8 Conclusions

The general longshore sediment transport in Ystad municipality is concluded to have an eastern bound net direction. The CERC-model predicted a predominantly eastern direction in Ystad Sandskog and Löderups Strandbad, explained by a primarily southwest direction of incident waves. The direction was further validated by artificial indicators displaying an impoundment of sediment on the updrift side of the structures. These areas also presented the greatest magnitude of sediment transport, which was found to be reasonable since it coincides well with historically observed erosion. Along Nybrostrand and Hammars backar, the predicted direction was found to alternate. This was concluded to be due to waves approaching close to parallel with the shoreline, which would also explain the smaller magnitude of transport present there. An altering direction of sediment transport was confirmed by the position of river outlets relocating between years.

The CERC model is applicable to the coast of Ystad municipality in the sense that modelled transport directions coincide well with directions deduced by natural and artificial indicators along the coast. Further, the active profile on the eastern coastline is to a great extent compromised of mobile sediment, although not unlimited, facilitating suspended transport and the use of the CERC model. It was concluded that the prediction is sensitive to stretches where the shoreline orientation drastically changes within a short distance, as in Kåsehuvud, and the sensitivity to shoreline orientation was further confirmed by the sensitivity analysis. This concluded that for stretches where waves approach close to parallel with the shoreline, a small change in orientation can have a large impact on both magnitude and direction of transport.

It is recommended that CERC is calibrated for the site-specific conditions, which was also concluded in this study where the transport coefficient was lowered significantly from the recommended value of 0.39 to 0.018. This further supports the importance of calibrating K when modelling for a low energy coastal climate, which was also observed in other studies. This study used EPR from a digitized shoreline analysis to calibrate the model prediction. Compared to using in-situ measurements for sediment transport, EPR requires minimal computation and time in order to obtain an extensive dataset for observed values. With regards this coastline, however, EPR does not appear to be an optimal method. Since the majority of the sediment loss along the coast of Ystad occurs underneath the surface with marginal impact on the shoreline, erosion becomes underestimated and is not fully reflected in the EPR. If the loss and gain of sediment is not correctly accounted for by EPR, it causes a discrepancy between actual and predicted transport irrespective of model fit. Despite this, although not calibrated, the Bayram formula resulted in transport of very similar magnitude to the CERC model.

Regardless of model fit or whether the predicted magnitude of transport equals the actual transport, the model results can be used to compare transport magnitude between beaches. Although the extent of erosion would be difficult to assess, locating stretches with higher risk for erosion is still possible without a correct transport coefficient. This might, however, require a large awareness of local sediment dynamics and beach condition since the CERC model assumes an unlimited supply of sediment. Although CERC predicts a large transport for a stretch, it might not consist of mobile sediment or has historically been depleted of fine

sediment, which instead relocates the risk of erosion downstream where less sediment input is received.

To obtain a better understanding of sediment dynamics, correlation analyses were performed on beach characteristics. The results showed a correlation between eroded beaches and coarser, less sorted sediment and a steeper beach face slope. Accumulated beaches were correlated with a finer, more well sorted material and a gentler slope. These findings were in accordance with previously established patterns by other studies. Furthermore, the beach sediment was expected to coarsen along the direction of transport, whilst becoming more sorted. This was true for Löderups Strandbad and Sandhammaren. At Ystad Sandskog and Nybrostrand, although the sorting did improve, the median grain size instead coarsened with distance. Probable explanations for the unexpected grain size pattern are the influence of finer nourished material at Ystad Sandskog or coarser native material from the ridge east of Nybrostrand.

While beach nourishment mitigates erosion and reforms beaches to a high recreational value, it also influences analyses of beach characteristics. Aside from impacting the shape of the beach profile, transport patterns derived from field samples are impacted by the addition and distribution of nourished material along the direction of transport, leading to field sample analyses that might become inconclusive if the amount of influence is unknown. As seen, nourished beaches have a more similar grain size distribution that non-nourished beaches, as they are not formed by natural disturbances. The inclusion of nourished beaches lowered the correlation of beach face slope and grain size.

8.1 Future studies

To achieve a more all-encompassing insight regarding the impact of nourishing on low energy coastlines, continuous data collection throughout the nourishing timeline can be of use. This would also include samples from right before a nourishing event to reflect the beaches "natural" state. Further, samples from unattainable stretches, such as Kabusa military field to Kåseberga, should be included to extend the dataset from this study and provide a greater comprehension of grain size patterns. If possible, samples from several points along the profile is desirable to receive a more accurate assessment of sediment distribution and grain size variation.

Investigating the look and slope of the active profile and comparing with the equilibrium profile could be of interest to see if the beach is in morphological equilibrium and whether much sediment has been lost underneath the surface. The loss of subsurface sediment could lead to beach erosion, which might happen quickly if the loss has undermined the beach. This type of inquiry would need extensive bathymetry of the coast, which was not available at the time of this study.

Should the inquiry confirm an extensive loss or gain of sediment beneath the surface, it would also confirm a need for a different method to obtain observed values rather than using EPR. Alternatively, a method to correct EPR for subsurface loss could be investigated. Additionally, evaluating whether the CERC model can be applied to the coastline west of Ystad harbour, or if another model is better suited, is recommended. The sediment transport should also be compared between years, to assess how the coast responds to a varying wave climate.

9 References

Adell, A., Hallin, C., & Nyberg, J. (2021). OPEN-ACCESS PORTAL WITH HINDCAST WAVE DATA FOR SKÅNE AND HALLAND. *VATTEN – Journal of Water Management and Research*, *77*(2), 10.

Ahrens, J. P. (2000). A Fall-Velocity Equation. *Journal of Waterway, Port, Coastal, and Ocean Engineering*, *126*(2), 99–102.

Almström, B., & Hanson, H. (2014). *Strandfodringen i Ystad 2011 - bakgrund, uppföljning, framtid (In Swedish)*. SWECO.

Bascom, W. N. (1951). The relationship between sand size and beach-face slope. *Transactions, American Geophysical Union*, *32*(6), 866–874.

Bayram, A., Larson, M., & Hanson, H. (2007). A new formula for the total longshore sediment transport rate. *Coastal Engineering*, *54*(9), 700–710. https://doi.org/10.1016/j.coastaleng.2007.04.001

Booij, N., Ris, R., & Holthuijsen, L. (1999). A third-generation wave model for coastal regions, Part I, Model description and validation. *Journal of Geophysical Research*, *104*(C4), 7649–7656.

Clinton Marine Survey. (2020). *Mätrapport - Ystad sandskog och Löderups strandbad (In Swedish)*.

Davidson-Arnott, R. (2010). *Introduction to Coastal Processes and Geomorphology*. Cambridge University Press.

Dean, R. G., & Dalrymple, R. A. (2001). *Coastal Processes with Engineering Applications*. Cambridge University Press.

Dubois, R. N. (1972). Inverse Relation Between Foreshore Slope and Mean Grain Size as a Function of the Heavy Mineral Content. *GSA Bulletin*, *83*(3), 871–876. https://doi.org/10.1130/0016-7606(1972)83[871:IRBFSA]2.0.CO;2

Fredriksson, C., Almström, B., Hanson, H., Larson, M., & Persson, O. (2017). Sandbehov för att motverka stranderosion utmed Skånes sydkust under perioden 2017–2100 Estimation of required beach nourishment volumes along the south coast of Sweden during 2017–2100. *VATTEN – Journal of Water Management and Research*, *73*, 77–84.

Hågeryd, A.-C., Rankka, K., Rankka, W., & Rosqvist, H. (2005). *Strandmorfologi. Studie av kuststräckan Ystad till Sandhammaren* (VARIA No. 554). Swedish Geotechnical Institute.

Hallin, C., Almström, B., Larson, M., & Hanson, H. (2019). Longshore Transport Variability of Beach Face Grain Size: Implications for Dune Evolution. *Journal of Coastal Research*, *35*(4), 751–764. https://doi.org/10.2112/JCOASTRES-D-18-00153.1

Hanson, H. (2012). *Profilmätningar vid Löderups Strandbad och Ystad Sandskog (In Swedish)*. Teknisk Vattenresurslära, Lunds Universitet.

Himmelstoss, E. A., Henderson, R. E., Kratzmann, M. G., & Farris, A. S. (2018). *Digital Shoreline Analysis System (DSAS) Version 5.0 User Guide*. U.S. Geological Survey.

Hughes, M. G., & Baldock, T. E. (2020). 8 - The swash zone. In D. W. T. Jackson & A. D. Short (Eds.), *Sandy Beach Morphodynamics* (pp. 155–186). Elsevier. https://doi.org/10.1016/B978-0-08-102927-5.00008-4

IPCC. (2019). 4 Sea Level Rise and Implications for Low-Lying Islands, Coasts and Communities [Oppenheimer, M., B.C. Glavovic , J. Hinkel, R. van de Wal, A.K. Magnan, A. Abd-Elgawad, R. Cai, M. Cifuentes-Jara, R.M. DeConto, T. Ghosh, J. Hay, F. Isla, B. Marzeion, B. Meyssignac, and Z. Sebesvari]. In *IPCC Special Report on the Ocean and Cryosphere in a Changing Climate* [H.-O. Pörtner, D.C. Roberts, V. Masson-Delmotte, P. Zhai, M. Tignor, E. Poloczanska, K. Mintenbeck, A. Alegría, M. Nicolai, A. Okem, J. Petzold, B. Rama, N.M. Weyer (eds.)] (pp. 321–445). Cambridge University Press.

Irminger Street, S., Bjarke, M., & Lövstedt, C. (2016). *Kostnads-nyttoanalys av strandfodring, säkerställd kustlinje, planerad reträtt och naturlig utveckling som alternativa strategier för att möta erosions- och översvämningshot vid Ystad Sandskog och Löderups Strandbad (In Swedish)*. SWECO.

ISO. (2017). *Geotechnical investigation and testing - Identification and classification of soil - Part 1: Identification and description (ISO 14688-1:2017)*. International Organization for Standardization.

Kamel, A. M. (1962). *Littoral studies near San Francisco using tracer techniques* (Technical Memorandum No. 44). U.S Army Beach Erosion Board.

Komar, P. D. (1976). *Beach processes and sedimentation*. Prentice-Hall.

Komar, P. D. (1983). Chapter 2 Nearshore Currents and Sand Transport on Beaches. In B. Johns (Ed.), *Elsevier Oceanography Series* (Vol. 35, pp. 67–109). Elsevier. https://doi.org/10.1016/S0422-9894(08)70500-2

Kriebel, D. L., Kraus, N. C., & Larson, M. (1991). *Engineering methods for predicting beach profile response*. Proceedings of Coastal Sediments, Seattle.

Larson, M., & Hanson, H. (1992). *Analys av klimatologiska och hydrografiska data för ystadbukten (In Swedish)*. Teknisk Vattenresurslära, Lunds Universitet.

Malmberg Persson, K., Nyberg, J., Ising, J., & Rodhe, L. (2016). *Skånes känsliga stränder - erosionsförhållanden och geologi för samhällsplanering (In Swedish)* (SGU-rapport 2016:17). Swedish Geological Survey.

Marin Miljöanalys AB. (2012). *Rapport och sjömätning före sandfodring - Ystad Sandtäkt (In Swedish)*.

Masselink, G., & Gehrels, R. (2014). *Coastal Environments and Global Change* (1st ed.). American Geophysical Union.

McFall, B. (2019). The Relationship between Beach Grain Size and Intertidal Beach Face Slope. *Journal of Coastal Research*, *35*(5), 1080–1086. https://doi.org/10.2112/JCOASTRES-D-19-00004.1

McLean, R. F., & Kirk, R. M. (1969). Relationships between grain size, size-sorting, and foreshore slope on mixed sand - shingle beaches. *New Zealand Journal of Geology and Geophysics*, *12*(1), 138–155. https://doi.org/10.1080/00288306.1969.10420231

Mil-Homens, J., Ranasinghe, R., van Thiel de Vries, J. S. M., & Stive, M. J. F. (2013). Re-evaluation and improvement of three commonly used bulk longshore sediment transport formulas. *Coastal Engineering*, *75*, 29–39. https://doi.org/10.1016/j.coastaleng.2013.01.004

Nyberg, J., Goodfellow, B., & Ising, J. (2021). *Fysiska och dynamiska förhållanden längs Skånes kust – underlag för klimatanpassningsåtgärder (In Swedish)* (SGU-rapport 2021:02). Swedish Geological Survey.

Nyberg, J., Goodfellow, B., Ising, J., & Hedenström, A. (2020). *Kustnära sedimentdynamik (In Swedish)* (SGU-Rapport 2020:04). Swedish Geological Survey.

Quadrado, G. P., & Goulart, E. S. (2020). Longshore sediment transport: predicting rates in dissipative sandy beaches at southern Brazil. *SN Applied Sciences*, *2*(8). https://doi.org/10.1007/s42452-020-03223-x

Reis, A. H., & Gama, C. (2010). Sand size versus beachface slope — An explanation based on the Constructal Law. *Geomorphology*, *114*(3), 276–283. https://doi.org/10.1016/j.geomorph.2009.07.008

Russell, R. D. (1955). Effects of Transportation on Sedimentary Particles. In P. D. Trask (Ed.), *Recent Marine Sediments* (Vol. 4, p. 0). SEPM Society for Sedimentary Geology. https://doi.org/10.2110/pec.55.04.0032

Skoog, M. (2008). *Bakgrundsmaterial - Policy för förvaltning och skydd av kusten (In Swedish)*. Ystad Kommun.

Skoog, M. (2020). *För kännedom - Information om strandfodring längs Ystad kommuns kust (In Swedish)*. Ystad Kommun.

Skoog, M. (2022). *Sandfodring Ystad* [Personal communication].

SMHI. (2021). *Havsvattenstånd, RH2000, Ystad Sjöv, 201116 - 201121 [Dataset]*. Https://Www.Smhi.Se/Data/Oceanografi/Ladda-Ner-Oceanografiska-Observationer#param=sealevelrh2000,Stations=all,Stationid=35159.

SMHI. (2022, January 19). *Tidvatten*. https://www.smhi.se/kunskapsbanken/oceanografi/vagor/tidvatten-1.321

Smith, E. R., Wang, P., Ebersole, B. A., & Zhang, J. (2009). Dependence of Total Longshore Sediment Transport Rates on Incident Wave Parameters and Breaker Type. *Journal of Coastal Research*, *25*(3), 675–683.

Smith, E., Wang, P., & Zhang, J. (2003, May 21). *Evaluation of the CERC Formula Using Large-Scale Model Data*. Coastal Sediments Conference, Clearwater Beach.

U.S. Army Corps of Engineers. (1984). *Shore Protection Manual*. Coastal Engineering Research Center.

Wang, P., & Kraus, N. C. (1999). Longshore Sediment Transport Rate Measured by Short-Term Impoundment. *Journal of Waterway, Port, Coastal, and Ocean Engineering*, *125*(3), 118–126. https://doi.org/10.1061/(ASCE)0733-950X(1999)125:3(118)

Wright, L. D., & Short, A. D. (1984). Morphodynamic variability of surf zones and beaches: A synthesis. *Marine Geology*, *56*(1), 93–118. https://doi.org/10.1016/0025-3227(84)90008-2

Ystad Municipality. (2018). *Handlingsplan för förvaltning och skydd av kusten (In Swedish)*.

Ystad Municipality. (2021, June 24). *Strandfodring i Ystad*. https://www.ystad.se/bygg-miljo/miljo-och-avfall/natur-miljo-och-klimat/integrerad-kustzonsforvaltning/strandfodring-i-ystad/

A Appendix

A1 Marine Geology and Soil Composition

West of Ystad Harbour

The marine sediment is mainly composed of cobble and boulders throughout the active profile. The soil composition is dominated by postglacial sand closes to the shoreline and then transitions into mainly clay till and clay till with a clay content of 15-25% (Figure A 1).

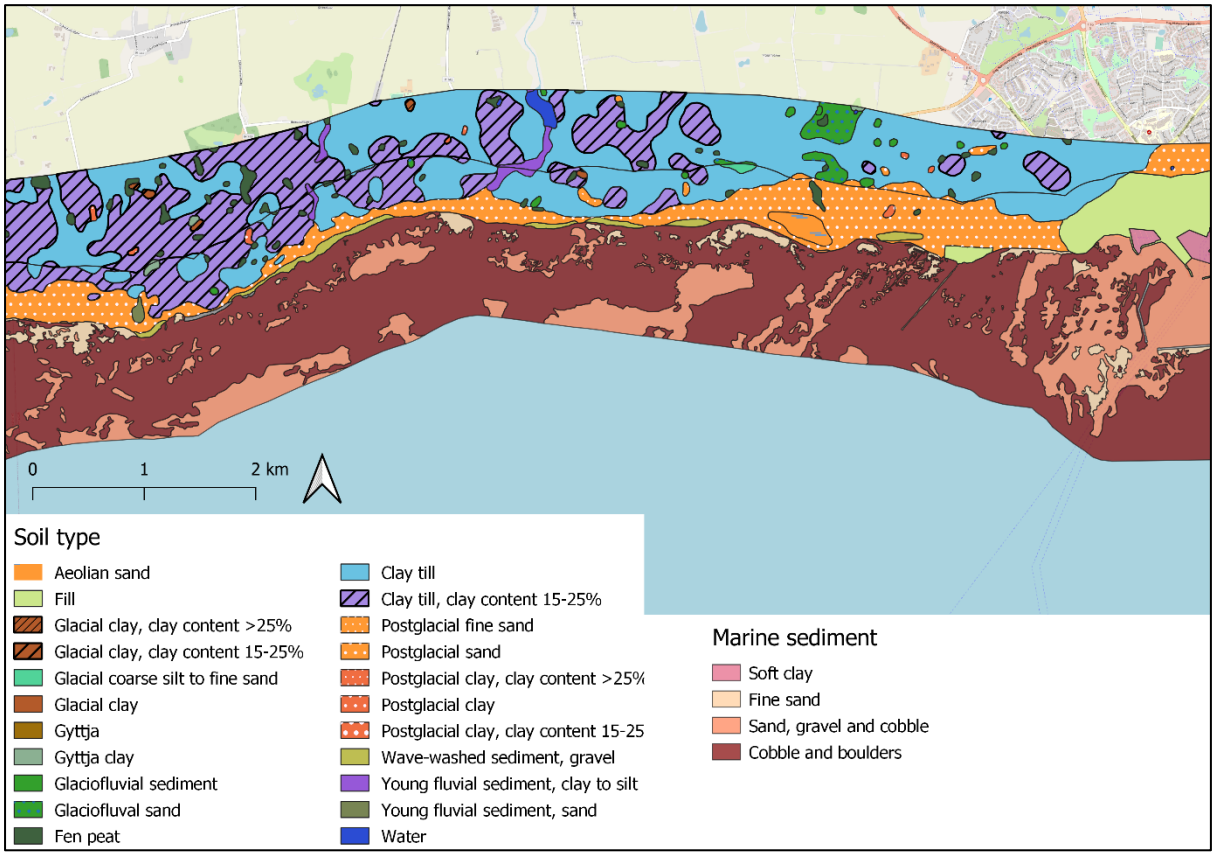

Figure A 1. Soil composition and marine geology of the western shore of Ystad municipality. Data acquired from the Swedish Geological Survey. The marine geology layer uses combined data from the topmost layer and the underlaying layer. Background map obtained from OpenStreetMap.

Ystad Sandskog

Marine geology analyses conducted in the area reveals sediments ranging from larger boulders to fine sand (Figure A 2) (see Table 2.1 for a classification of grain sizes). A few hundred meter offshore, boulders and gravel tend to dominate the bottom whereas finer sand is found along the shoreline. Sand is the dominating soil on land, stretching a few hundred-meter inwards. Closest to shore, there is dune build-up whereas further inland vegetation binds the sand and make out a small forestry area.

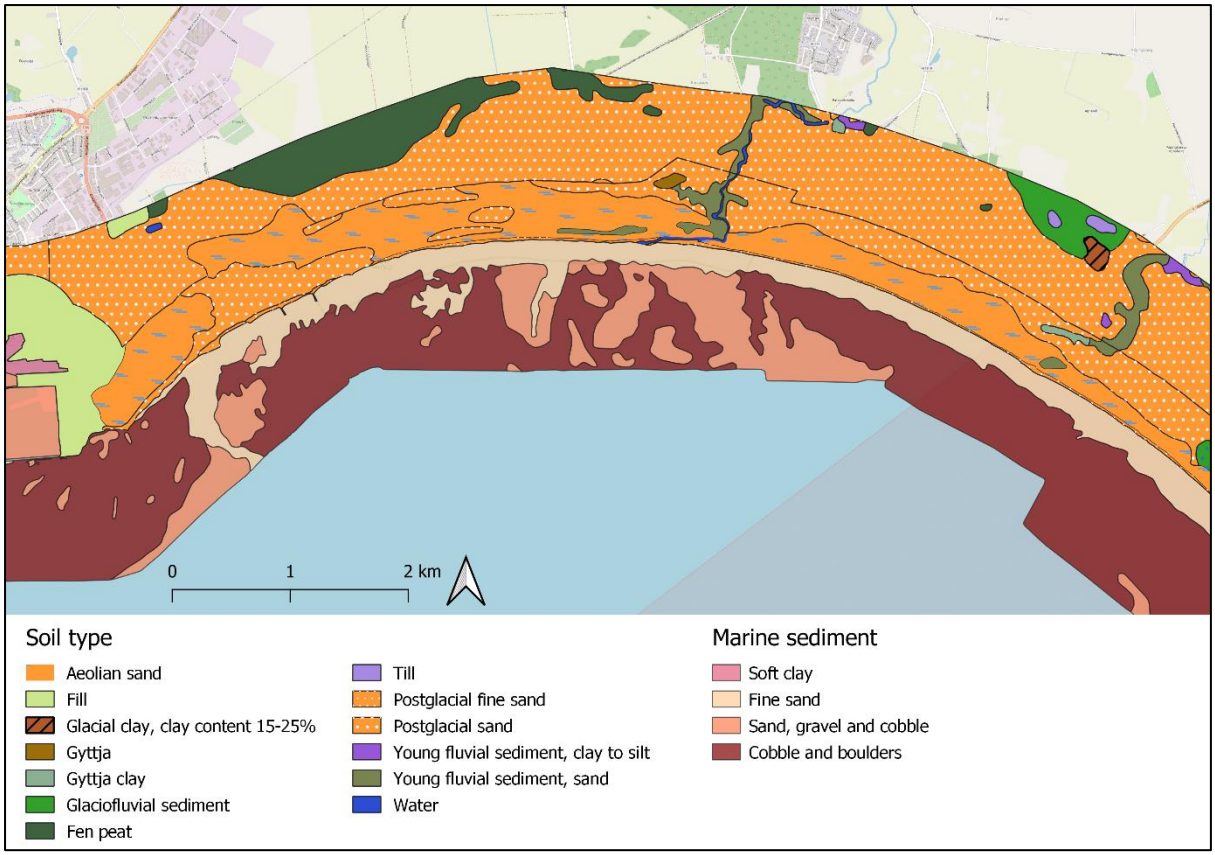

Figure A 2. Soil composition and marine geology of the stretch Sandskogen - Nybrostrand. Data acquired from the Swedish Geological Survey. The marine geology layer uses combined data from the topmost layer and the underlaying layer. Background map obtained from OpenStreetMap.

Nybrostrand

Sediments range from fine sand to blocks (Figure A 2). The first 200 meters out to sea is dominated by fine sand transcending into an area defined by larger sediments like boulders. Although still harbouring some finer sediments as well, such as gravel and sand, larger sediments seem to dominate from here on and throughout the surf-zone. These are the characteristics for a large part of the stretch, however, directly east of Nybroån the section of fine sand transcends into slightly coarser sediments such as sand and gravel with little or no occurrence of boulders throughout the active beach profile.

The soil is completely dominated by sand, both postglacial stretching a kilometre inland, and close to shore with aeolian deposition of sand (Figure A 2). Additionally, flood plain deposits of sand are present in the vicinity of both rivers.

Kabusa Military Field, Hammars Backar and Kåseberga

The marine sediment outside the Kabusa field is mainly composed of fine sand for the first 200 meters (Figure A 3). Seaward of this the sediment transitions into being dominated by cobble and boulders. Outside of Hammars backar the sediment ranges from fine sand to boulders for the first 200 meters, which then transitions into cobble and boulders, whereas outside of Kåsehuvud the sediment is dominated by cobble and boulders, which transitions into a combination of sand, gravel, and cobble after 100 meters. The marine sediment in the area stretching from Kåseberga village to Löderups Strandbad is mainly composed of sand, gravel,

and cobble (Figure A 3). Since this area is mainly composed of the Kåseberga ridge at various degrees of erosion, the soil is coarser in the eroded areas and finer in the less eroded areas.

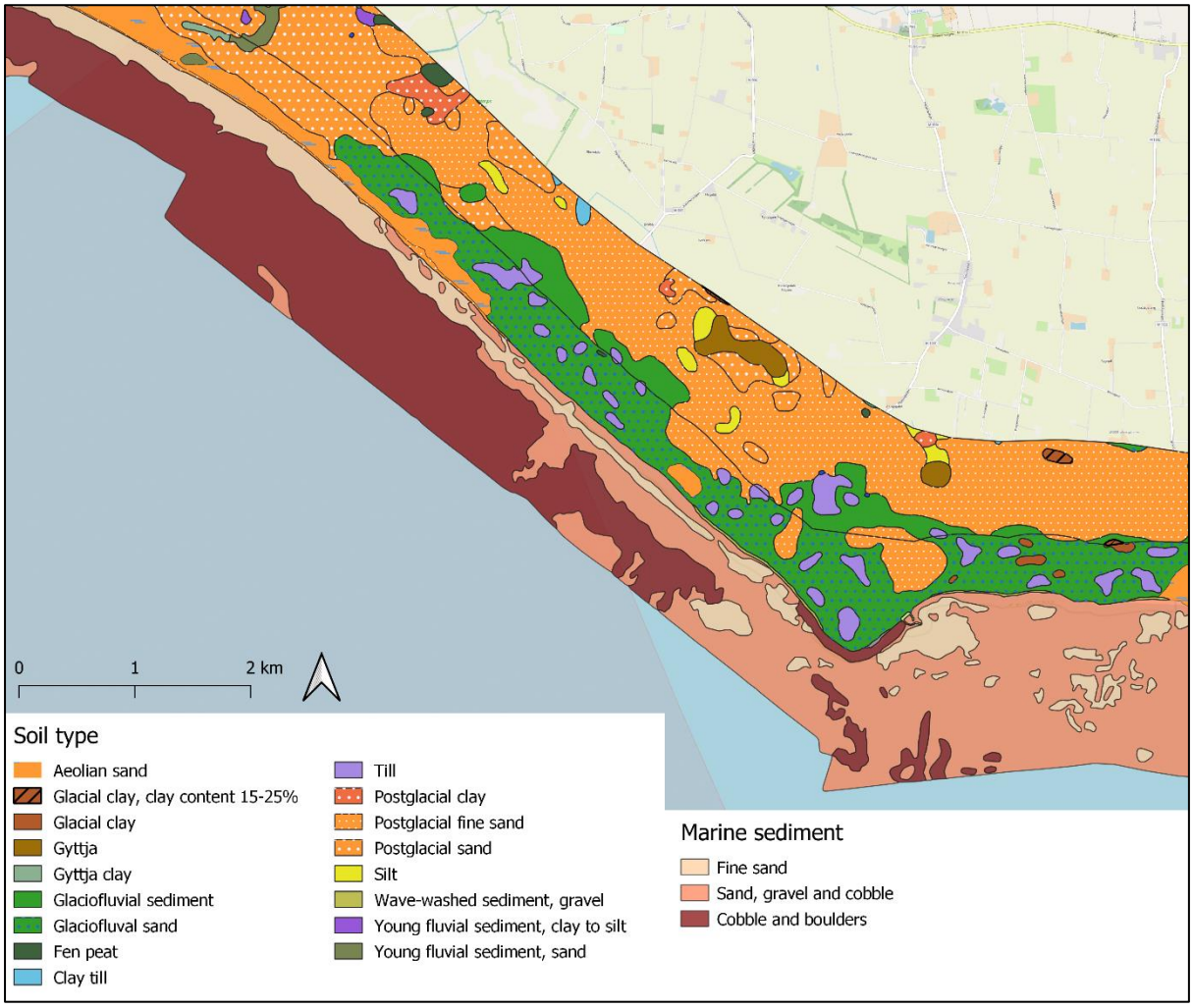

Figure A 3. Soil composition and marine geology of the stretch Kabusa Military Field - Kåseberga. Data source geology: SGU (2021). Background map: OpenStreetMap.

Löderups Strandbad

The marine sediment in the active profile is dominated by fine sand (see Table 2.1 for classification of sediment), except for the far eastern part where sand is intermixed with gravel and boulders (Figure A 4). The natural beach sediment is almost completely eroded from parts of the shoreline. The soil is composed of mainly aeolian sand.

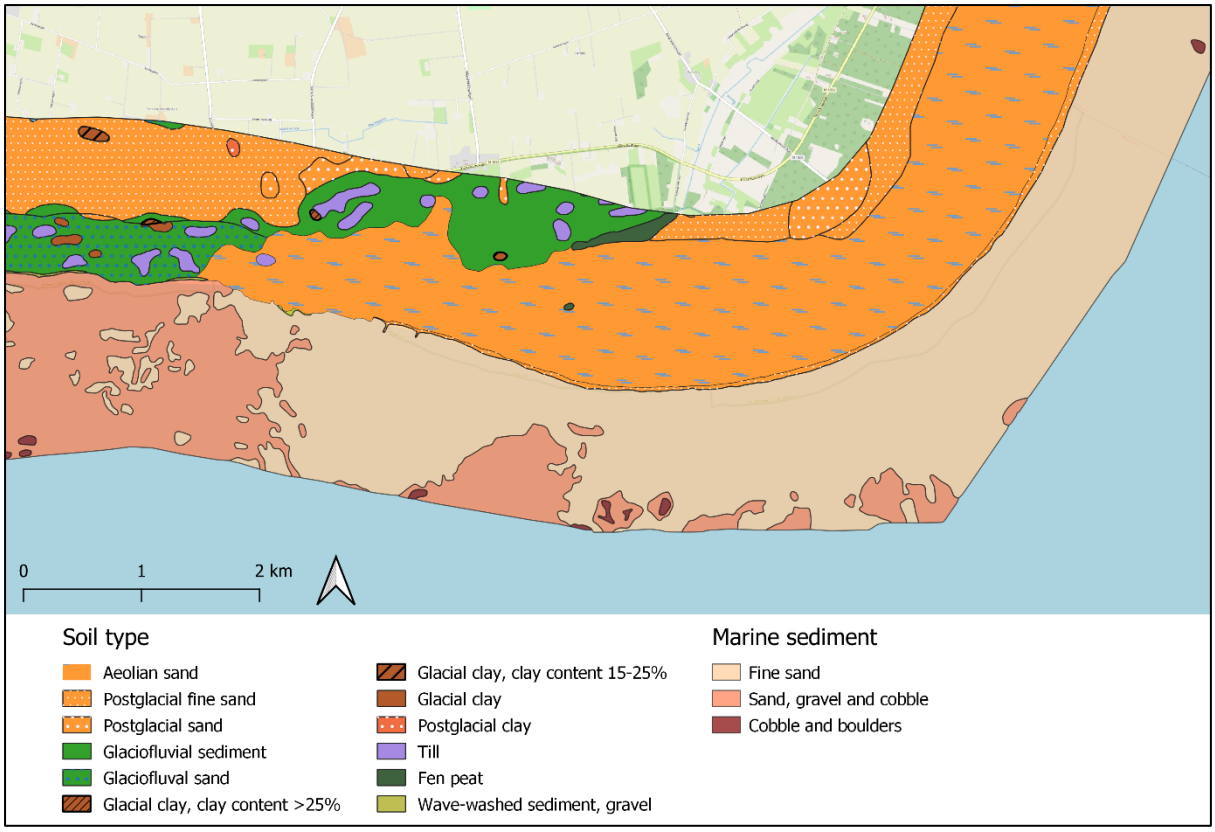

Figure A 4. Soil composition and marine geology of the stretch Löderups Strandbad - Sandhammaren. Data source geology: SGU (2021). Background map: OpenStreetMap.

Sandhammaren

The marine sediment outside Sandhammaren is completely dominated by fine sand for the entire length of the active profile. The soil is mainly comprised of aeolian sand (Figure A 4).

A2 Table of Grain Size Statistics of Field Samples

The below table contains the median grain size and the beach face slope obtained through field sampling.

Location	**Sample**	**d_{50} (mm)**	**Sorting, d_{84}/d_{16}**	**Beach face slope (m/m)**
West of Svarte	1	225.5	1.92	0.11245
	2	216.6	1.46	0.10302
	3	181.1	1.64	0.07229
Svarte	4	670.6	1.69	0.12728
	5	829.2	2.74	0.18648
	6	359.2	2.18	0.11206
	7	460.2	2.10	0.17126
	8	407.3	1.69	0.16256
	9	623.8	1.58	0.17042
Lilleskog	10	392.3	1.61	0.17195
	11	352.8	1.67	0.12243
	12	532.7	2.42	0.09698
	13	353.1	2.29	0.13076
	14	287.6	1.53	0.14251
	15	353.2	1.92	0.14003
	16	882.3	3.02	0.16912
	17	250.5	1.68	0.13596
	18	307.7	2.79	0.15951
	19	314.8	2.02	0.13024
	20	601.0	3.23	0.13905
	21	307.2	1.96	0.10299
Ystad	22	754.2	1.88	0.13584
	23	780.9	2.16	0.17671
	24	297.4	2.01	0.09903
	25	359.9	2.67	0.10789
Ystad Sandskog West	26	491.8	4.32	0.11902
	27	397.7	2.94	0.09790
	28	229.7	1.73	0.09094
	29	350.2	1.98	0.09811
	30	337.6	1.89	0.11817
	31	328.3	1.84	0.06858
	32	337.9	2.14	0.19401
	33	351.0	1.90	0.11442
	34	298.9	2.26	0.13601
Ystad Sandskog East	35	329.9	1.71	0.13181
	36	281.5	1.77	0.12152
	37	350.3	1.91	0.17550
	38	432.5	1.80	0.11333
	39	403.4	1.68	0.12760

Location	Sample	d_{50} (mm)	Sorting, d_{84}/d_{16}	Beach face slope (m/m)
Nybrostrand	40	438.4	1.75	0.12336
	41	414.0	1.89	0.13399
	42	399.0	1.64	0.15088
	43	479.6	1.93	0.13880
	44	701.5	1.65	0.25664
	45	488.5	1.71	0.16320
	46	414.5	1.95	0.16230
	47	568.7	1.68	0.17488
	48	594.1	1.86	0.15103
	49	630.0	1.85	0.15837
Löderups Strandbad	50	661.3	2.27	0.13406
	51	333.1	2.32	0.17083
	52	375.7	1.81	0.13630
	53	317.4	1.96	0.08411
	54	283.6	1.61	0.13934
Sandhammaren	55	243.6	1.67	0.02609
	56	279.7	1.66	0.06310
	57	235.0	1.63	0.07165
	58	214.0	1.37	0.07913
	59	228.6	1.68	0.07960
	60	230.3	1.66	0.08399

A3 Sorting vs. Beach Face Slope

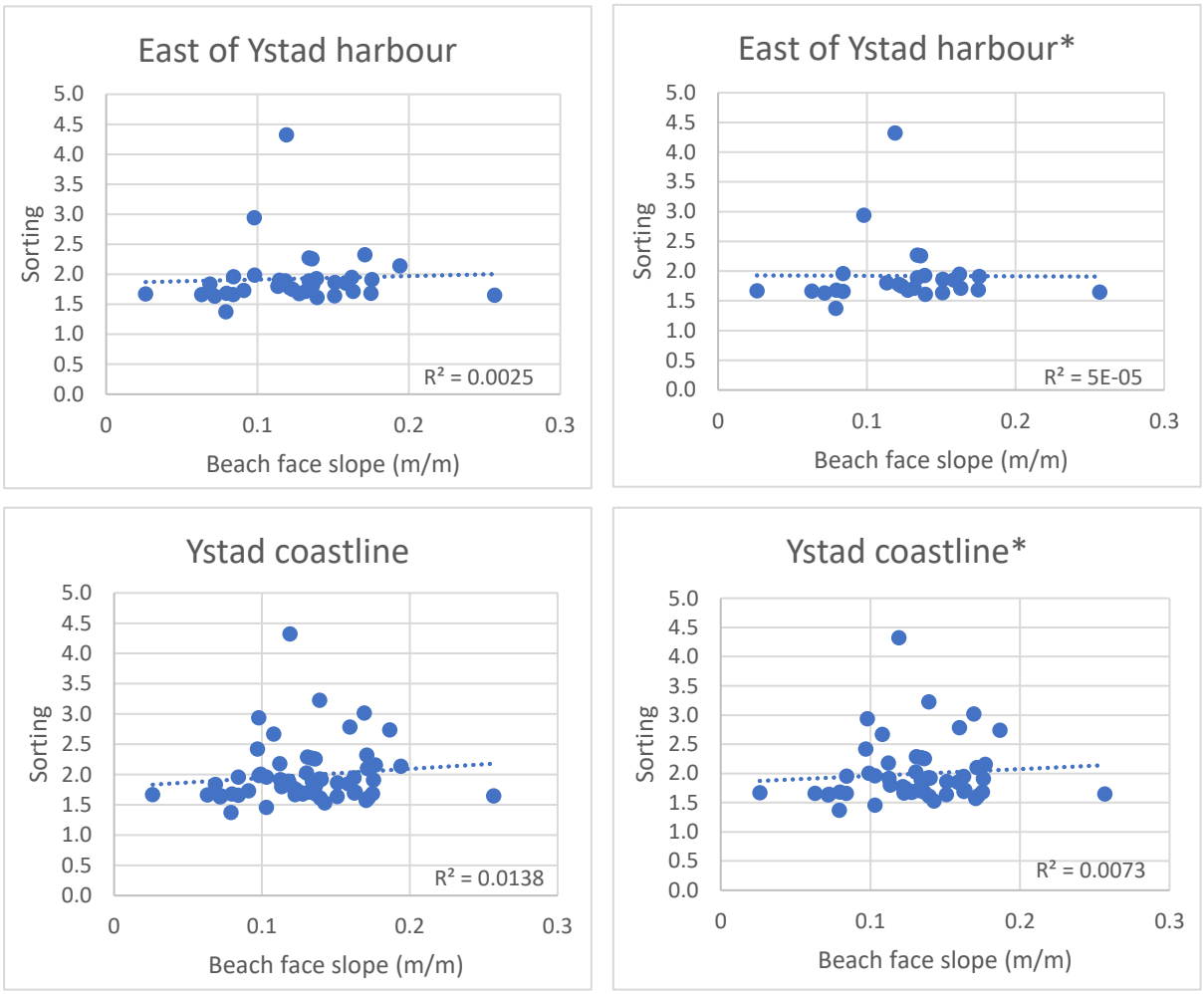

*Figure A 5. Sorting plotted against beach face slope in m/m. * Nourished stretches have been excluded from the plot.*

A4 Cumulative Distribution Curves

This appendix contains the cumulative distribution curves for all sediment samples collected during the field survey. Note that the x-axis, denoting grain size, varies between plots.

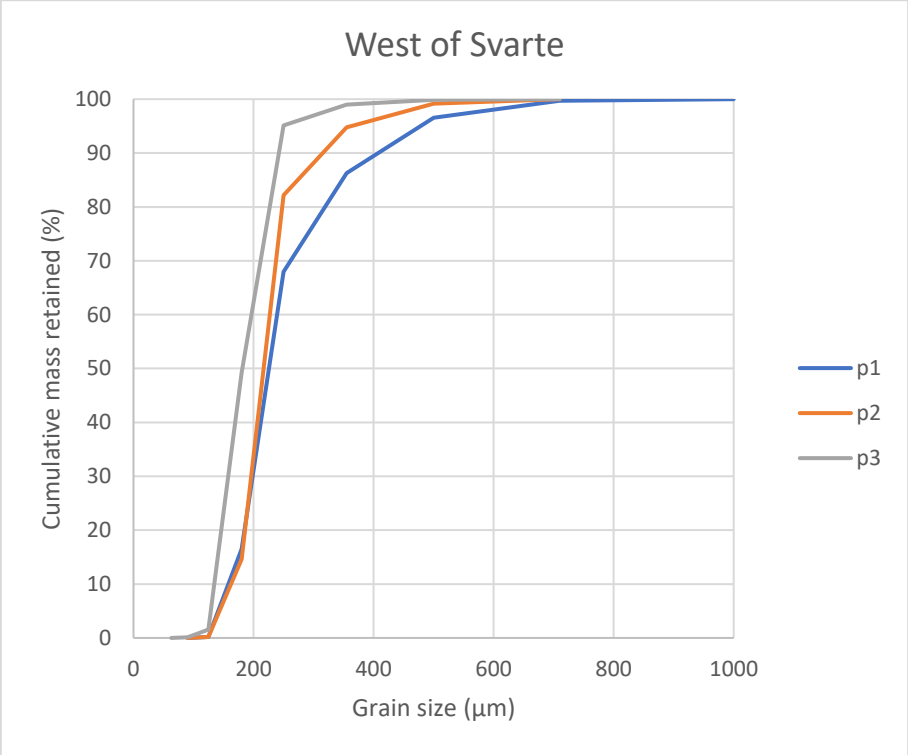

Figure A 6. Cumulative distribution curves of grain size samples from West of Svarte.

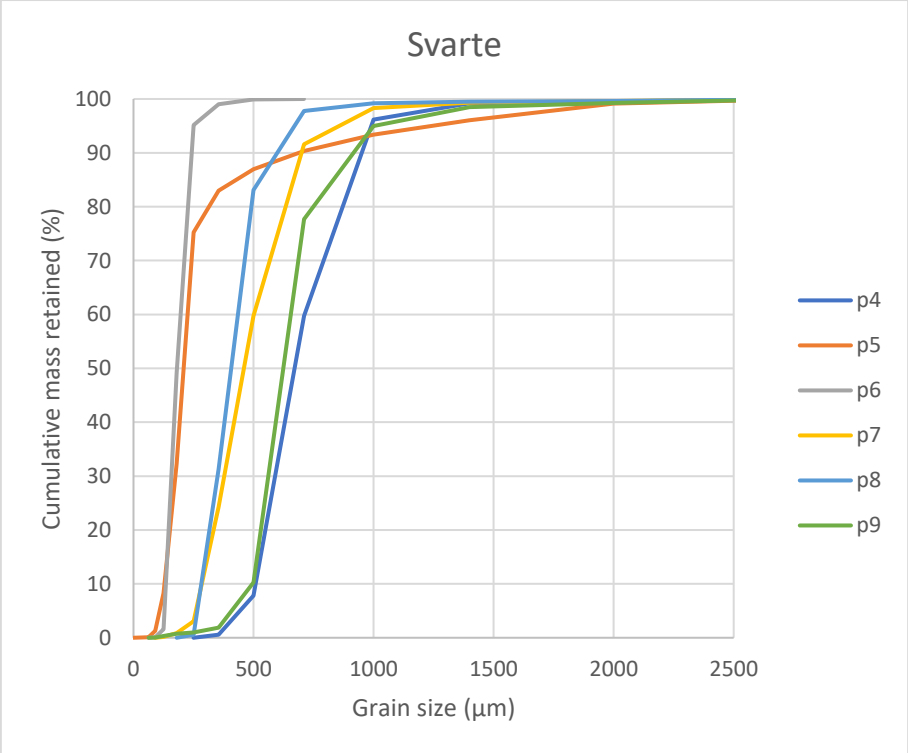

Figure A 7. Cumulative distribution curves of grain size samples from Svarte.

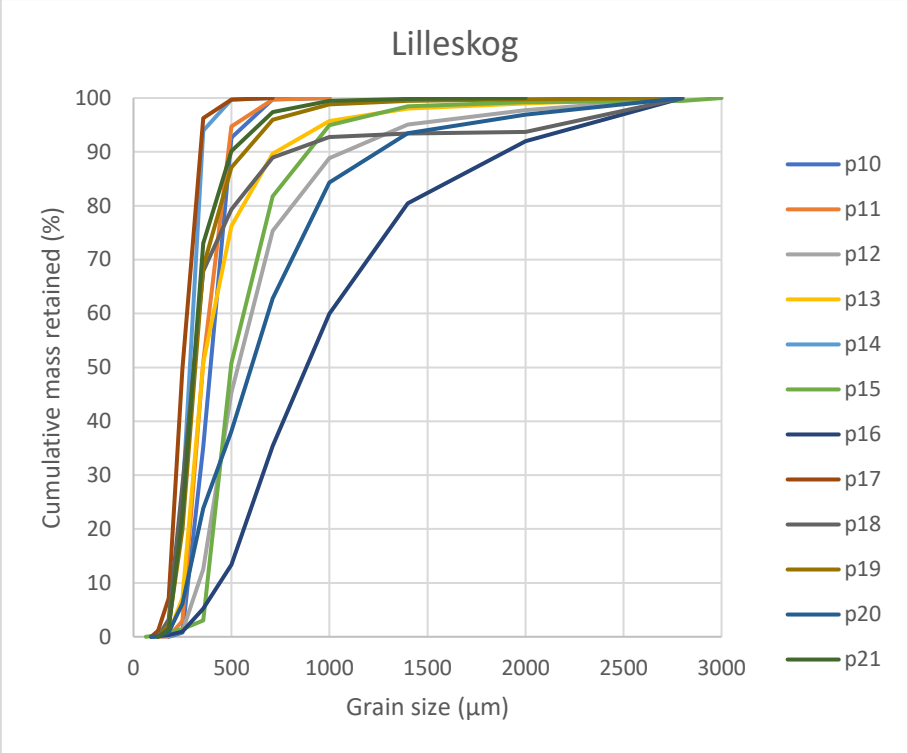

Figure A 8. Cumulative distribution curves of grain size samples from Lilleskog.

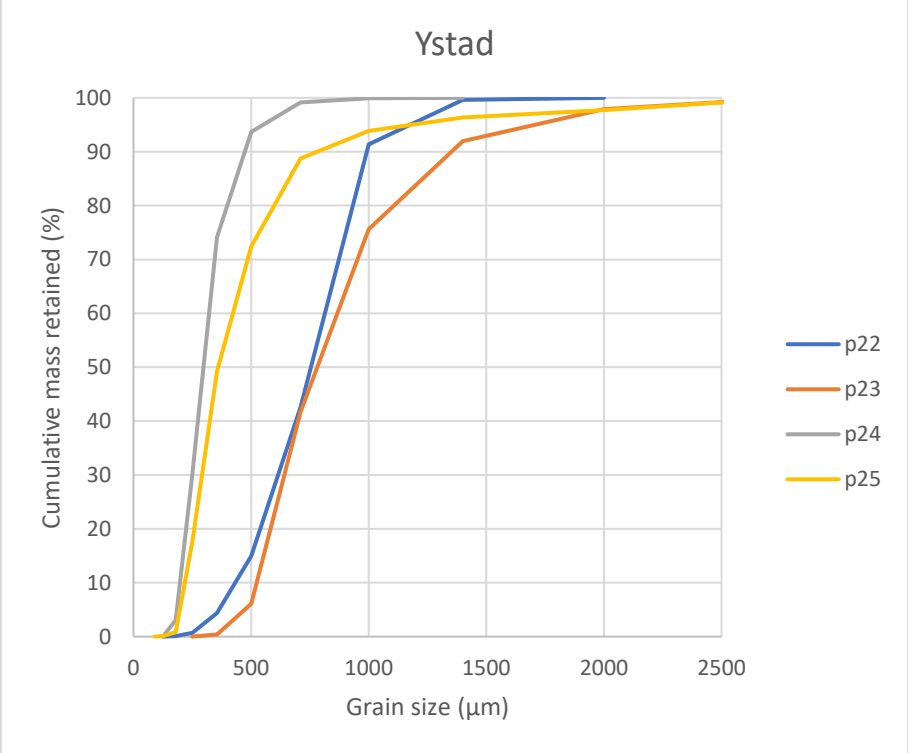

Figure A 9. Cumulative distribution curves of grain size samples from Ystad.

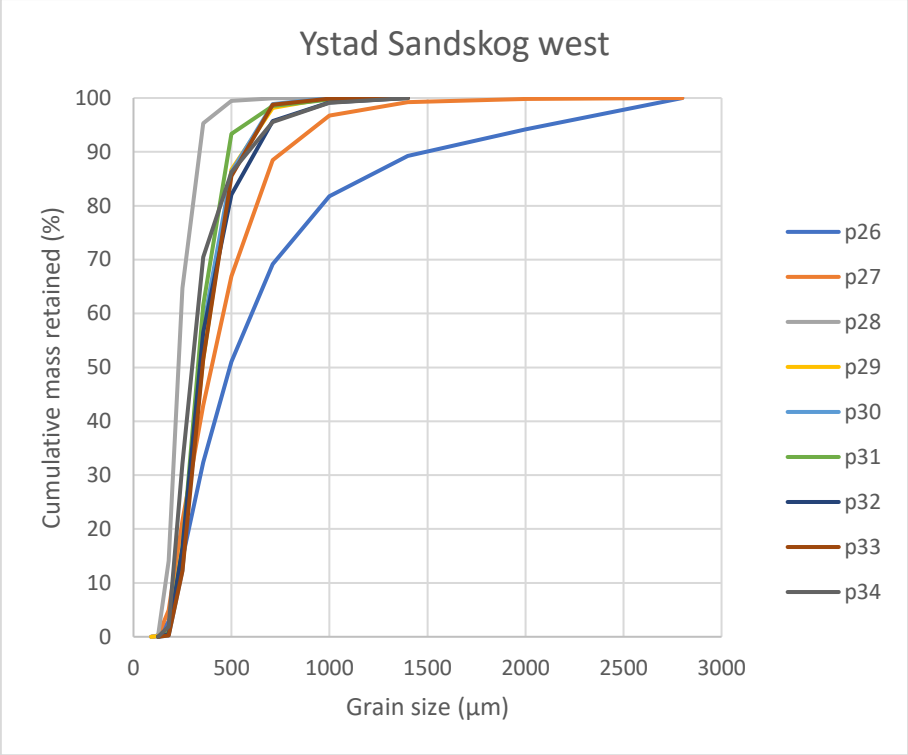

Figure A 10. Cumulative distribution curves of grain size samples from Ystad Sandskog west.

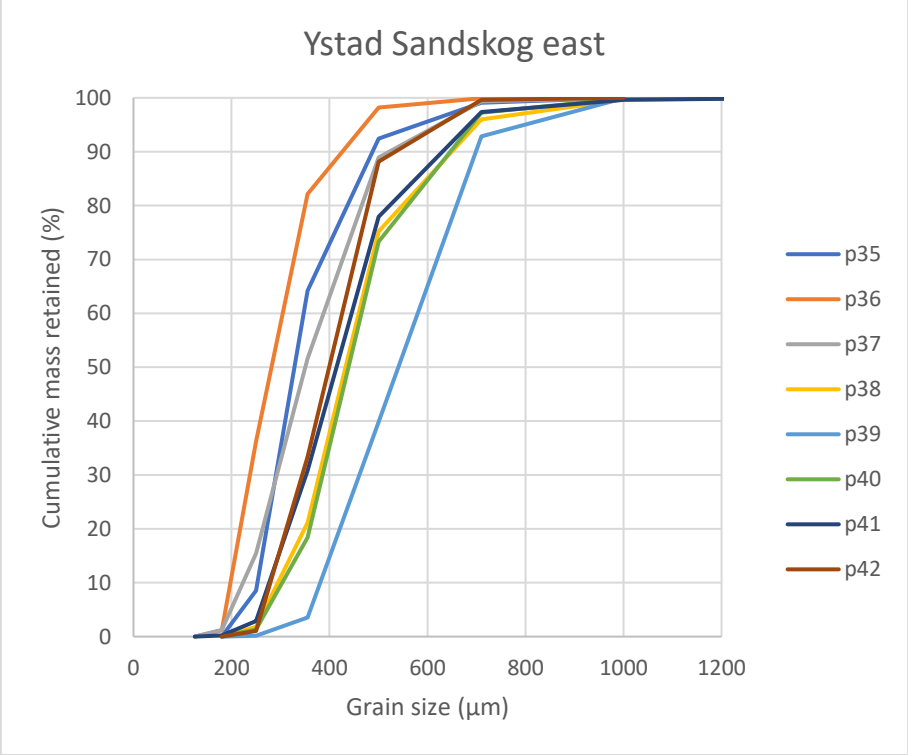

Figure A 11. Cumulative distribution curves of grain size samples from Ystad Sandskog east.

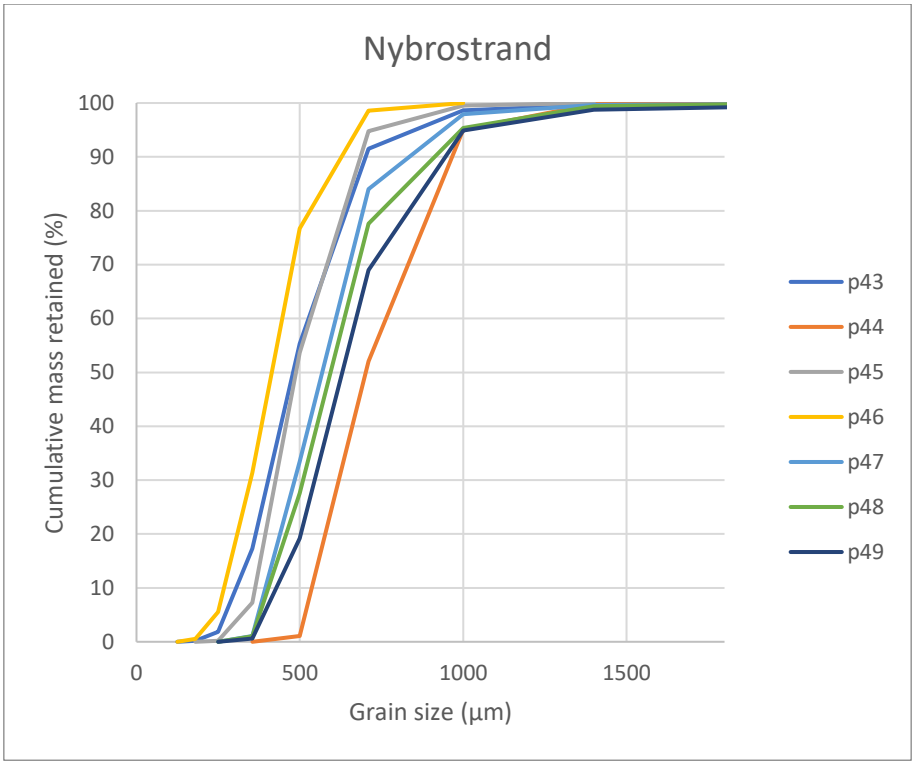

Figure A 12. Cumulative distribution curves of grain size samples from Nybrostrand.

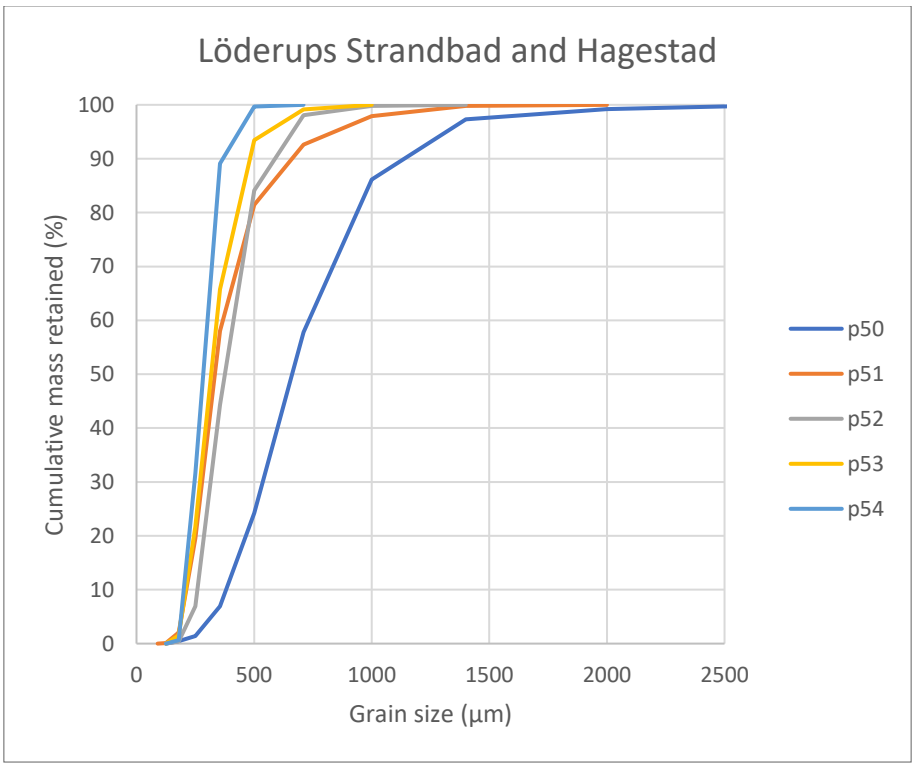

Figure A 13. Cumulative distribution curves of grain size samples from Löderups Strandbad and Hagestad.

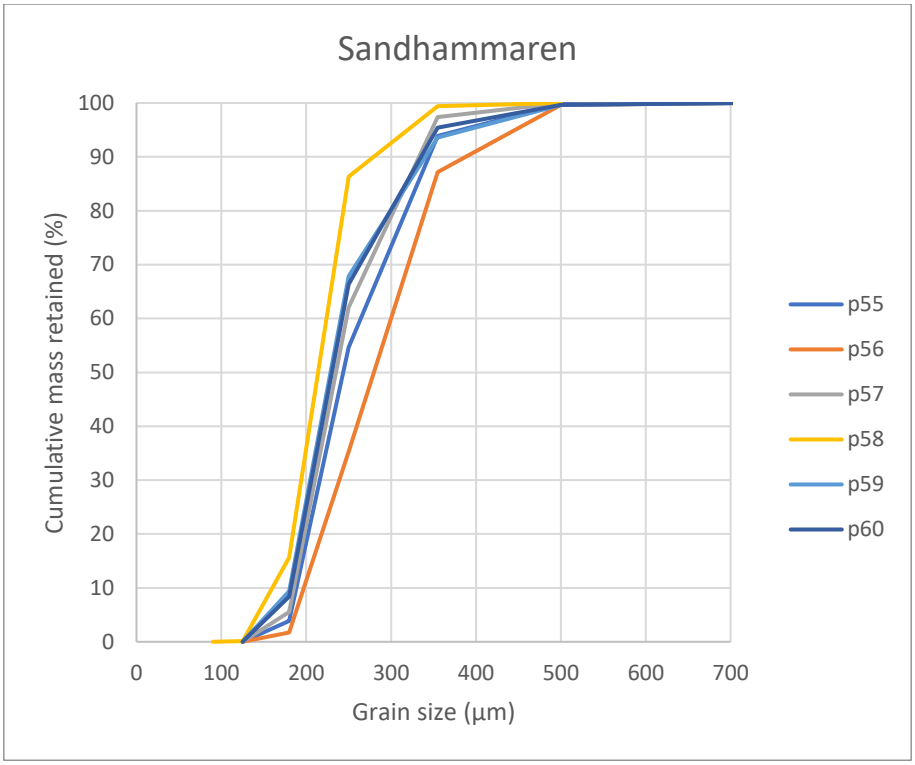

Figure A 14. Cumulative distribution curves of grain size samples from Sandhammaren.

A5 Sieving Data

Data from sieving and weighing of sediment samples are compiled in the table below.

	Sieve size (mm)												
	>2	1.4	1	0.71	0.5	0.355	0.25	0.18	0.125	0.09	0.063	<0.063	
Sample	weight retained (g)												Sum retained (g)
1	0	0	0	0.6	6.3	20.5	36.6	102.9	32.7	0.3	0	0	199.9
2	0	0	0	0	1.4	8.7	24.7	132.8	28.4	0.3	0	0.2	196.5
3	0	0	0	0	0.2	1.8	7.7	91.7	95.3	2.9	0	0.2	199.8
4	0.9	0.7	6	72.5	103.3	14.5	1.1	0	0	0	0	0	199.0
5	26	7.9	15.4	85.4	48	14	2.3	0.2	0	0	0	0	199.2
6	0.9	1.3	3.7	9.1	29.9	56.4	83.3	11.4	2.3	0.5	0.3	0.2	199.3
7	0.8	0.6	2	13.4	64	71.1	42.5	4.5	1.4	0.3	0	0	200.6
8	0.7	0.3	0.6	2.8	29.3	103.4	61.4	1.1	0	0	0	0	199.6
9	1.5	1.5	7	34.7	135	16.8	1.7	0.5	0.8	0.6	0.1	0	200.2
10	0	0	0	0.5	14.3	114.8	69	1.2	0	0	0	0.4	200.2
11	0	0	0	0.6	10	87.2	96	5.7	0.1	0	0	0	199.6
12	4.5	5.4	12.4	27	60	65.5	23.1	1.7	0.3	0	0	0	199.9
13	2	1.9	4.6	12.1	26.8	50.8	87	13.2	1.1	0	0	0	199.5
14	0	0	0	0	0.6	11.5	136.3	47.4	3.1	0.2	0	0	199.1
15	1	0.5	1.6	7	26.3	61.9	95.4	3.3	1.1	1.1	0.3	0.3	199.8
16	15.9	23	40.8	48.8	43.9	16.2	8.5	1.3	0.4	0.2	0	0	199.0
17	0	0	0	0	0.6	6.9	92.6	85.1	12	2.2	0	0	199.4
18	12.6	0.5	1.3	7.6	19.2	22.9	79.2	49.8	6.4	0	0	0	199.5
19	0.5	0.5	1.4	5.7	17.6	36.7	97.4	35.5	4.1	0	0	0	199.4
20	6.3	7	18.6	43.9	50.3	29.1	36.1	10.8	1.6	0.1	0	0	203.8
21	0	0.3	0.8	4.1	14.4	34.1	100.9	41.8	2.9	0	0	0	199.3
22	0	0.7	16.5	97.5	55.1	21.1	7.4	1.2	0.2	0	0	0	199.7
23	4.2	11.9	32.6	67.7	71.1	11.4	0.8	0	0	0	0	0	199.7
24	0	0	0.2	1.5	10.9	39	87.7	54	6.1	0	0	0	199.4
25	4.6	2.7	5	10.1	32.6	46.3	63	33.6	1.4	0.2	0	0	199.5
26	11.6	9.8	14.9	25.1	36	37.2	35.6	23.1	5.5	0.2	0	0	199.0
27	0.4	1.1	5.1	16.7	43.5	48.4	43.3	33.4	9.6	0.4	0	0	201.9
28	0	0	0	0.1	1	8.2	61	100.9	27.5	0.5	0	0	199.2
29	0	0	0	3.7	22.8	70.1	69.3	31.8	1.6	0.2	0	0	199.5
30	0	0	0	2.3	25	57.5	90	24.1	0.5	0	0	0	199.4
31	0	0	0.6	2.4	10.3	63.4	90.5	30	2.3	0	0	0	199.5
32	0	0	1.6	6.9	27.2	50.9	79.7	32	0.9	0	0	0	199.2
33	0	0	0.2	2.3	26.4	67.7	78.3	23.8	0.5	0	0	0	199.2
34	0	0	1.8	7.1	18.6	31.3	76.4	60.3	3.8	0	0	0	199.3
35	0	0	0	1.9	10.8	59.8	109.4	15	0.3	0	0	0	197.2
36	0	0	0	0.2	3.4	32	91.5	69.9	2.3	0	0	0	199.3
37	0	0	0	1.3	20.7	74.4	72.1	28.2	2.5	0	0	0	199.2
38	0	0	0.6	7.4	41.6	108.1	38.5	3.7	0	0	0	0	199.9
39	0	0	0	1.6	29.7	102.4	61.2	4.2	0	0	0	0	199.1

	Sieve size (mm)												
	>2	1.4	1	0.71	0.5	0.355	0.25	0.18	0.125	0.09	0.063	<0.063	
Sample	weight retained (g)												Sum retained (g)
40	0	0	0.3	5.2	47.7	109.3	34	2.7	0	0	0	0	199.2
41	0	0	0.7	4.6	38.7	93.9	55.7	5.4	0.4	0	0	0	199.4
42	0	0	0	0.7	22.9	109.2	64.5	2.1	0	0	0	0	199.4
43	0.3	0.4	2	14	71	74.7	30.4	3.3	0.3	0	0	0	196.4
44	0	0.3	9.6	85.9	101.8	2.2	0	0	0	0	0	0	199.8
45	0	0	0.9	9.5	81.9	92.6	14	0.4	0	0	0	0	199.3
46	0	0	0	2.8	43.7	90.5	51.6	10	1.1	0	0	0	199.7
47	0.3	0.4	3.4	27.8	100.9	64.7	2.1	0	0	0	0	0	199.6
48	0.2	1	8	35.5	99.9	53.1	2	0	0	0	0	0	199.7
49	1.2	1.3	7.7	51.7	99.3	37.1	1.2	0	0	0	0	0	199.5
50	1.6	3.8	22.2	56.5	66.8	34.5	11	1.9	0.9	0	0	0	199.2
51	0	0.4	3.7	10.5	21.9	46.1	75.9	34.3	3.9	0.2	0	0	196.9
52	0	0	0.4	3.4	27.7	78.9	74.2	12.9	0.8	0	0	0	198.3
53	0	0	0	1.7	11.4	55.1	87.8	40.3	3	0	0	0	199.3
54	0	0	0	0	0.6	21.1	114.9	61.7	1.3	0	0	0	199.6
55	0	0	0	0	0.4	11.8	78.3	101.5	7.7	0	0	0	199.7
56	0	0	0	0	0.7	24.9	103.5	67	3.5	0	0	0	199.6
57	0	0	0	0	0	5.3	72.4	116.1	11.3	0	0	0	205.1
58	0	0	0	0	0	1.2	26.1	141.3	31	0.2	0	0	199.8
59	0	0	0	0	0.7	12.1	51.3	116.6	18.7	0	0	0	199.4
60	0	0	0.2	0	0.5	8.4	57.7	115.2	16.6	0	0	0	198.6